2021

THERMOMECHANICAL MECHANISMS THAT CAUSE ADHESION OF ALUMINUM HIGH PRESSURE DIE CASTINGS TO THE DIE

Alex Monroe
Michigan Technological University, akmonroe@mtu.edu

THERMOMECHANICAL MECHANISMS THAT CAUSE ADHESION OF ALUMINUM HIGH PRESSURE DIE CASTINGS TO THE DIE

By

Alexander K. Monroe

A DISSERTATION

Submitted in partial fulfillment of the requirements for the degree of

DOCTOR OF PHILOSOPHY

In Materials Science and Engineering

MICHIGAN TECHNOLOGICAL UNIVERSITY

2021

This dissertation has been approved in partial fulfillment of the requirements for the Degree of DOCTOR OF PHILOSOPHY in Materials Science and Engineering.

Department of Materials Science and Engineering

Dissertation Advisor:	*Paul G. Sanders*
Committee Member:	*Kevin R. Anderson*
Committee Member:	*Douglas J. Swenson*
Committee Member:	*Stephen A. Hackney*
Department Chair:	*Walt Milligan*

Table of Contents

List of Figures

List of Tables

Acknowledgements

Many thanks to my family, friends, and colleagues who were critical to the success of this adventure. Our discussions were invaluable in my learning and development of the work in this document. I am also thankful for the support from my employer, Mercury Marine, and professional organization, the North American Die Casting Association. Most of all, I want to thank my wife, Esther, for her support and encouragement.

Abstract

In high pressure die casting (HPDC) of aluminum, cast material adhering to die is a significant defect. Adhesion occurs in two primary ways. The casting may stick preventing its removal from the die. Aluminum can also adhere to the die and buildup in local areas on the die surface with additional casting cycles. This second form of adhesion is called soldering. Lubricant is the best technology to control all forms of adhesion, but it comes at the cost of casting porosity, blisters, reduced die life, and increased die casting machine wear. New strategies to prevent adhesion are desired to eliminate the downsides of spray lubricants.

Thermodynamically, there is a drive to form intermetallic phases between the aluminum casting and steel die. The kinetically controlled formation of these phases has been understood as the primary mechanism which causes sticking and soldering. Assuming this mechanism, adhesion should be eliminated by coating the die surface with a non-reactive material, but laboratory and industrial experiments show that this approach is partially effective. Also, kinetics based predictions cannot identify the areas where adhesion is most severe. Additional mechanisms are needed to further predict and reduce these defects.

Friction is such a mechanism, and it has been overlooked as a significant cause of sticking and soldering in HPDC. Sticking results from the thermal contraction of the casting onto the die. This creates a friction force that resists ejection and may be larger than the ejection force capability of the die casting machine. Soldering is a special case where the local shear stress due to friction exceeds the local shear strength of the casting. This typically happens at high temperatures and can be predicted by the ratio of the local ejection shear stress and temperature dependent shear strength.

Four aspects of HPDC adhesion were investigated to support this friction mechanism. First, the accepted theory of a kinetically controlled approach to the thermodynamic equilibrium does not adequately predict sticking and soldering. Next, the decrease in sticking force with increasing draft angle is predicted by a friction model. Third, soldering is shown to occur when the shear stress at ejection exceeds the strength of the casting via hot ejection test and computer models of industrial castings. Finally, the friction approach is applied to a range of casting conditions and alloys with discussion of optimization opportunities.

1 Introduction

High Pressure Die Casting (HPDC) is the most common casting process for complex non-ferrous castings, and it is favored to produce aluminum components for both automotive powertrain and body in white structures. The importance of the process is evidenced by foundries in the United States shipping over two billion pounds of aluminum die castings per year over the last decade [1]. High production rates offset the initial tooling investment making it a low-cost process. HPDC components are also lightweight because 2 mm thick walls can be achieved. Rapid cooling of these thin walls refines the microstructure offering the potential for high strength and ductility [2]. Recent alloy developments have enabled a broader use of secondary aluminum sources improving the renewability of HPDC [3].

Advantages of HPDC are achieved by forcing molten aluminum into a permanent mold, called the die, with high velocities and pressures (Figure 1). Lubricant, a water-based emulsion of waxes and oils, is sprayed on the die prior to filling [4]. Next the die is closed and clamped with many tons of force. Molten aluminum is poured into a horizontal tube called the cold chamber. A piston, called plunger tip, forces the casting alloy into the die. Pressure is applied by the plunger after the die is filled to feed solidification shrinkage. After solidification and cooling is complete, the die is unclamped, opened, and the casting is ejected from the die. The next casting cycle is started immediately after the casting is removed, and castings are produced semi-continuously.

Metal velocities in the gating system can exceed 100 km/h and fill the die in less than 100 milliseconds. High velocity is required to avoid solidification while filling the casting [5]. Thermal gradients are large because the die surface temperature is roughly 250°C while the cast material enters at nearly 700°C. Depending on the section thickness, a wide range of cooling rates are experienced both exceeding 100°C/s and falling as low as 1°C/s. Due to the short filling, solidification, and cooling times the cycle times are rapid, roughly 30 to 300 seconds.

Solidification shrinkage is fed by pressure from the injection system. It is called intensification pressure and often exceeds 600 bar. Ejection forces increase with the size of the casting, and large castings can require over 50 metric tons of force. With these high forces it is possible to distort and fracture the casting or die. The summation of this extreme intensification pressure and ejection force requires robust dies that weigh upwards of 60 metric tons.

Die casting machines must resist the die opening force due to the intensification pressure. This force is roughly the product of the projected area of the casting in the parting direction and the intensification pressure. Larger castings require higher clamping force, and the machine size is determined by this clamping force. Typical machines range from 50 to over 5000 metric tons. The square root of the projected area gives the equivalent edge length of a square casting. This serves as a rough estimate of the casting size capability as a function of machine size (Table 1).

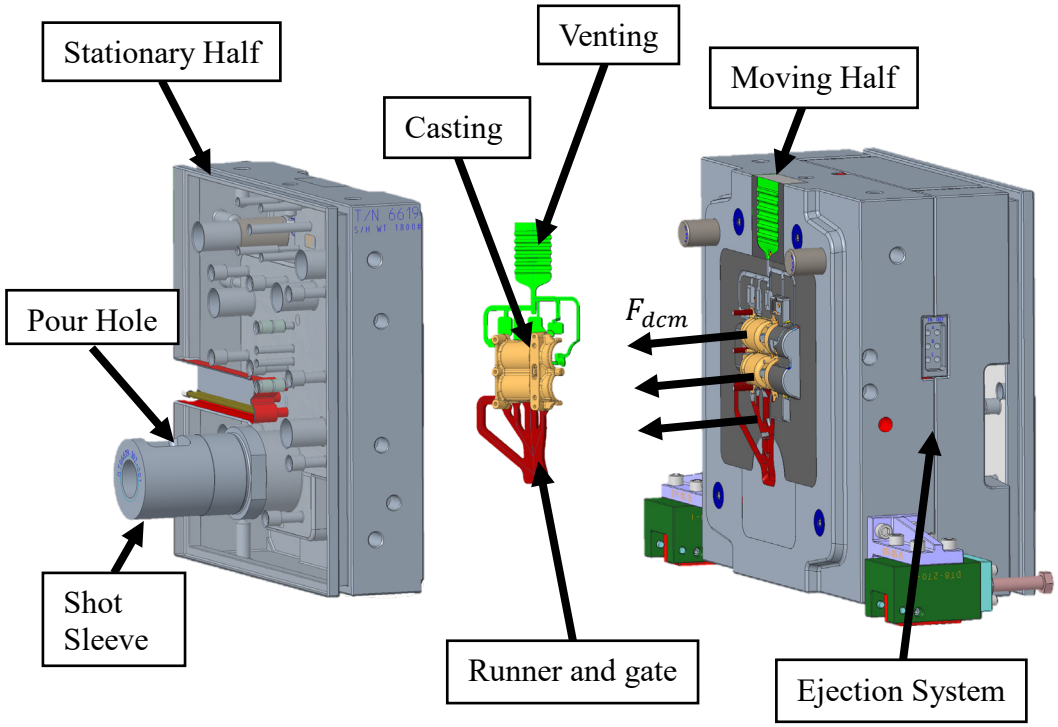

Figure 1: The moving half of a typical die casting die [2].

Numerous challenges face the HPDC designer and the foundry to achieve high quality castings. High velocities required to fill the die cause erosion of the dies. Thin vent passages are required to prevent the metal from escaping the die, but inadequate venting causes entrapped air porosity and filling defects. This leads to blisters during solution heat treatments [6]. Internal shrinkage voids are also difficult or impossible to feed because the process relies on feeding exclusively through the gating system, and the gates freeze prior to the thickest areas of the casting causing shrinkage porosity [7].

Table 1: Approximate casting size capability based on clamping tonnage.

Tonnage	**Projected Area (m^2)**	**Equivalent square casting edge length (m)**
50	0.006	0.08
500	0.064	0.25
5000	0.645	0.80

These challenges are increased by the interaction of the lubricant with the die casting machine, casting, and die [8]. Applying the lubricant can take nearly 30% of the die casting cycle time limiting productivity [8]. Dies fail from the thermal shock of the air atomized spray that is used to apply the lubricant. The lubricant may be trapped in the

surface of the casting, and this reduces paint adhesion. It also contributes to porosity when the lubricant penetrates the cast skin during solidification. Overspray contributes to rapid corrosion on the dies and die casting machines. It also coats much of the die casting plant floor causing workplace slip hazards.

Lubricant caused production and quality concerns justify the goal to reduce or eliminate them. This is difficult because lubricants reduce adhesion of aluminum to the die [9]. Adhesion in HPDC occurs in two primary ways. The most damaging form is when the casting cannot be removed from the die, and it is called sticking, (Figure 2 (a)). Downtime and die damage are the common consequences of sticking, and lubricants have been shown to reduce sticking [10]. Solder is the other form of adhesion, and it is local regions of the casting that adheres and builds up on the die (Figure 2 (b)). Over time it wears the tooling and damages the castings. Lubricants reduce soldering, but they cannot eliminate it.

(a)

(b)

Figure 2: (a) An example of sticking. Both images courtesy of Mercury Marine. (b) An example of soldering on a die insert.

Adhesive mechanisms in HPDC have been studied as thermodynamically driven reaction between the casting and die because aluminum dissolves and forms intermetallic phases with iron [9]. The effect of these reactions is exhibited on failed die components. Permanent die coatings have been primarily investigated to prevent the casting/die reaction and eliminate both forms of adhesion [11]. They do prevent dissolution and phase formation but have not been effective at preventing adhesion [8]. Similarly, models based on these reaction mechanisms are partially effective suggesting additional adhesion mechanisms are required to accurately predict adhesion in HPDC [12], [13].

Friction is a mechanism that has been overlooked, and friction-based models make good predictions of the adhesion observed in HPDC. The insight of friction research is that adhesion always occurs where any two materials touch. Bond strength depends on the nature of the interface contact. Good contact equates to high friction forces and poor contact has low friction force. Variables such as surface roughness, contact pressure, elastic modulus, and material strength affect the interface contact [14]. In HPDC, thermomechanical interference develops between the cooling/shrinking casting and the warming die. The resulting contact pressure increases the strength of the casting/die interface, and this increases the casting ejection force.

HPDC sticking and soldering can both be illustrated as special cases of friction. Sticking occurs when the ejection force is larger than the machine capability. Soldering appears where the ejection shear stress is greater than the casting strength. Since the critical ejection force or shear stress is relative other values, they can be expressed as dimensionless ratios. The force to eject the casting, F_{ej}, is scaled by the force capability of the die casting machine, F_{dcm}, to create a dimensionless ejection force, F_{ej}^*. Local shear stress at ejection, τ_{ej}, is scaled by the local temperature dependent shear strength of the aluminum, τ_{Al}, to create a dimensionless shear stress. This dimensionless ratio is also known as the Tresca friction factor, $Tr = \tau_{ej}/\tau_{Al}$, from hot forming literature [15]. Adhesion in HPDC is reduced by minimizing both dimensionless ratios (Figure 3)

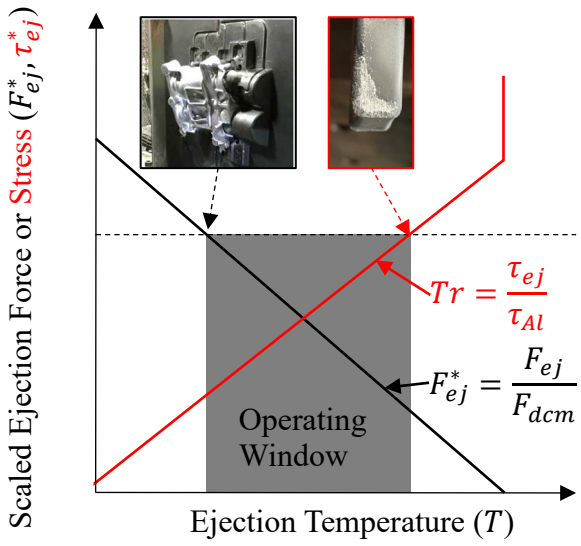

Figure 3: Temperature dependence of the proposed dimensionless ejection force, F_{ej}^* and ejection shear stress, Tr.

Many variables such as the casting design, material choice, and coefficient of friction affect these dimensionless ratios, but they are all linked to temperature (Figure 3). This allows general statements to be made about the behavior of the sticking and

soldering parameters. Sticking will generally increase as the ejection temperature decreases because the ejection force increases with the increasing thermal interference. Soldering decreases with decreasing temperatures because the shear strength of the aluminum increases faster than the local shear stress for ejection (Figure 4).

Modeling these critical ratios requires the application of two friction models, Coulomb and Tresca. The Coulomb model, where the friction force is the product of the normal force, F_n, and the coefficient of friction, μ, is sufficient for most cases (Figure 4). However, high normal forces cause the Coulomb model to no longer apply. This is because the aluminum will fail rather than the casting/die interface. Hot forming of aluminum is such an example and it requires calculation of the Tresca friction factor, Tr [15]. This factor is the ratio of the frictional shear stress to the shear strength of the material. With these two models, Coulomb friction occurs at low ejection temperatures when the aluminum is strong (Figure 4 a) [10], [16]. Soldering occurs at high temperatures when the strength of the aluminum is near zero, and this requires the Tresca approach (Figure 4 b) [17].

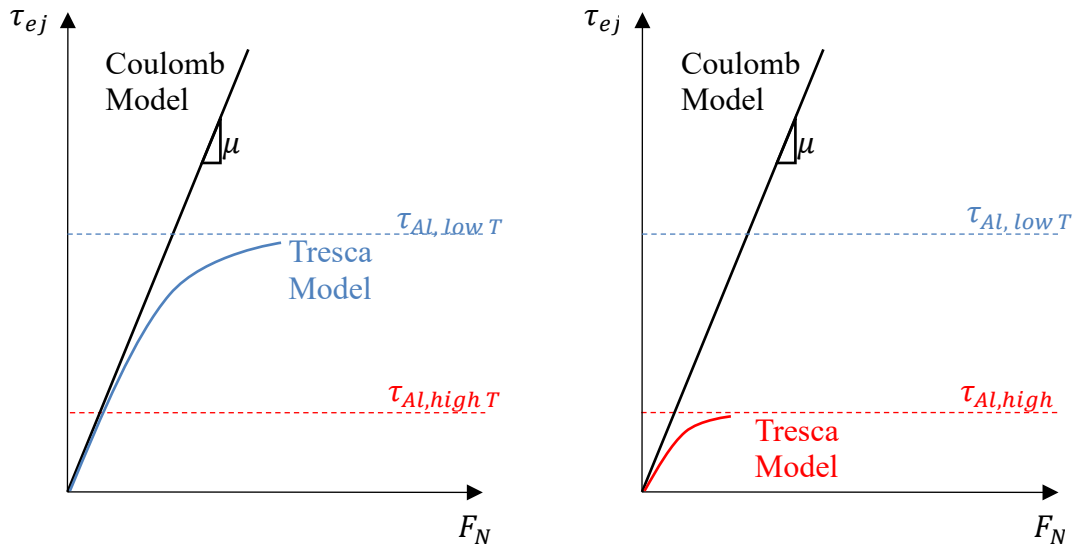

(a) (b)

Figure 4: (a) Conceptual plot of the Coulomb model where the ejection stress is low relative to the part strength at low temperatures, and the part sticks to the die. (b) Conceptual plot at high temperature where all ejection stresses will be large relative to the part strength, and the part fails. Figure adapted from Widerøe and Welo [15].

The friction approach to HPDC adhesion was evaluated in four ways, and these evaluations are presented in separate chapters. First, the literature review shows the accepted adhesion mechanism is a thermodynamically driven reaction between the casting and die. Friction has also received little attention despite being applied in analogous manufacturing processes. Second, predictions based on casting/die reaction

kinetics are demonstrated to be incapable of predicting failures observed in HPDC. Third, an application of the Coulomb friction model shows that ejection force at room temperature behaves as a friction joint. Finally, the Tresca friction model is applied at high temperatures. As predicted, hot ejection tests create soldering in a single cycle, and computer simulations of the Tresca friction factor match industrially observed soldering locations on production tooling. This discovery of the applicability of friction is applied to identify opportunities to optimize the HPDC process to reduce adhesion.

2 Literature Review

2.1 HPDC Soldering:

Soldering is the most studied adhesion failure in HPDC. The consensus is that it is the result of kinetically favorable intermetallic phase formation, and this reaction is the cause of both sticking and soldering adhesion in HPDC [8]. Based on this hypothesis, hot dip aluminizing of steel is the accepted analogous process [18].

Despite the common name, HPDC soldering should not be confused with the multi-material joining technique. It has a similar appearance, but HPDC soldering differs in important ways. Traditional soldering starts with heating the materials to be joined. Then a low melting temperature metal is melted against the hot substrates and flows into the joint driven by capillary forces. Once cooled a joint is created [19]. The strength of the interface is dependent on wetting and mechanical interlocking between the substrate and filler. When wetting is difficult the formation of intermetallic phases can improve the strength. Soldering uses filler materials that melt below 450°C and brazing uses higher melting temperature alloys. Aluminum fillers melt above 450°C meaning that joints between aluminum and steel would technically be considered brazing.

Brazed joints have characteristics that are not found in HPDC. First, the surface temperature of the base material (i.e., the die) must exceed the temperature of the filler metal. Long *et al.* measured the surface temperature of a die during HPDC and the die surface never exceeded the melting temperature of the casting alloy [20], [21]. Second, the filler material should form a strong joint with the base material. Wang *et al.* created an adhesion test by holding a cylinder of liquid aluminum with a steel base for 15 minutes. Joint strengths with bare H13 die steel had a low strength of 0.12 MPa [11]. This strength is over 1000 times lower than the strength of the base aluminum filler materials. Finally, soldering and brazing rely on the filler material flowing into small gaps between the base materials. Capillary forces and excellent wetting enhance the strength of the assembly. Without this small gap, such as in HPDC, the thermal expansion mismatch between aluminum and steel causes the joint to crack during cooling.

Therefore, HPDC solder is unique. It is a rough appearance unlike the smooth wetted surface typical of traditional soldering or brazing (Figure 2a) [22], [23]. There are two stages to failure from HPDC soldering. Initially, there is buildup on the die surface [22], [23]. Overtime this buildup erodes and/or corrodes the die. The rough surface that results in the casting can often be tolerated. Defective castings result when the soldering causes poor surface appearance, leaking, dimensional non-conformance or other customer requirement violations [9], [24], [25].

Solder initiation can occur in less than 10 cycles [22], [23]. Damage after the initiation is slow and may take many thousands of castings to cause failure [26], [27]. The failure rate can be reduce by changing the die material or employing coatings [22], [23]. In the early 1990's, Chu *et al.* proposed that solder initiation and progression was

caused by thermodynamically favorable reactions between the casting and die (Figure 5) [9]. The hypothesis was soldering is a kinetically favorable approach to the thermodynamic equilibrium between the casting and die. Attaining this equilibrium requires dissolution of the steel and formation of intermetallic phases. It is believed these phases are responsible for the adhesion. The rough surface occurs due to spalling of some weaker phases and dissolution of the iron into the aluminum, and it causes mechanical interlocking with the aluminum casting which ultimately breaks the die component [9], [22]–[24], [26], [28]–[33]. This reasoning motivates the historic focus on the thermodynamics and kinetics of aluminum interacting with steel to reduce HPDC adhesion.

2.1.1 History and overview of soldering:

Soldering has always been a problem that reduces the efficiency of a die casting machine, and it is accepted that sticking has already been resolved otherwise serial production of castings would not be possible. Stern discussed this defect during a presentation on the progress of HPDC in 1930 [34]. A member of the conference presentation asked whether the silicon content affects the soldering tendency of the alloy. This is the earliest mention of soldering in the American Foundry Society's transactions, a mere 16 years after the invention of the aluminum HPDC process. Solder was discussed again near the end of World War II and in the early 1950's while new HPDC alloys were under development [35]–[38]. These early references discussed soldering qualitatively. Quantitative measurements of soldering occurred much later.

Early references established cast alloy composition as an important variable that affects soldering progression [10], [35]–[37], [39]–[41]. Colwell and Tichy said iron and manganese exceeding 1 and 0.4 weight percent, respectively, helps to reduce soldering , but no data was presented to support this claim [36]. Holz echoed this claim without supporting evidence [40]. These authors appear to be reflecting an the consensus of industrial observations in 1964 that elevated iron in the alloy reduced soldering [42].

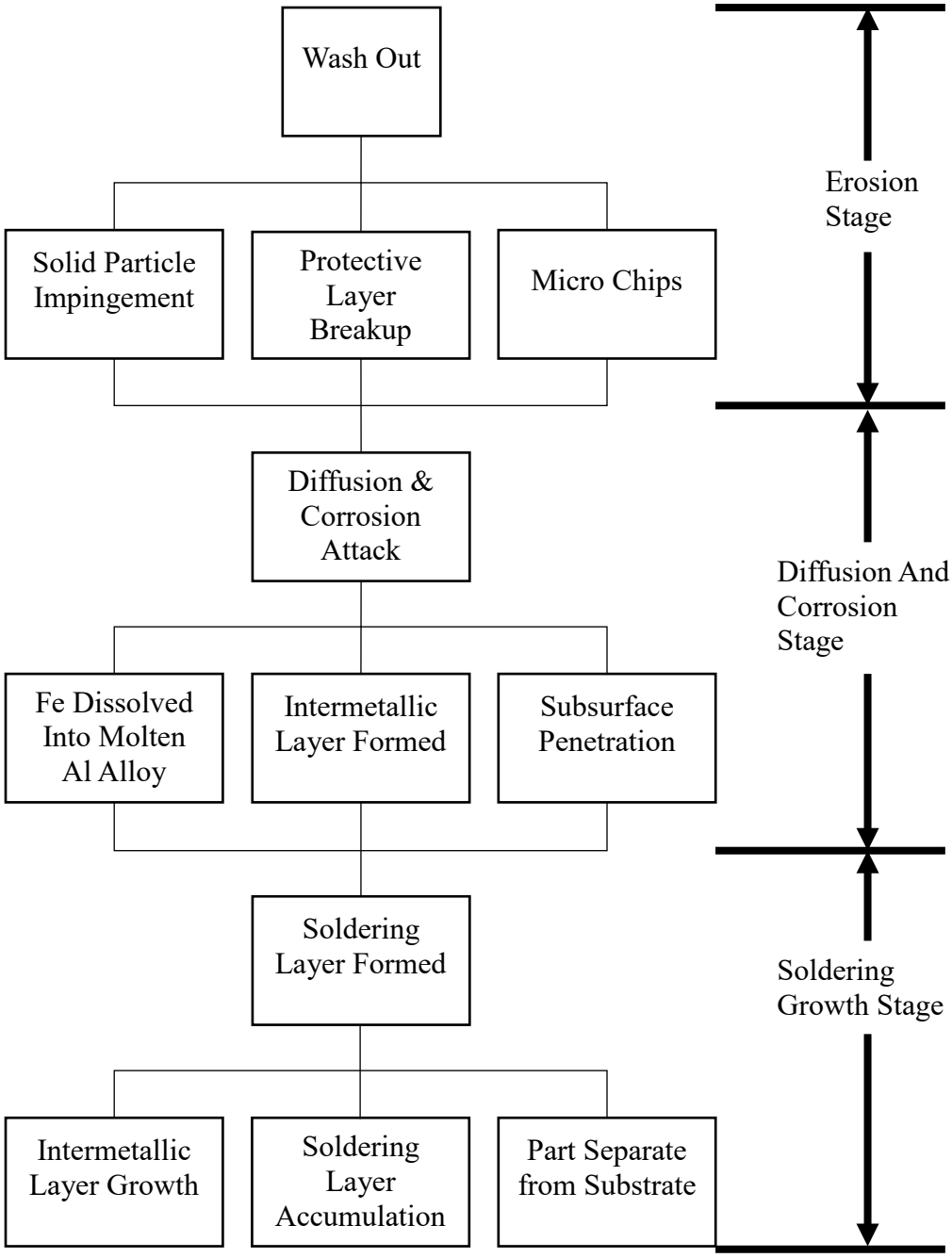

Figure 5: Stages of soldering as proposed by Chu et al. in 1993 [9].

Other authors performed quantitative measurements based on the alloy composition. Tosa and Urakami showed ejection force reduced with increasing iron content, but the effect was small and not clearly related to soldering [10]. Kojach and Fajkiel proposed that soldering was like friction welding. They performed ball in ring friction tests where a steel ball was rotated in a conical shaped seat on a ring of aluminum. The normal load on the ball was increased until the steel and aluminum adhered to each other. They found that the joining load increased with increasing iron content, but a mechanism was not proposed [41]. Occasionally processing conditions were offered as a stronger variable affecting soldering, but this is the exception, not the rule [35], [39].

The scarcity of quantitative measurements of soldering during HPDC production reflect the difficulty to obtain them. HPDC is capital intense and adapted for high production rates making it hard to replicate in a lab environment. When HPDC machines are available for research, test conditions and times are designed to minimize costs. This is clear from the few test dies which were designed to create severe soldering conditions in order to reduce study costs [22]–[24]. Chu *et al.* created a die which caused the injected metal to impinge directly on a series of core pins to cause rapid erosion [43]. Chen in 2005 as well as Zhu *et al.* in 2008 performed similar tests with a single core pin [22], [23]. Wang *et al.* coated a full die cavity and implemented it within a production HPDC facility [8]. Beyond these examples industrial trials to failure are common, but rarely replicated to achieve statistical confidence [33], [44]. Due to their specialized design or application, the results of these studies cannot be generalized for all HPDC conditions.

2.1.2 Industrial Experiments:

The few industrial trials have been combined with many industrial observations to provide an approximate understanding conditions that cause HPDC soldering. Die temperature, initial casting metal temperature, injection velocity, die lubricant composition, casting alloy, and die material have been identified as key variables [9], [10], [33], [40], [41]. They all have multiple effects on the process conditions, but primarily they affect the casting/die interface temperature. Assuming kinetically driven reactions to form intermetallic phases [29], increasing the temperature would increase the rate of reaction [45]. Prevention of contact would also prevent reaction rationalizing the effect of lubricant composition and the potential effect of high injection velocity, "washing" the lubricant away. Replacement of the die material with a less reactive alloy would also reduce the reaction rate [29].

Barnhurst *et al.* investigated the effect of die temperature and draft angle on soldering in zinc HPDC experiments [46]. Higher die temperatures resulted in increased soldering like aluminum. This is notable because zinc does not dissolve steel like aluminum. In addition, the authors show that increasing the draft angle from zero degrees to one degree reduced the soldering by nearly 50%. A strong interaction between die temperature and draft angle was also found where soldering is reduced at low draft angles when the die temperature is lower.

Chen designed a die casting die that caused soldering to occur within a few casting cycles. Soldering was observed within 4 casting cycles. The soldered core pin was removed and examined for intermetallic phases, and none were found. Phases began forming on the core if it was cycled 15 times [22]. Zhu *et al.* performed similar tests on a vertical squeeze casting machine [23]. Different die materials and preparations were examined. Soldering was quantified by dissolving it with NaOH and measuring the weight loss of the core pins. The authors did not perform metallography in search of intermetallic phases.

2.1.3 Laboratory Experiments:

Due to the challenges of *in situ* testing, many studies have been performed with laboratory analogs to test soldering hypotheses. Diffusion couples where die materials are either dipped into a bath of molten aluminum or placed at the bottom of a small crucible of molten aluminum have been considered the primary analog for HPDC soldering [11], [23], [24], [27]–[29], [31], [32], [45], [47], [48]. Occasionally, diffusion couple experiments are supplemented by sessile drop tests to measure wettability [24].

Shankar and Apelian performed diffusion coupling experiments and found that small cast alloy compositional changes could affect the intermetallic growth rate [49]. Chu *et al.* performed similar experiments and also found a dependence of steel dissolution rate on the alloy composition [9]. Zhu *et al.* investigated the effect of die material composition and found that refractory metals react slower than iron based tool steels [23]. Wang *et al.* investigated the effect of coatings on the die steel and found that many ceramic coating systems prevent interaction between the casting and die [11].

Die steel surface conditions have also been extensively studied [26]. Duarte *et al.* found that nitriding and oxidizing the surface reduced the erosion/corrosion rate of die steel dipped in molten aluminum [48]. Cathodic Arc Emission (CAE) and Physical Vapor Deposition (PVD) coatings have been identified as an alternative to refractory die materials [26]. These coatings attempt to create a non-wetting and non-reactive layer between the casting and die to prevent soldering. Early tests confirmed that vanadium carbide and titanium nitride are non-wetting, non-reactive, and they have a lower the coefficient of friction compared to nitriding the die material [24]. Soldering failures were delayed by these coatings in dedicated HPDC soldering test dies [25], [30].

Wang *et al.* performed extensive testing of CAE and PVD coatings with a novel adhesion test. In this test the liquid aluminum was held in contact with uncoated and coated steel surfaces for over 15 minutes and allowed to cool to room temperature. Uncoated steel would develop a bond with the solidified aluminum, and the force to remove the aluminum was measured. Six of the twelve candidate coatings had no bond, or a negligible bond strength compared to a bare H13 steel baseline. Intermetallic formation and adhesion were eliminated with the use of permanent die coatings in a laboratory adhesion test [8], [11]. Two of these coatings were tested in full scale die casting production with partial success. The die continued to run at Mercury Marine, and soldering has continued to form during its 100,000+ casting cycle lifetime (Figure 6).

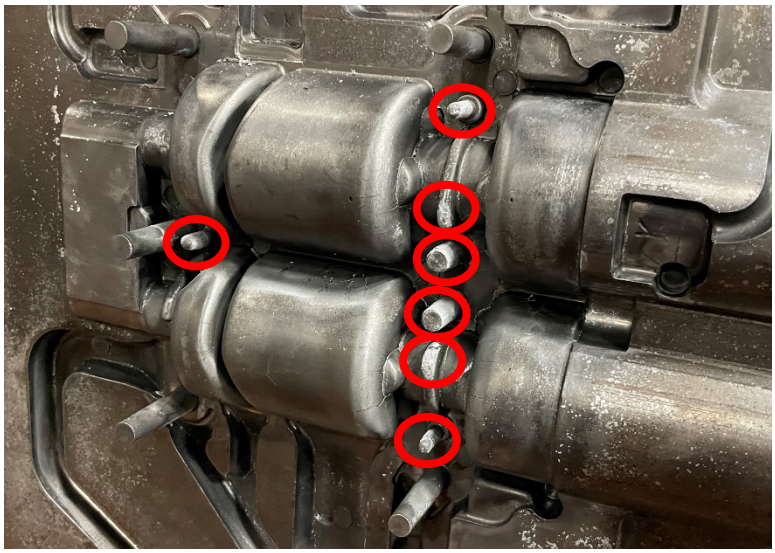

Figure 6: Soldering that occurs on a die that has a non-reactive coating identified by Wang *et al.* [8]. Lubricant spray was reduced, but the soldering (red circles) and sticking still occur (Image courtesy of Mercury Marine).

Han and Viswathanan proposed a critical soldering temperature to be the solidus temperature of the alloy at the casting/die interface [28]. To test temperatures below solidus a sample of steel was dipped into molten aluminum and removed to create a thin layer of aluminum on the pin. The sample was then placed into a furnace at the desired test temperature for test time. Air gaps formed between the aluminum and steel for experiments below the solidus temperature. This gap would prevent intermetallic formation. Therefore, the conclusion that a critical soldering temperature exists reflects the test design and not a fundamental material property.

Die wear during ejection has also been studied but less often than diffusion couples. Vilaseca *et al.* used pin on disk wear tests to optimize die composition and hardness to reduce the wear rate during dry sliding [50]. Terek *et al.* poured aluminum around a core pins with various wear resistant coatings and roughness. The pins were removed at room temperature and the force was recorded. They found no dependence of ejection force on the coating composition [51]. Kajoch and Fajkiel also noted black oxidized steel resisted soldering in their friction welding based testing [41].

2.2 Sticking Relationship with HPDC Soldering:

Sticking is considered a more severe form of soldering [11]. There are some unique differences between soldering and sticking. Soldering leaves a rough layer of aluminum on the surface of the die. Sticking prevents the removal of the casting from the die. Soldering is repaired by mechanical abrasion to remove the adhered materials. Sticking is overcome by reheating the stuck casting, lubricating the interface, and increasing the ejection force [52]. Once the stuck casting is removed, the surface of the

die is clean with little or no evidence of aluminum adhered to the steel surface [8]. These differences suggest that sticking is more closely related to the available ejection force.

Wang *et al.* proposed that the sticking is a widespread and undetectable form of soldering. The hypothesis is that the same soldering intermetallic phases are present at a much finer scale in sticking. The authors developed a severe solder test and identified coatings that were non-reactive and non-sticking on the flat die interface tested [11]. This test has been replicated by others and similar adhesion performance was found based on the coating composition [53]. The hypothesis was tested by applying the non-sticking coatings to a full HPDC die. Sticking and soldering still occurred (Figure 2a and Figure 6) [8].

Stuck castings at least partially result from thermomechanical interference between the casting and die. Tosa and Urakami measured ejection force as a function of cooling time in 1972. Wang and Loong did a similar test in 1999. Both teams found that ejection force increased with longer cooling time [10], [16]. These findings make sense as the mechanical interference increases as the casting cools and contracts. The normal force on the die/casting interface creates a friction force that increases with increasing interference. However, all these papers presented their research from the perspective that reactions occur at the casting/die interface causing friction.

Terek *et al.* also recognized the potential for frictional wear to cause soldering and examined the effects of coating, surface finish, and casting condition on the ejection of the casting [51]. They found that surface roughness was a strong indicator of ejection force. Coatings were not found to alleviate the observed soldering. In later work, Terek *et al.* looked at the effect of filling and solidification path on the soldering when cores were ejected at room temperature [54]. Ejection forces was highest when the core was at the bottom of the mold and metal was poured over the top of it. This is opposed to dipping the pin into a solidifying casting or hanging the pin over an open top casting mold. The authors suggest that the different ejection behavior is due to potentially different oxides between the casting and core. They do not discuss the possibility that the casting contraction is radically different near the top (riser pipe formation) and bottom (well fed and chilled) of the mold. In addition, neither paper investigated whether the soldered aluminum had formed intermetallic phases. Instead, it was simply observed that aluminum remained on the core pins after ejection [51], [54].

Researchers in Australia have also shown aluminum adheres to the die before intermetallic phases form [22], [25], [55]. Chen most clearly showed this by interrupting the die casting process as soon as soldering was observed and found no intermetallic phases present at the interface. These phases only formed after subsequent castings were made on the stuck aluminum. Similar soldering occurred on cores coated with vanadium carbide, but additional cycles could not produce intermetallic phases [22].

Aoyama *et al.* created a novel die for measuring the friction between the casting and die when a die casting was produced. A disc of aluminum equivalent to the diameter of the plunger was cast onto the moving half of the die. After solidification, the die was

opened a few millimeters while the plunger maintained a known normal force on the disc. The moving half cavity was then pulled vertically sliding perpendicular to the normal load from the plunger force [4]. The authors found that the friction coefficient was reduced when lubricants were applied. It was also found that the un-lubricated coefficient of friction dropped with an increasing cooling time prior to ejection. This is similar behavior to that observed in elevated temperature friction tests where cooler temperatures result in lower friction coefficients [56].

Kimura *et al.* measured the ejection force reduction when replacing water/wax emulsion lubricants with water free lubricants. Ejection force decreased and die temperature increased with the water free lubricants. From the data presented it is not clear whether the ejection force reduction is from lower friction, or increased ejection temperature relaxing the thermal contact pressure. Also, heat transfer was noted to be reduced improving the filling of the die [57]. Nishi made a similar observation in zinc die casting [58].

2.3 Models of Casting Adhesion in HPDC

Domkin *et al.* developed a model for soldering based on the intermetallic growth theory [13]. Soldering strength was proposed to relate to the predicted thickness of the intermetallic layer. An example casting was simulated, and the soldering strength was strongest at inside corners of the casting where the highest temperatures were predicted. Five modeled cases were presented with the hottest die temperature predicted as having the most severe soldering. The most severe soldering case was predicted to produce a 25 μm thick intermetallic layer after 10,000 casting cycles. Experiments were not presented to validate the model.

Kim *et al.* extended the intermetallic growth rate model by including the effect of mold erosion. Sticking is accepted to be the result of the soldering reaction, but it was observed that the location of soldering is often over-predicted by a thermodynamics-based model. An attempt to correct this was proposed by including mold erosion and scaling with a correction parameter, alpha [12] (eq. 1). When alpha approaches 1 the soldering parameter is purely due to intermetallic growth and if alpha is zero then only mold erosion is accounted for. This brute force approach does improve the soldering prediction, but there is not a good first principles argument for why mold erosion could increase soldering at the expense of intermetallic growth. Commercial solidification codes have similar rules based soldering intensity calculations without rigorous physical principles support [59].

$$S = alpha * Intermetallic\ Growth + (1 - alpha) * Mold\ Erosion \qquad \text{(eq. 1)}$$

2.4 Wear Relationship to HPDC Soldering and Sticking

The observations of galling from Terek *et al.* coupled with the inconsistencies of the kinetics driven theory models for soldering suggests that friction analogies could be useful to understand adhesion in HPDC. Plastic injection molding is analogous to die casting without the potential for reaction between the part and mold. Frictional wear

between aluminum and steel would also be a useful analogy because ejection of the casting requires sliding of aluminum against steel. Finally, hot forming of aluminum by extrusion, stamping, plastic forming, and other methods are other analogies of HPDC.

2.4.1 Plastic Injection Molding Analogy

Thermo-mechanical interference models have been applied to prediction of sticking and die life in plastic injection molding. Cedorge and Colton investigated the ejection force required to separate an injection molded plastic part from a 3D printed mold [60]. They proposed that the ejection force follows a simple Coulomb friction model. A free body diagram was used to derive an expression that predicts ejection force as a function of draft angle. Interestingly, this model predicts the observed reduction in ejection force with increasing draft in HPDC of zinc alloys [46]. Colton continued this work with Palmer and Pham including experimental studies and Finite Element Analysis (FEA) to match experiments [61], [62]. Good agreement was found using the model. Bataineh and Klamecki predicted the ejection force of a real injection molded component using FEA. Their results correlated well with experiment measurements [63].

Sasaki *et al.* experimented with the ejection force of plastic injection molded components due to the roughness of the die surface, die coating, and the injection pressure. Three polymers, polypropylene, methacrylate resin, and polyethylene terephthalate were tested. Ejection force was reduced as the roughness was reduced from 0.7 to 0.2 μm Ra. Smoother surfaces (<0.2 μm Ra) increased ejection force. Coatings were also found to be effective at reducing ejection force [64].

Sorgato *et al.* machined micro injection molding cores using both EDM and milling. The effect of machining method and process parameters were observed. Higher mold temperatures, injection velocity, and packing pressure created increased ejection force. The machining methods created similar roughness, but they interacted with the injection temperature and pressure. This means the surface topography interaction with the process is complex [65]. Ejection temperature was not measured, and it would have been a good parameter to measure based on the increasing thermal interference with decreasing ejection temperature predictions from Cedorge and Colton [60].

Encouraged by the injection molding models, Monroe *et al.* performed preliminary simulations of HPDC sticking assuming a friction model [66]. In the simulations, the contact stress was calculated by considering the casting shrink and the die expansion. It was proposed that the ejection force could be predicted by multiplying the contact pressure by the contact area and a friction factor. In other words, the Coulomb model of friction was applicable in predicting ejection force. A full factorial experiment was simulated showing the ejection temperature was the strongest variable to determine sticking.

2.4.2 Melt Spinning Analogy

Altieri and Steen investigated the sticking distance of aluminum to a copper wheel in the melt spin casting process [67]. A model was developed based on the thermal stress

buildup in the ribbon. It was shown that these stresses overcome the adhesion between the aluminum and the roll to cause detachment. The thermomechanical model had good agreement with experimental results. It also predicted that sticking increases as the roll temperature increases.

2.4.3 Hot Forming Analogy

Hanna investigated the galling behavior of aluminum and magnesium at temperatures up to 450°C in a novel galling test [68]. Incipient galling was detected by applying a voltage difference between the aluminum and steel. This difference dropped to zero when galling occurred. It was found that the sliding distance required to gall decreased with increasing temperature. The coefficient of friction also increased with higher test temperatures. The normal load was 100 N for an undefined sample size.

Jerina and Kalin measured the transfer of aluminum to H13 tool steel in a single pass dry sliding wear experiment at various temperatures from 20°C to 500°C [56]. Material transferred from the aluminum to the steel within 2 mm of sliding distance for all temperatures. However, the severity of the transfer was dependent on test temperature. The calculated Hertzian contact pressure was 600 MPa which is much higher than the strength of the aluminum. At both 400°C and 500°C transfer of aluminum to the H13 was observed without any sliding. Increasing the sliding distance increased the volume and surface area of the transferred material. In a similar experiment Kitano *et al.* evaluated a model to predict the material transfer [69]. The model was dependent on material properties, sliding distance, pressure, and temperature. It was effective for short sliding distances.

Local sticking of aluminum to the workpiece occurs frequently in hot forming [70]. This is particularly true in extrusion [71]. Ma *et al.* provided a comprehensive model of the friction in the extrusion die [72]. In follow up work, the authors matched the model of sticking and sliding friction with a combination of the Coulomb and Tresca friction models [73]. Wang and Yang used a similar friction model to accurately predict the ram pressure required for an extrusion under different processing conditions [71], [74]. Sticking friction is the term used to describe the aluminum sticking to the extrusion die surface.

Coulomb friction is the widely known friction model where friction force, F_f, is proportional to the normal load, F_N (eq. 2). The proportionality constant, μ, is known as the coefficient of friction. This model recognizes that the contacting surfaces observed at the macro scale do not match the actual contact area. Instead, the contacting surfaces are rough, and they touch via Hertzian contact at disparate locations. Increasing the normal load increases the actual contact area. Tabor provided an excellent review of this model in 1981 [14].

$$F_f = \mu F_N \qquad \text{(eq. 2)}$$

At high normal loads, the Coulomb friction model no longer applies. This is because the friction force approaches the shear strength of the weaker contacting material. The Tresca friction model (eq. 3) does consider this strength, and it is appropriate when sticking friction can occur. In this model the friction force is expressed as a frictional shear stress, τ_{ej}, and it is the product of the Tresca friction factor, Tr, and the shear strength of the aluminum, τ_{Al} [73]. This friction model is called the Tresca model because it assumes the Tresca failure condition. The more familiar ultimate tensile strength is related to shear strength of the cubed root of three ($UTS = \sqrt{3}\tau_{Al}$) [75].

$$\tau_{ej} = \tau_{Al} Tr \quad \text{(eq. 3)}$$

Predicting the local frictional shear stress is often simply the Coulomb model, and the Tresca factor simply determines if this Coulomb friction is high enough to cause failure of the casting. This approach replaces the ejection shear stress with the product of the contact pressure and a coefficient of friction (Figure 4). Widerøe and Welo described this approach in relation to hot compression and twist testing of 6061 aluminum. They were searching for the value of the Tresca friction factor where sticking occurred. It was discovered that sticking occurred when the factor was 0.6 for temperatures above 300°C. Lower temperatures were not investigated thoroughly, but the critical factor increased to 0.7 at 250°C.

2.5 Literature Summary

HPDC soldering is not the same as the multi-material joining technique called brazing or soldering. This is clear from the literature. Soldering is the most studied adhesion defect in HPDC. It has been accepted that the causal mechanism is the formation and growth of intermetallic phases on the die surface. Sticking is considered an extreme form of soldering where the adhesion of the casting to the die exceeds the strength of the ejection system. Minimizing phase formation and growth with die coatings has had limited success in preventing adhesion defects. Friction models of adhesion appear to be promising to identify the adhesion mechanism. Therefore, a friction model of soldering and sticking was developed.

3 Summary of Research Approach

As previously stated, *in situ* testing of HPDC is difficult. This work is focused on making novel predictions of the common adhesion defects in HPDC, sticking and soldering. Prediction requires that the bulk of the work be modeling. One-dimensional modeling was completed by deriving relationships and implementing them in Excel, or solving numerically in Matlab [76]. Thermophysical and thermomechanical properties of the casting alloy are critical for the modeling. Thermocalc was combined with literature review to obtain these properties [77]. Experiments were developed to test hypotheses based on the one-dimensional model predictions. Finally, 3D computer simulations were performed with the casting simulation software MAGMASOFT [59].

Both models and experiments were primarily focused on a cylindrical die (core) in a tubular shaped casting. Axial symmetry allows the solidification, cooling, and thermal interferences to all be modeled in one dimension (Figure 7). Close formed solutions exist for the stress/strain state in the tube casting. Experiments are also simple to produce and evaluate.

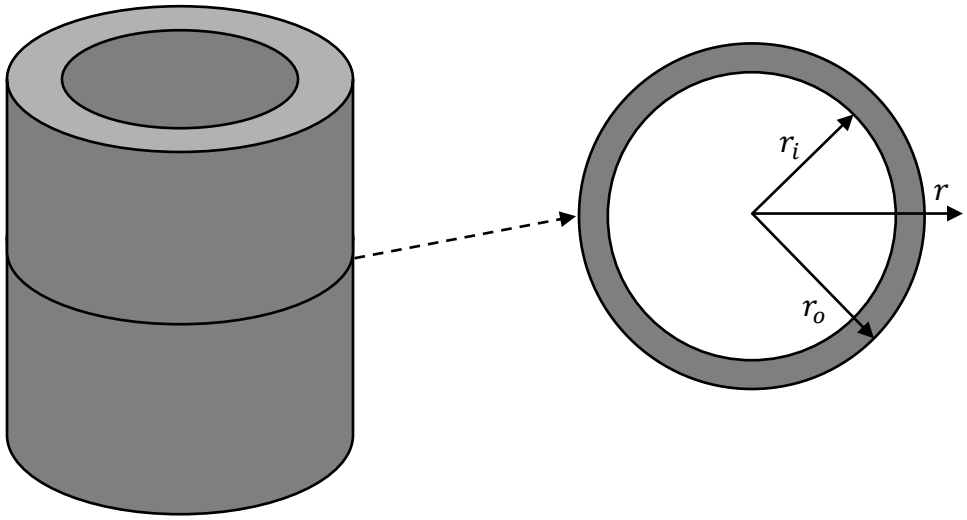

Figure 7: Conceptual casting for developing a thermomechanical theory of soldering and sticking. Radii smaller than r_i are the die steel core, and radii greater than r_o are the die steel mold.

Four facets of adhesion in HPDC were investigated in detail to support the proposed friction mechanism. First, the predictions of the thermodynamics and kinetics theory of soldering is evaluated. Second, the Coulomb friction model is applied to casting ejection. Third, Tresca friction factor calculations are applied to HPDC soldering. Finally, the Coulomb and Tresca model are combined to find optimum alloy and process design parameters to minimize adhesion in HPDC.

Three non-trivial hypotheses were generated and tested to support the four facets of HPDC adhesion. They are:

- If soldering is the result of kinetically driven phase formation, then laboratory diffusion couple experiments should match industrial observations.
- If the draft angle is increased, then the ejection force should be reduced by an amount greater than the reduced contact area. This is because friction models predict a force component in the ejection direction.
- If the ejection temperature is increased, then soldering will occur because the alloy is not strong enough to overcome the friction force.

4 Thermodynamics and Kinetics of HPDC Soldering

The assumption in the HPDC literature is that all forms of adhesion are caused by the reaction of the casting material with the die material. Erosion from dissolution of the iron may cause undercuts; intermetallic phases readily form between aluminum and iron. While some Kirkendall porosity forms at the reacted interface, the interface is still bonded [78]. Together, the erosion and corrosion of the die face are believed to cause adhesion, in this case HPDC soldering (Figure 8). Thicker intermetallic layers and deeper undercuts are believed to cause increasing ejection forces [12], [43], [55]. In this way, HPDC sticking has been hypothesized to be the result of these reactions [8], [11].

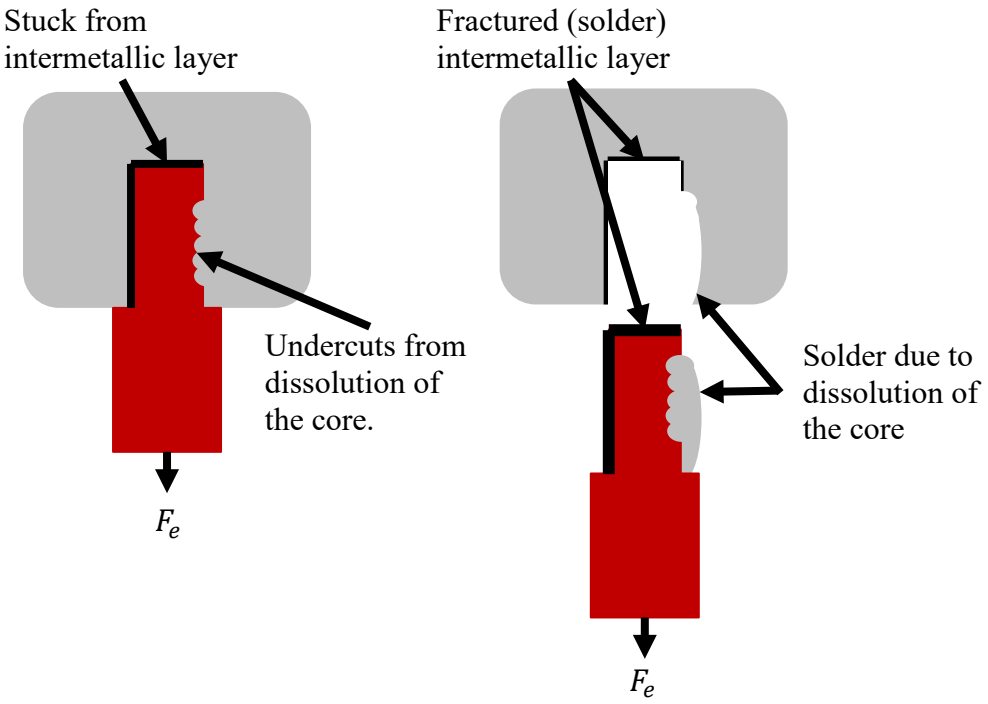

Figure 8: Schematic of the common thermodynamics and kinetics-based theory of soldering and sticking.

4.1 Hypothesis

It is true that failed die components often exhibit reaction between the casting and die [18], [43]. These components appear like laboratory prepared diffusion couple specimens. However, the existence of similar phases does not require that they be the cause of HPDC soldering. To evaluate the causal link between thermodynamically driven phase formation and soldering, a simple hypothesis was generated. If soldering is the result of intermetallic phase formation, then laboratory diffusion couple experiments should mimic industrial observations.

A detailed analysis of the literature data invalidates this hypothesis because the laboratory results do not match industrial observations in three ways. First, the measured

reaction rates are too slow. Second, the effect of alloy composition is not consistent. Finally, the intermetallic layer is brittle and weakens the bonded joint.

4.2 Intermetallic Reaction Rate

In aluminum-iron diffusion couples, the total thickness of the intermetallic layers, x, grows proportional to the square root of the exposure time. This follows Fick's law for one-dimensional diffusion (eq. 4). The diffusion constant depends on temperature, T, following an Arrhenius relationship with an activation energy, Q, a pre-exponential constant, k_o, and the ideal gas constant, R [79].

$$x = k_0 \, exp\left(-\frac{Q}{RT}\right)\sqrt{t} \qquad \text{(eq. 4)}$$

Springer *et al.* investigated the activation energy and growth rate of these intermetallic phases between pure aluminum and steel above and below the solidus temperature of aluminum [79]. The authors found, through their experiments and by citing others, that the activation energy is approximately 190 kJ/mol. This constant adequately fits the data above and below the solidus temperature. In other work, Jindal *et al.* and Springer *et al.* friction stir welded and roll bonded joints between aluminum and steel. They annealed these joints at various temperatures and found that the activation energy was also 190 kJ/mol for these solid-solid diffusion couples [78], [80] (Figure 9). This suggests that deviations other authors have observed between solid-solid diffusion couples relative to liquid-solid is due to imperfections in the contact of solid-solid diffusion couples.

Using eq. 4, the time required to form 0.1 mm of intermetallic phases was calculated using the activation energy proposed by Springer *et al*. This critical thickness was chosen because soldering buildup exceeding this thickness is known to occur within a few casting cycles (Figure 9) [23], [81]. Terek *et al.* observed aluminum exceeding 0.1 mm thick stuck to a core in one casting cycle [51]. Die castings rarely contact the die steel for longer than 20 seconds. Measurements have shown that the maximum die temperature stays below the liquidus temperature at all times [82]. If the die surface were the liquidus temperature of pure aluminum, 660°C, it would take 250 seconds (more than 12 cycles) to produce 0.1 mm of soldering. Intermetallic phases cannot grow fast enough to be the cause of buildup within only a few cycles. This suggests that some mechanism causes the initial buildup of aluminum. After additional time, the intermetallic phases will start to grow [22].

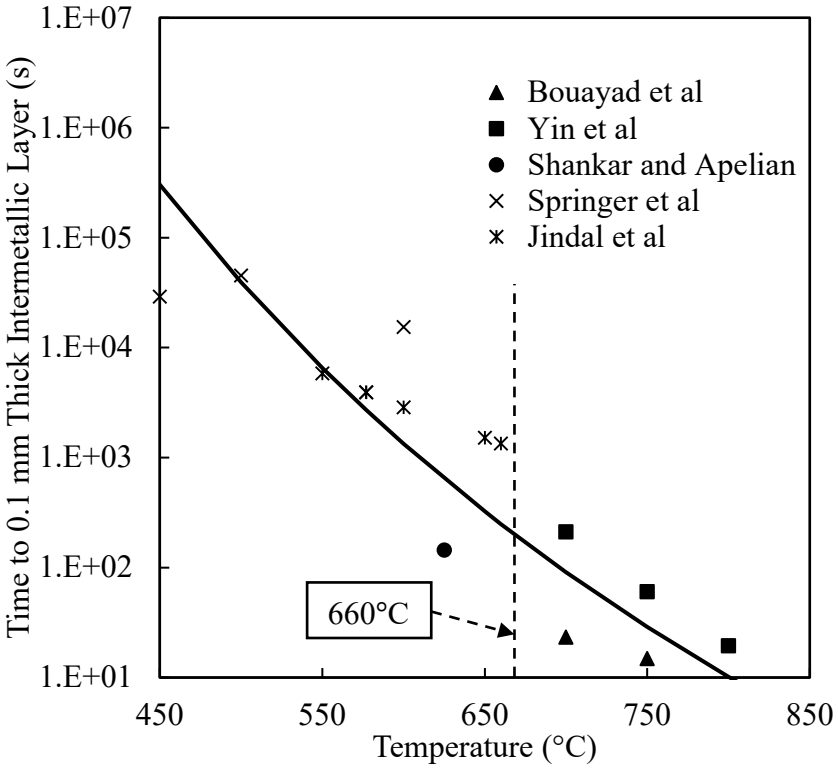

Figure 9: The predicted time to grow a 0.1 mm thick intermetallic layer [18], [79], [80], [83], [84]. A single activation energy of 190 kJ/mol provides reasonable agreement with measured reaction rates both above and below the melting temperature of 660°C

4.3 Effect of Alloy Composition

Die-casting experiments and observations suggest iron additions reduce ejection forces and soldering [10], [41]. When iron is dipped into pure aluminum it will initially dissolve, and once the aluminum is saturated intermetallic phases will form on the aluminum/iron interface (Figure 10a). The net effect is slow erosion of the iron and expansion of the solid intermetallic phases into the liquid aluminum. Often these two effects are combined into one overall growth from the original interface. If HPDC soldering is a kinetically controlled reaction, and adding iron reduces the occurrence of HPDC soldering, then the intermetallic growth rate should decrease with increasing iron content. This has been tested, and the opposite is true where iron saturated aluminum grows the intermetallic layer faster (Figure 10b). The faster growth rate makes sense because iron has to be dissolved to saturate the liquid aluminum prior to growing the intermetallic phases [85]. Similarly, manganese and silicon have been observed to reduce soldering, but they also increase the growth rate of intermetallic layers in diffusion couples [86], [87]. Thus, the best known HPDC solder reducing alloy elements increase the growth rate of the intermetallic layer; this contradicts the accepted kinetically controlled reaction theory.

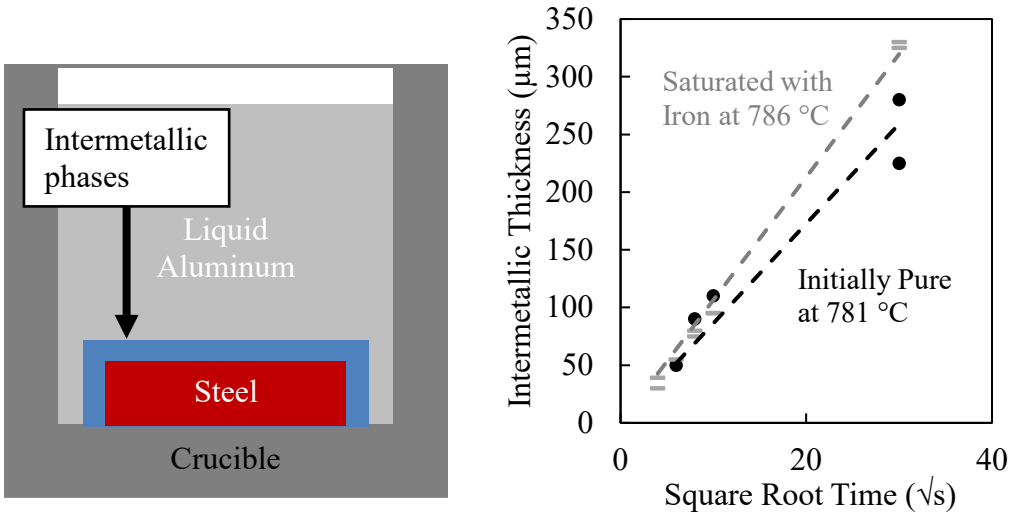

(a) (b)

Figure 10: (a) Illustration of a typical aluminum iron diffusion couple [18]. (b) One dimensional intermetallic growth rate when the liquid is either initially pure or saturated with iron [85].

Dissolution also occurs in a diffusion couple. As steel dissolves into the liquid aluminum, the rate of dissolution could be a predictor of the HPDC soldering tendency. Previous work has shown that both pure aluminum and structural casting alloys, which have low iron content, dissolve steel at a slower rate than common commercial die-casting alloys (Figure 11) [9], [43], [88], [89]. This is the opposite trend observed in die casting process where pure aluminum and the low iron structural alloys erode and solder the die much faster than the conventional secondary alloys that have high iron contents. Dissolution rate is also a poor predictor of HPDC soldering tendency.

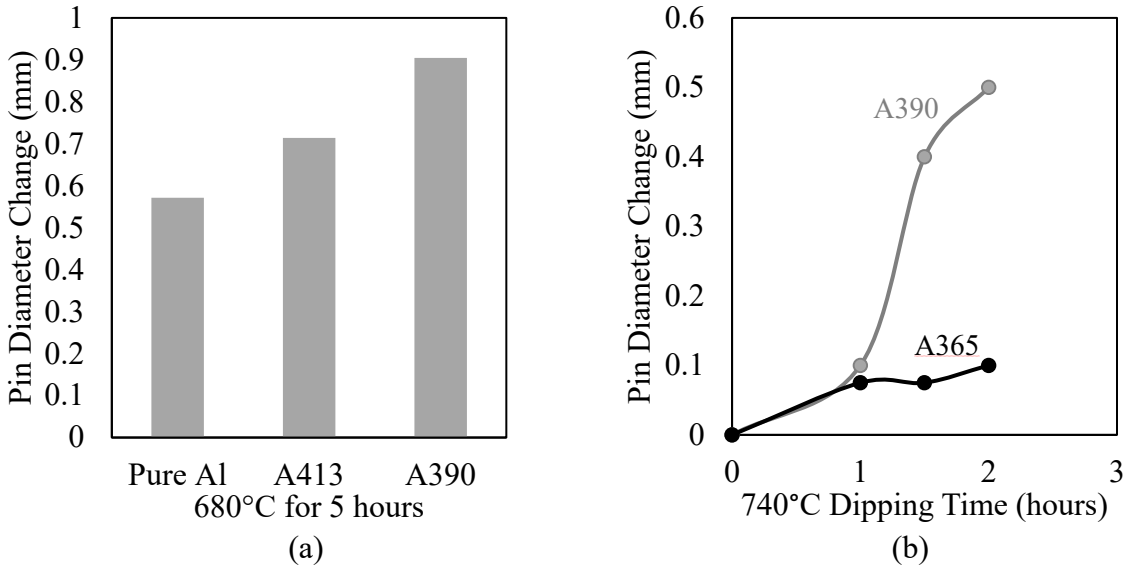

Figure 11: (a) Static steel cylinder (12.7 mm diameter) dip tests in various aluminum alloys showed that pure aluminum dissolves steel more slowly than commercial casting alloys [89]. (b) Static steel cylinder (12.7 mm diameter) dip tests showed that the structural alloy Silafont 36 (A365) dissolves steel slower than the more common A390 diecasting alloy [88].

4.4 Strength of Intermetallic Bonding

Implicit in the study of intermetallic growth as the cause of HPDC soldering is the idea that a metallic bond is required for the buildup to occur. These phases are assumed to be a required transition layer for the buildup to occur. Examining the strength of joints between aluminum and steel can test this hypothesis, and the result is that multi-material bonding studies show intermetallic phases reduce the interface strength rather than enhance it.

Roll bonding and friction stir welding create a joint between aluminum and steel without forming a detectable intermetallic layer [78], [80], [90]–[92]. There are three locations that the joint can fail; fracture can occur in the steel, the aluminum, or at the interface. Fracture will occur at the joint (Figure 12a) when the two metals have poor contact implying limited metallic bonding; otherwise, the aluminum side of the joint is likely to fracture for well bonded interfaces due to its lower strength compared to steel (Figure 12b). Annealing these joints at temperatures above 450°C causes an intermetallic layer to form and grow. Once grown, the fracture occurs within the intermetallic layer (Figure 12c), with a reduced joint strength [78], [80], [90]–[92]. In contrast, failed die cast components exhibit an unusual behavior where an intermetallic layer exists on the die surface but fracture occurs in the aluminum casting (Figure 12d) [29].

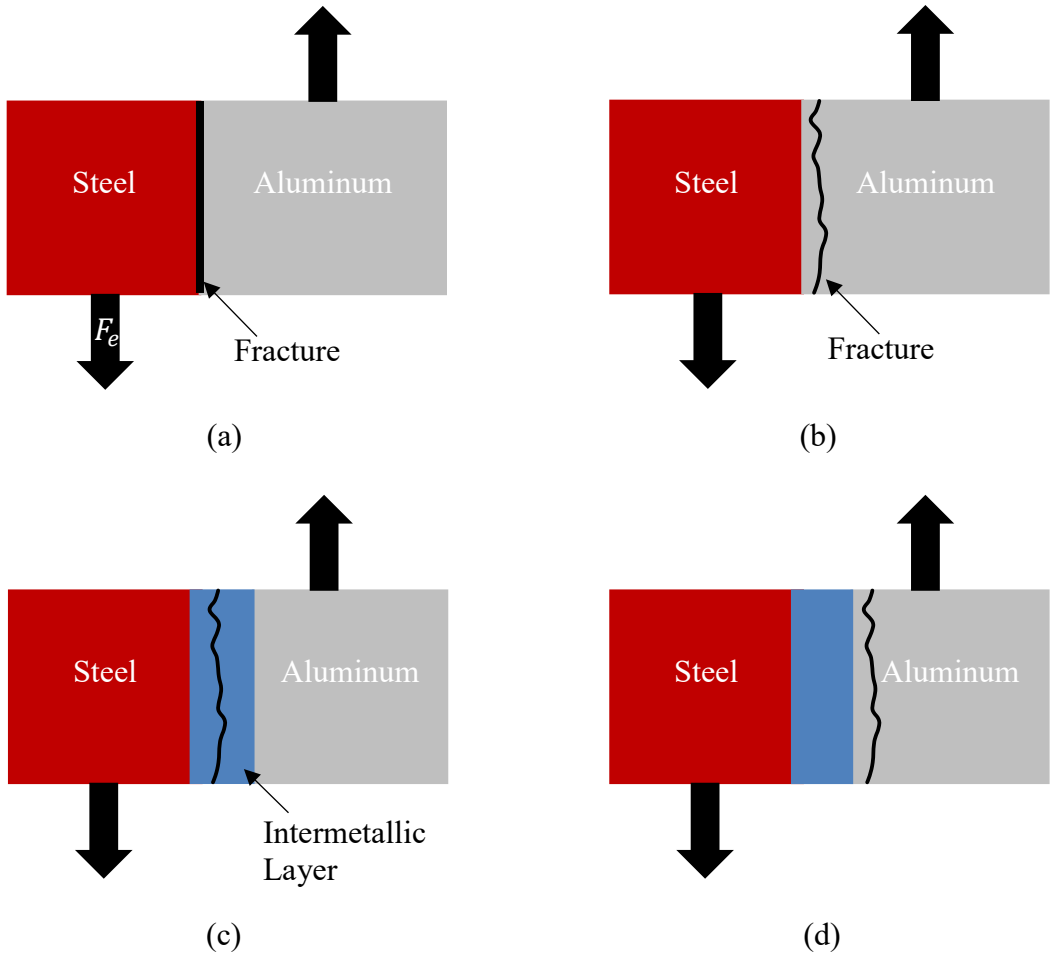

Figure 12: Illustration of joints between steel and aluminum under the shear of the ejection force, F_e without (a,b) and with an intermetallic layer (c,d). When the bond strength is low a clean separation at the aluminum/steel interface is normally observed (a) Casting failure may occur due to the low strength of aluminum at elevated temperature. (b). Roll bonded, brazed, and friction stir welded joints typically fracture within the intermetallic layer when it is present (c), while HPDC conditions often contain an intermetallic layer with the fracture in die casting (d).

4.5 Summary of the Thermodynamics and Kinetics of HPDC Adhesion

Since laboratory-scale diffusion couple and roll bonding experiments do not match industrial observations, it is safe to conclude that these are not the mechanisms that cause adhesion in HPDC. This is not to say intermetallic phases cannot form between the casting and die. They appear to be the symptom of a different mechanism which causes the adhesion. Chen made this observations in 2005 when an initial buildup of aluminum on a core pin occurred without intermetallic formation, and subsequent casting cycles imparted enough energy and time for the intermetallic phases to form and grow [22].

5 Thermomechanics of Sticking

A thermal interference will occur on all die components that form internal features to the casting. This is because the coefficients of thermal expansion (CTE) for both the casting and die are mismatched. Even if they were identical, the casting cools while the die stays roughly the same temperature or slightly heats up. So, a thermal interference will always occur. This makes some component of HPDC adhesion behave like a common press fit, or interference fit. The interference would be expected to increase with lower ejection temperatures. If the resulting friction force is large relative to the die casting machine ejection force capability the casting will stick (Figure 13).

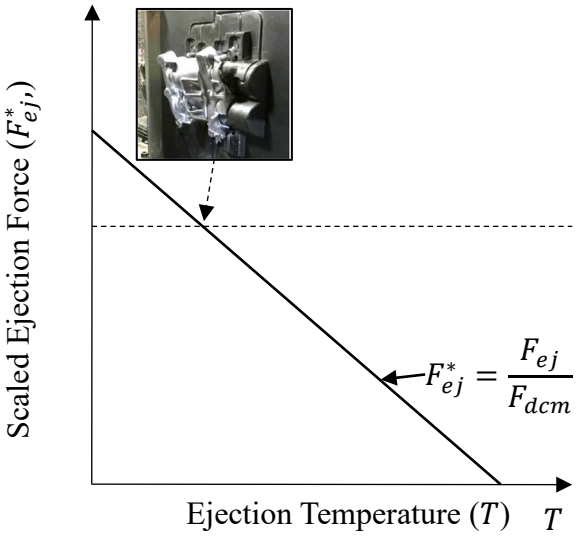

Figure 13: A simplified schematic based on Figure 3 where only the sticking factor is considered.

This ejection force, F_{ej}, depends on two factors; the strength of the interface and the area that must be separated (Figure 14). The contact area, A_c, is an apparent area because many factors affect the actual contact area in tribology [14]. Sticking in HPDC occurs when both the shear strength of the aluminum, τ_{Al}, and iron die, τ_{Fe}, are higher than the shear strength of the interface, τ_{ej}, and the contact area is large enough to prevent ejection. Heating a stuck parts reduces the strength of the interface, and the stuck casting is often cleanly removed from the die. Thus, the study of sticking in HPDC involves the key variables that control the strength of the interface.

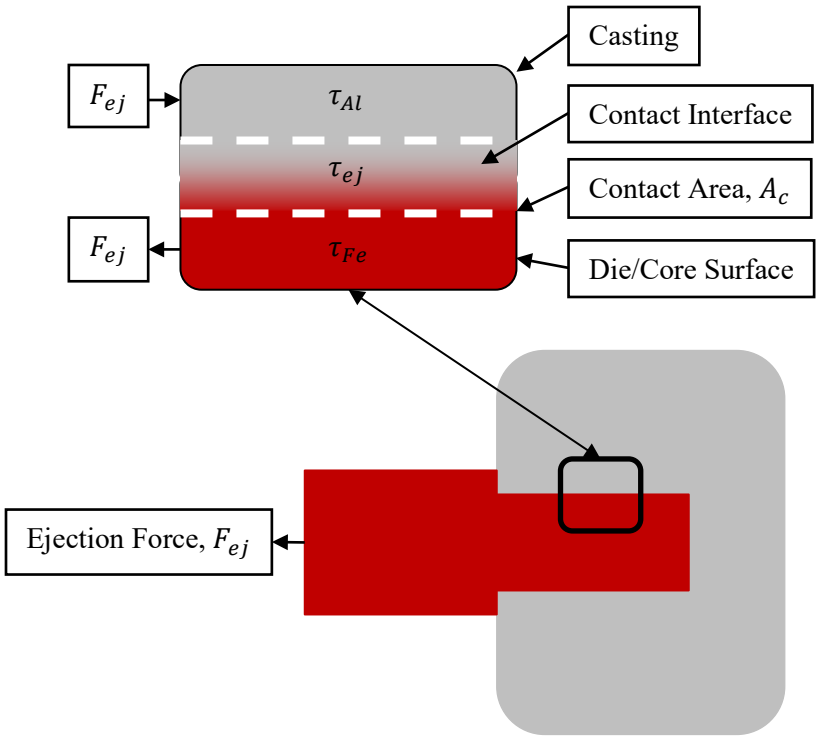

Figure 14: Conceptual model of the casting/die interface where F_{ej} is the ejection force and A_c is the total contact area. τ_{Al}, τ_{ej}, and τ_{Fe} are the shear strength of the casting, interface, and die, respectively.

The strength of the contact interface (Figure 14) is potentially affected by five factors. These factors can be illustrated and described in time order of the HPDC process (Figure 15). First, liquid metal contacts the die. This initial interaction establishes the true contact area through wetting. Good wetting can increase the mechanical interlocking and bonding potential with the die. Next, the porosity feeding intensification pressure contact between the casting and the die. During cooling of the liquid and early in solidification, there is an opportunity to form intermetallic phases. After solidification, the casting develops strength and contracts onto the die. The die is also absorbing heat and expanding. The relative temperature changes increase the interference and increases the contact area. Finally, uneven ejection may apply a moment which locally increases the contact area.

Symmetry is required to achieve uniform ejection. A single core in a cylindrical casting can be assumed to be axis-symmetric minimizing non-symmetric ejection effects (Figure 15 far right). This leaves 4 potential factors that affect the strength of the interface. Assuming a consistent casting process, then the remaining factors are split between interface interactions and friction. Friction was hypothesized to be the only significant component of ejection force. It can be calculated as the product of contact pressure, P_c, contact area, and the effective coefficient of friction, μ_{eff}, in this simple case (eq. 5 left term). Casting to die interactions could affect the strength of the interface, τ_{adh}, and would affect ejection force proportional to the contact area (eq. 5 right term).

$$F_e = \mu_{eff} P_c A_c + \tau_{adh} A_C \quad \text{(eq. 5)}$$

Cedorge and Colton did a free body analysis of the effect of draft angle, θ, [60]. They showed that draft angle reduces the ejection force due to reaction forces aligned with the ejection direction. The effective coefficient of friction (eq. 5) can be expanded to take these reaction forces into account (eq. 6). The resulting equation has 3 unknowns: the shear strength from adhesion, the contact pressure, and the coefficient of friction. These variables are not likely to depend on draft angle as adhesion results from aluminum in contact with the steel and contact pressure can be viewed as a stack of infinitesimally thin rings and the draft angle cannot affect any one ring in the stack. The coefficient of friction depends on the casting conditions and local roughness of the steel core. All three of the unknowns can be determined by testing a minimum of three different draft angles.

$$F_e = A P_c (\mu \cos\theta - \sin\theta) + \tau_{adh} A \quad \text{(eq. 6)}$$

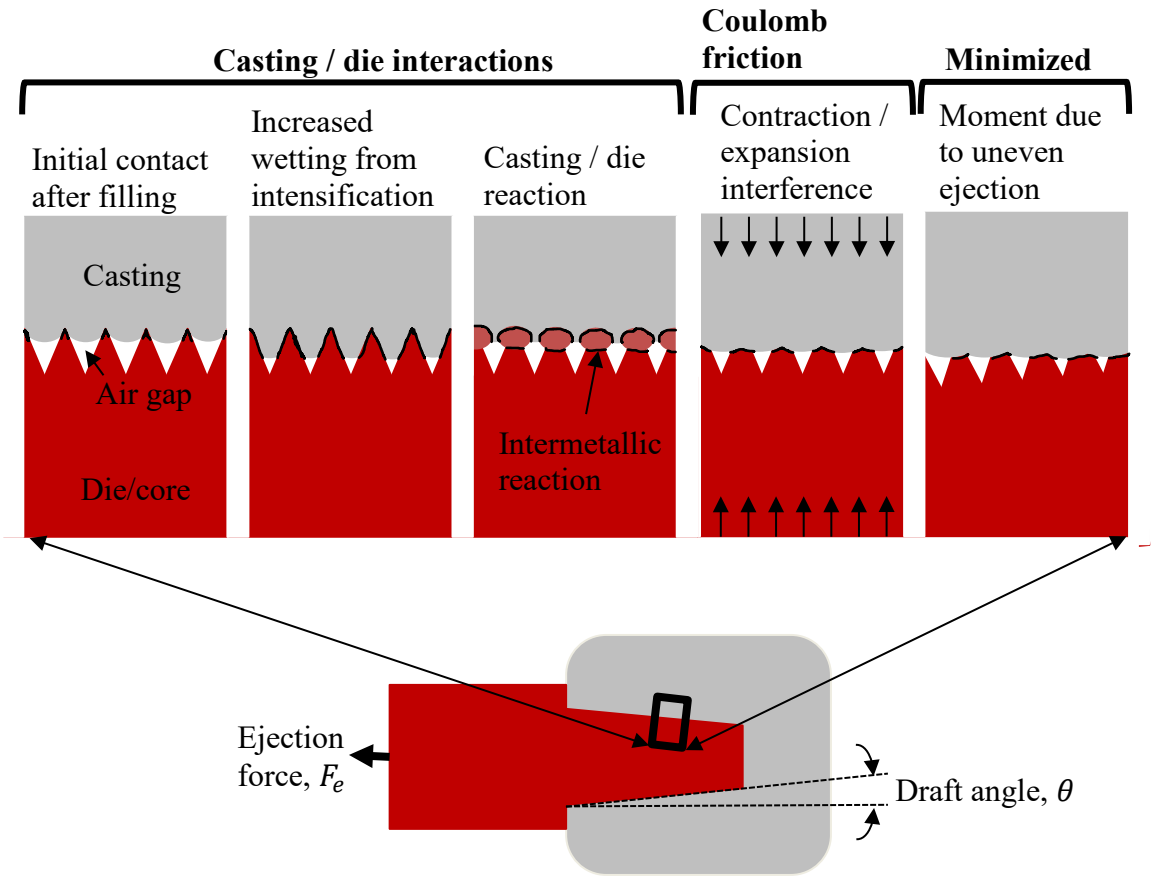

Figure 15: Different factors that affect the local contact area in the die casting process.

5.1 Hypothesis:

There are three possibilities with this friction model (eq. 6): either the casting to die interactions or the thermal interference are important, or both are significant. It is hypothesized that friction is the primary sticking mechanism, and this can be tested with a room temperature ejection test. If the draft angle is increased, then the ejection force is reduced by an amount greater than the reduced contact area. This is because the interference model (eq. 6) predicts a force component which acts in the ejection direction as a function of the draft angle. Also, the measured strength of the casting to die interaction are low making them insignificant [11].

5.2 Room Temperature Ejection Experimental Method

The test employed a consistent casting condition with only the draft angle and cast alloy as factors to determine if the coefficient of friction behaves like dry sliding measurements. Alternatively, it could be different when measured *in situ*. A single 12.7 mm diameter core pin was centered in a cylindrical mold. The casting outer diameter was 76.2 mm, and aluminum was poured into the open top of the mold. To control temperature and geometry, the alloy was taken from an HPDC holding furnace at the alloy specific temperature and the mold was filled completely to a 63.5 mm height (Figure 16 and Appendix A.1).

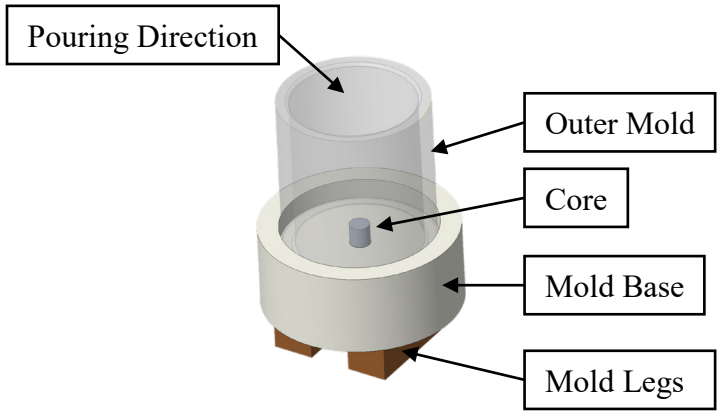

Figure 16: Schematic of room temperature ejection mold.

Seven core pins were prepared with the following draft angles 0.5°, 5°, 10°, 15°, 20°, 22.5°, 25° per side (Figure 21). Two alloys (362 and 380) were tested (Table 2). These alloys represent the most common and easy to cast 380 alloy compared to a more difficult to cast structural 362 alloy. The pouring temperature of 380 was 650±10°C and 362 was 680±10°C. These two different temperatures reflect the production holding furnace temperature for die casting. The 380 alloy has a lower solidus temperature due to its copper content. For this reason, it is typically held and cast at a lower temperature than the essentially copper free 362 alloy. Castings were produced by hand ladling alloy from an approximately 2700 kg HPDC holding furnace. Between each draft angle the casting and mold were cooled for at approximately 3 hours until they were at room temperature.

Three replicates of each alloy were poured for a total of 42 castings tests. After each ejection test the cores were inspected for any evidence of solder. The cores were reused without any cleaning or polishing because in all cases the inspection did not reveal any aluminum buildup.

Table 2: Chemical composition limits for the two alloys under study.

Alloy	**Si**	**Mg**	**Fe**	**Mn**	**Cu**	**Zn**
362	10.5-11.5	0.55-0.75	<0.45	0.25-0.35	<0.2	<0.1
380	7.5-9.5	<0.1	<1.2	<0.5	3.0-4.0	<3.0

Between each casting trial the pins were ejected from the castings at room temperature with a Tinius and Olsen tensile machine. An Omegadyne 0-30,000 lbf (133 kN) model TH-LPM4 load cell was used to measure the ejection force. Crosshead speed was constant for all tests at 1 mm/min. Only the maximum ejection force was used for analysis, but the load and crosshead displacement versus time was collected and archived for each test. During test development, it was discovered that the alignment of the crosshead was critical for reproducible results. At large draft angles, this is less important but, it is critical at drafts less than 5°. The fixture design was optimized with pivots in the top and bottom plate to allow for crosshead to align to the core during the early loading stages (Figure 17).

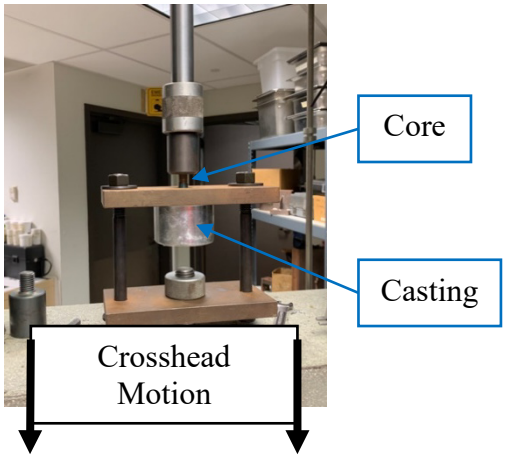

Figure 17: Image of the fixture for measuring the ejection force. The top and bottom of the fixture could pivot by a few degrees to correct for misalignment.

5.3 Results and Discussion:

All the ejection forces were plotted versus the draft angle (Figure 18) and increasing the draft angle reduces the ejection force as hypothesized. There appears to be an insignificant effect of alloy. A paired Student's T test was performed on the data from the two alloys, and the t-statistic was calculated as 0.94 for the paired test. This is less than the critical value of 1.71 assuming 95% level of significance. This implies that the

362 and 380 ejection force are not different, because the alloy and pouring temperature did not affect the results of the test. Further analysis and results are presented using the combined data from both alloys.

Pooled summary statistics were calculated for each draft angle (Table 3) with standard error as a fraction of the mean ejection force in the last column. The error is consistent regardless of draft angle suggesting that filling, solidification, and ejection loading were consistent. Shrinkage away from the surface of the core was minimized because the mold acted as a chill controlling solidification and the pouring rates were slow to avoid trapped gas porosity around the core. The data was collected with a 133 kN load cell and at the high draft angles, the load was only 1-2% of the rated load capacity.

Table 3: Summary of all the ejection force tests at room temperature.

Draft angle (degree)	**Average ejection force (kN)**	**95% standard error (2*std dev/sqrt(n))**	**Standard deviation (kN)**	**Standard err / average ejection force**
0.5	12.2	1.5	2.0	0.12
5	11.2	1.5	1.8	0.13
10	6.8	0.6	0.8	0.08
15	4.9	0.3	0.5	0.07
20	3.0	0.2	0.3	0.08
22.5	2.4	0.1	0.1	0.03
25	2.3	0.5	0.6	0.21

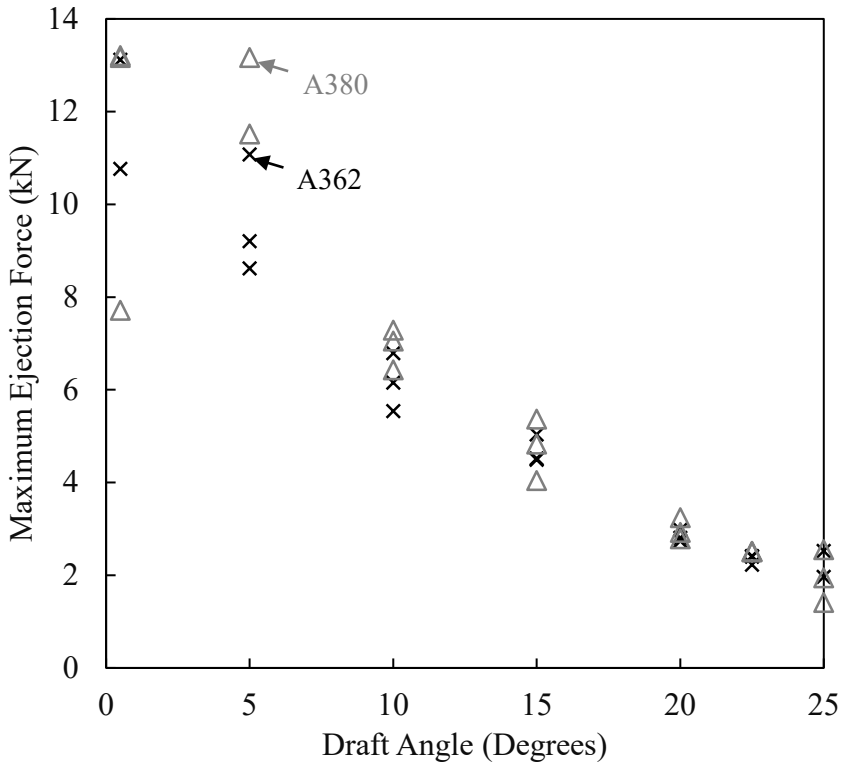

Figure 18: A plot of all ejection force measurements showing a trend of decreasing ejection force with increasing draft angle but little effect of alloy.

Eq. 6 was fit to all the data in Figure 18. Fitting was performed in Excel using the Solver tool to minimize the sum of the squares difference between the model and the experimental data. Interfacial strength, contact pressure, and coefficient of friction were the fitting parameters. The contact area was assumed to be the designed area. The top of the core pin (Figure 19) was not included in the contact area of the first term in eq. 6, as it has a 90° draft angle. The friction correction term become undefined at this draft angle. The best fit occurs when the interfacial strength is set to zero, contact pressure is 5.9 MPa, and the coefficient of friction is 0.59. The best fit was plotted as the "Friction Model" line (Figure 20), and this approach was also plotted assuming adhesion from interfacial strength alone. This is the dashed "Adhesion Model" line, and it is a poor fit of the data. Sticking is dependent on contact pressure at the casting/core interface.

Previous work by Wang and Loong as well as Tosa *et al.* agree with this finding because they found ejection force increased with longer delays prior to ejection [16], [93]. They also found the coefficient of friction to be approximately 0.6 [16]. Longer ejection times allow the casting to cool and develop a larger contact pressure from thermal contraction, and cooler temperatures reduce the reaction rate for an adhesion model. Increasing ejection forces with cooler ejection temperatures suggest that the friction from contact pressure is more important than adhesion from casting to die reactions.

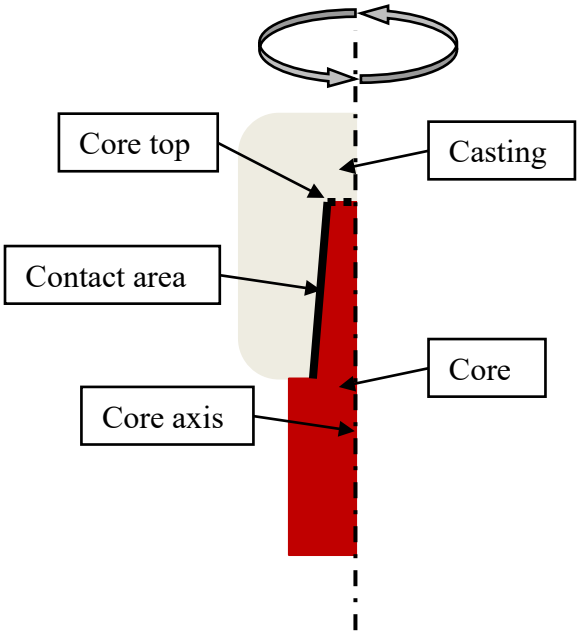

Figure 19: Schematic of core denoting the contact area used to fit (eq. 6) to the experimental data (Figure 18).

A friction is also consistent with the measured strength of the casting to die interface. Compared to previously reported values of the intermetallic adhesion strength, such as Wang *et al.* who reported a strength of 0.12 MPa [11], the ejection forces in this experiment were much higher with an interfacial shear stress of 3.5 MPa. This value is small relative to the typical strength of cast aluminum alloys but large compared to the intermetallic interfacial strength. Bulk visual deposition of aluminum or intermetallic phases on the surface of the core were not observed during the trial. Over 100 castings were produced without any polishing because the pins remained clean after each trial (Figure 21).

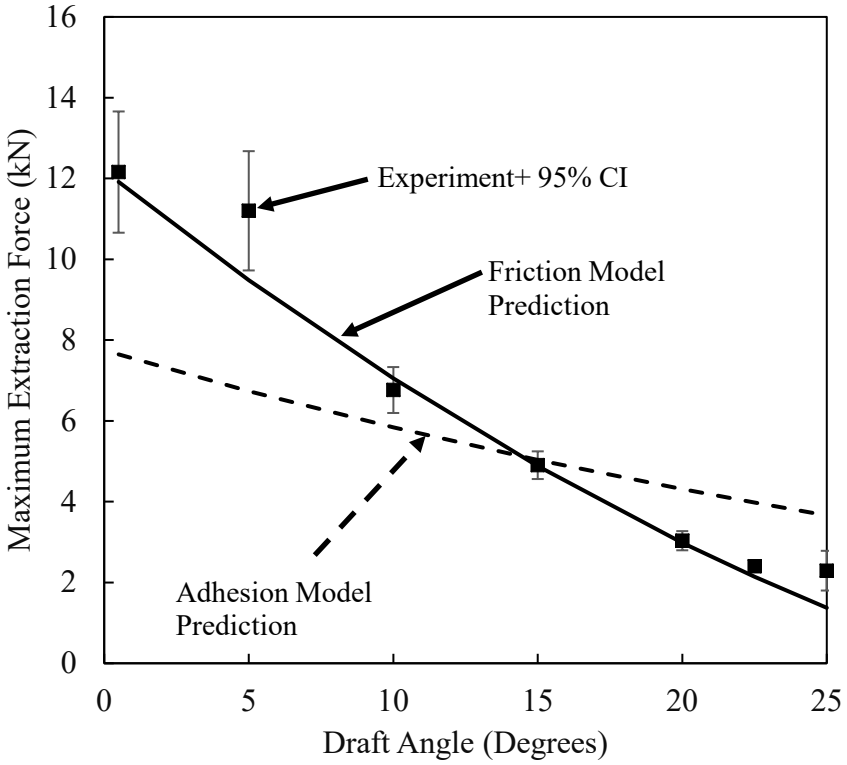

Figure 20: The best fit is achieved with the "Friction Model" and is not improved by adding the adhesion term. The adhesion only model does not match the data.

Figure 21: Image of all 7 cores after over 10 casting cycles showing no buildup from the cast aluminum.

A second set of 10 core pins were prepared with draft angles of 0.5, 5, 10, 15, and 20 degrees. Five of the cores were draw polished with a 220 grit stone (rough condition) and five were diamond polished to a 3 micron diamond finish (smooth condition). After preparation, all pins were coated with an AlCrN physical vapor deposition (PVD) coating. The coating, called Fortiphy+, was applied by Phygen, and it has been shown to resist reaction with aluminum under severe conditions [11].

The same casting trials were performed with 3 tests per pin and a total of 30 castings, and all the experimental results were plotted (Figure 22). There is no clear difference between coating condition. Perhaps this is because the castings were poured with the mold at room temperature, and the casting cooled too quickly to effectively wet the relatively rougher cores compared to the diamond polished cores. More tests with different initial mold temperatures may help further understand this difference, but the similarity was leveraged to pool the statistics of the dependence on coating and draft angle. This increased the number of experiments to six for each draft angle in the following analysis.

Ejection force for the coated cores was fit with eq. 6 and plotted in comparison with the uncoated cores (Figure 23). Coatings reduced the coefficient of friction by 18% from 0.59 to 0.5. This suggests that the primary reason coatings reduce sticking is by reducing friction. Abrasive wear resistance of the die is also improved by the hardness of the coatings, and this extends the useful life of the tooling. Adhesion is not a significant factor in the coated versus uncoated samples because the lowest error occurs when the adhesion term (right hand term in eq. 6) is set to zero meaning the friction only model fits the data best.

Generalizing the results of the coated cores is difficult because these tests were performed unlubricated. It is possible there is an interaction between the lubrication and the coating/surface finish of the cores in a production environment. Die lubricant manufacturers will often speculate that the smooth and coated finish is more difficult to coat with a lubricant. This interaction of lubricant should be investigated in the future.

Contact pressure and friction coefficient are the only factors that are necessary to predict the casting ejection force. This is a surprising result because of the literature suggests that interfacial reaction is the primary mechanism that controls ejection force. Further, the in-situ measurement of friction yields a similar friction coefficient to regularly reported for dry sliding friction between aluminum and steel [16]. It is true that the precise mechanism that causes friction is not well understood.

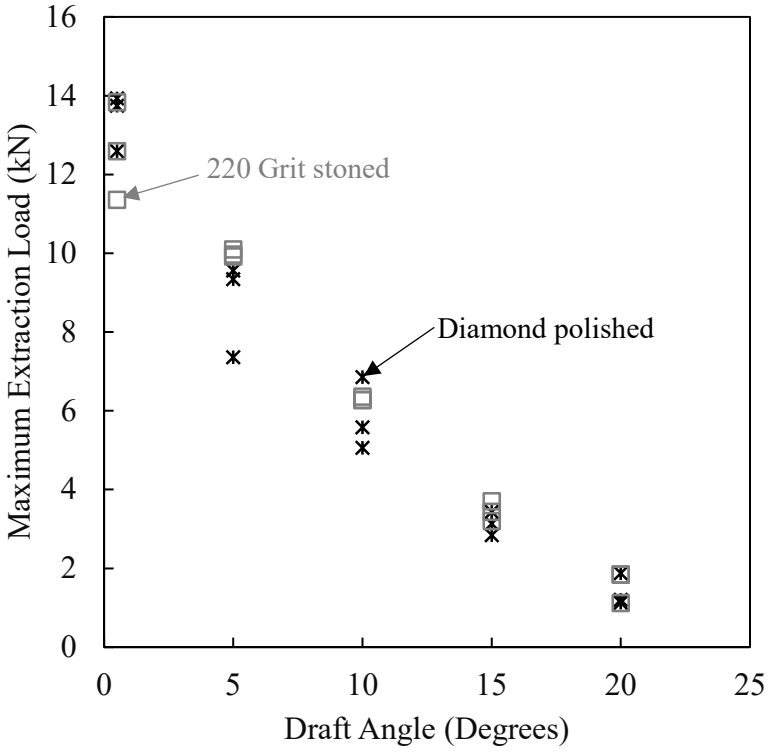

Figure 22: Comparison of AlCrN coated cores showing no difference between the smooth (Diamond Polished) and rough (220 Grit Stoned) surface preparation.

In situ measurement of friction in the die casting process has not been previously reported but measuring the dry sliding friction coefficient of permanent mold casting is helpful in understanding ejection force. This is because the during the casting process the aluminum has an opportunity to interact with the surface of the die. The cooling against the die/core surface affects the microstructure of the casting and its friction against the die. By leaving the surface undisturbed, it was possible measure the friction coefficient while keeping the casting surface unmodified.

Castings can stick because the die casting machine ejection force is relatively weak. A 300 ton machines can have a maximum ejection force of 100 kN [94], which implies eight cores like the test described above would exceed the machine ejection force capability and cause the casting to stick. This limitation can be reduced by relieving the contact pressure through increasing the casting ejection temperature. It can also be reduced by lubrication [10], [16].

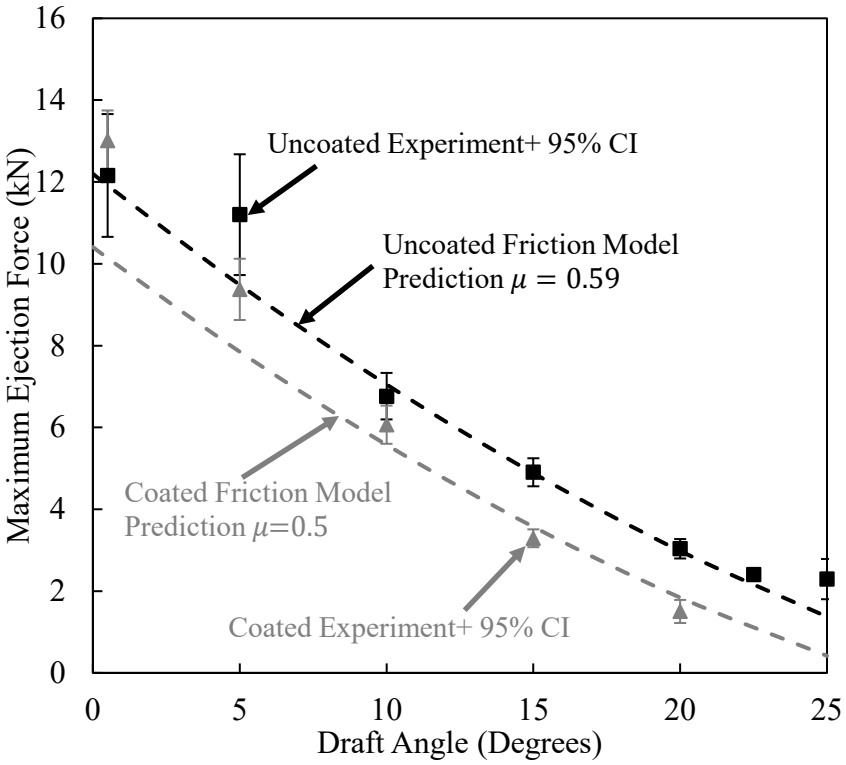

Figure 23: Friction model fit to the AlCrN coated cores versus the uncoated cores. The 95% confidence interval based on a minimum of six experiments for each data point is shown.

There is a low chance that the casting will fail by shearing instead of sticking at these lower ejection temperatures. The contact pressures were low in this test despite maximizing ejection force by ejecting at room temperature. The measured shear stress of roughly 3.5 MPa is low compared to the yield stress of aluminum which is at least 20 times higher. This means that there is a low chance that the aluminum would fail and buildup on the die when the ejection temperature is low, and the aluminum is strong relative to casting/die interfacial strength.

6 Thermomechanics of Soldering

HPDC soldering is a local failure of the aluminum casting during ejection. It can be predicted when the shear strength of the casting/die interface, τ_{ej}, exceeds the shear strength of the aluminum, τ_{Al} in which the Tresca friction factor, Tr, is the ratio of these shear strengths (eq. 7). Shear tests have shown that aluminum transfers to steel when the Tresca friction factor exceeds 0.7, but this form is difficult to apply directly to a casting [15].

$$Tr = \frac{\tau_{ej}}{\tau_{Al}} < 0.7 \qquad \text{(eq. 7)}$$

The numerator of eq. 7 is more simply defined as the scalar multiple of the local contact pressure, P_c, and a coefficient of friction, μ [15]. The denominator can be related to the ultimate tensile strength (UTS), σ_{UTS}, through the Von Mises failure criteria. Under pure uniaxial load the Von Mises failure stress is the ultimate strength divided by the square root of three. These substitutions yield an equation (eq. 8) where all the variables are temperature dependent. Both contact pressure and tensile strength increase as the temperature decreases, but they are not required to increase at the same rate. In particular, the non-linear increase in aluminum strength with decreasing temperature generally causes the Tresca friction factor to decrease with temperature (Figure 24).

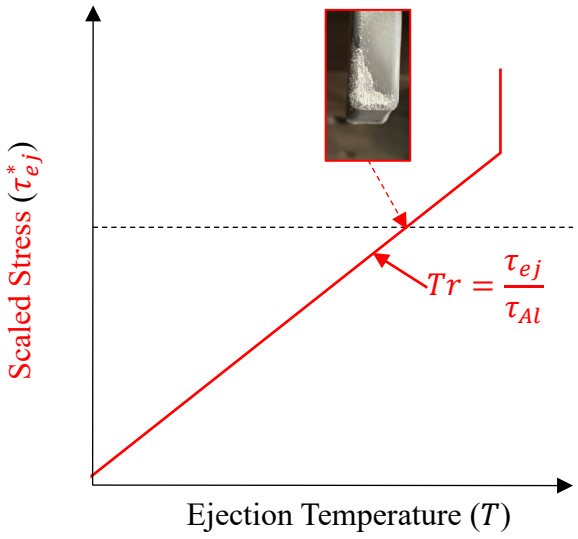

Figure 24: HPDC soldering occurs when the Tresca friction factor is larger than a critical value, and it decreases with lower ejection temperatures, (simplification of Figure 3)

Some evidence suggests that the coefficient of friction increases with increasing temperature [16], [56], [95]. However, temperature also affects the modulus and strength of aluminum and will in turn affect the Hertzian contact area depending on the friction test geometry. This makes a general statement about the friction coefficient's dependence on temperature challenging.

$$Tr = \sqrt{3}\mu \frac{P_c}{\sigma_{UTS}} \quad \text{(eq. 8)}$$

Temperature dependent mechanical properties are required to solve eq. 8. These properties can be approximated from the Ludwick-Hollomon (L-H) constitutive relationship proposed by Roy *et. al* [17]. Eq. 9 relates the stress, σ, to strain, ε, and the strain rate, $\dot{\varepsilon}$, with temperature, T, dependent parameters. $K(T)$ is the strength parameter (eq. 10). $N(T)$ is the strain hardening exponent (eq. 11), and $M(T)$ is the strain rate sensitivity (eq. 12).

$$\sigma = K(T)\varepsilon^{N(T)}\dot{\varepsilon}^{M(T)} \quad \text{(eq. 9)}$$

$$\mathrm{K}(T) = 8 \times 10^{-4}T^2 - 1.16T + 408 \quad \text{(eq. 10)}$$

$$N(T) = -0.06\, ln\, T + 0.4 \quad \text{(eq. 11)}$$

$$M(T) = 4.6 \times 10^{-11}T^{3.5} + 0.024 \quad \text{(eq. 12)}$$

Strain rates are small both during cooling and ejection because the strains are small. If the aluminum coefficient of thermal expansion is roughly 20 μm/m°C then at a cooling rate of 100°C/*s* the thermal strain rate is 0.002 s^{-1}. For simplicity, the strain rate was always assumed to be 0.001 s^{-1}.

The strain hardening exponent $N(T)$ was modified to better match all the experimental data (eq. 11). Roy *et al.* proposed a discontinuous behavior with a constant strain hardening exponent above 300°C [17]. They also report this constant coefficient to be negative suggesting that the material has a lower UTS than its yield strength. This behavior has been reported elsewhere in hot compression tests at very low strain rates, but it is not the most common trend [96]. Most of the raw data from Roy *et al.* indicate a positive coefficient, and it was matched with a logarithmic fit to that raw data (eq. 11). Another approach would be to set the exponent to zero above 300°C [97].

Using the L-H relationship, local contact pressure can be predicted using numerical simulations. The other material property in eq. 8, UTS, can be difficult to predict because it requires knowledge of the failure strain. Caceres proposed that the onset of necking is the highest possible uniform strain to failure while providing the rational for the Quality Index of aluminum [98]. If the local strain required to create a stress that overcomes friction exceeds the onset of necking, then the material will continuously plastically deform until it fails. Below this stress there is a good chance the material can strain harden sufficiently to survive the ejection shear making it a reasonable failure criterion for predicting HPDC soldering. The casting-die interface cannot be broken if the casting plasticly deforms till failure.

Nichols provided a summary of the necking criteria [99]. Strain rate insensitive materials necking when the strain equals the strain hardening exponent, $N(T)$. Strain rate sensitive materials have a non-zero strain hardening exponent, $M(T)$, and they will neck when the strain equals $N(T)/(1 - M(T))$. This strain was used in the Ludwick-

Hollomon model (eq. 9). The new term for UTS was then substituted into eq. 8 and the terms were rearranged to create a relationship for the maximum local contact pressure (eq. 13). If the ratio of contact pressure to the UTS exceeds the critical value of the right-hand side, then the aluminum casting is predicted to fail at ejection resulting in the observation of HPDC soldering.

$$\frac{\sqrt{3}\mu P_c}{K(T)\left(\frac{N(T)}{1-M(T)}\right)^{N(T)}\dot{\varepsilon}^{M(T)}} < Tr \lesssim 0.7 \qquad \text{(eq. 13)}$$

This general form for prediction of soldering can be directly implemented in solidification and cooling stress simulation codes [59], and it is novel because of the thermophysical and thermomechanical property basis (eq. 13). Soldering is directly proportional to the coefficient of friction and inversely proportional to the UTS of the casting material.

6.1 Hypothesis:

Based on this friction model, lubricants and coatings should reduce soldering as observed in industry because they reduce the coefficient of friction (eq. 13). The temperature dependence of UTS also leads to a testable hypothesis of soldering which is independent of the friction coefficient. If the ejection temperature is increased, then the soldering tendency will be increased because the ultimate strength approaches zero (Figure 25). This hypothesis was tested in two ways. First, a hot ejection test was developed to match a close-form prediction of contact pressure versus UTS. This test was important because the true values of P_c, UTS, μ, and Tr are difficult to know for die casting alloys at elevated temperatures. Second, 3D simulations in MAGMAsoft were compared with industrial examples [59].

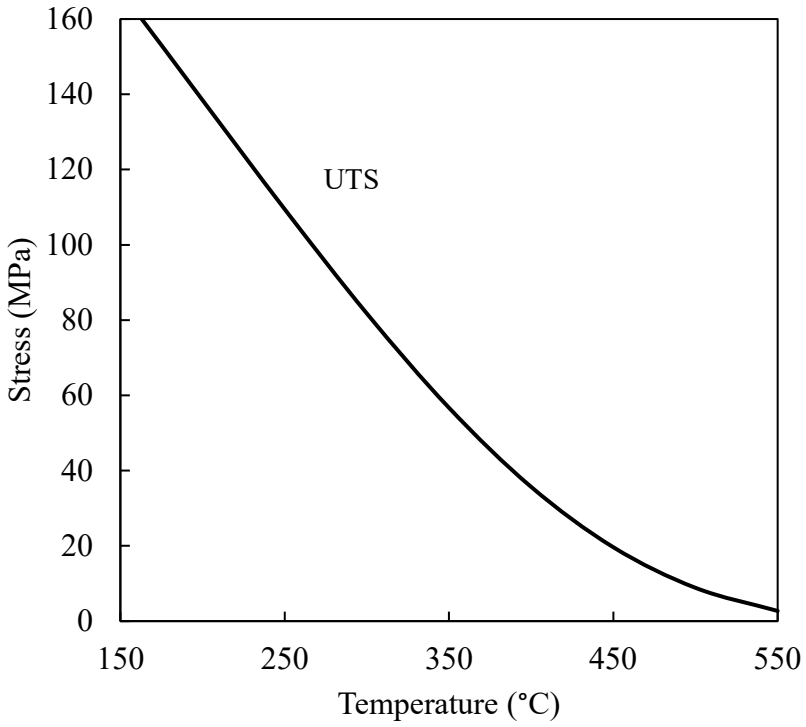

Figure 25: The L-H relationship as proposed in eqs. 9 through 12. UTS was calculated assuming the onset of necking where $N(T)/(1-M(T))$.

6.2 Model Application:

A solid core in a tubular casting (Figure 7) is an ideal example geometry to calculate the Tresca friction factor versus temperature. Interference fits like this have been studied for many years and exact solutions exist for the stress distribution through the casting thickness [75]. The stress state has two components, assuming no end effects, and they depend on radial position, r (Figure 26). Radial stress, σ_r, is normal to the casting/core interface (eq. 14). Tangential stress, σ_t, acts along the tangent of the casting radius (eq. 15). Contact pressure, P_c, occurs only at the casting/core interface and is related to the elastic modulus, E_{Al} and E_{St}, and Poisson ratio, v_{Al} and v_{St}, of the casting and core (steel), respectively. It also depends on the thermal interference, δ, and relative size of the inner, r_i, and outer, r_o, radii (eq. 16). The core is assumed to be solid, but the case with internal cooling may also be considered [75].

$$\sigma_r = \frac{r_i^2 P_c}{r_o^2 - r_i^2}\left(1 - \frac{r_o^2}{r^2}\right) \quad \text{(eq. 14)}$$

$$\sigma_t = \frac{r_i^2 P_c}{r_o^2 - r_i^2}\left(1 + \frac{r_o^2}{r^2}\right) \quad \text{(eq. 15)}$$

$$P_c = \frac{\delta}{\frac{r_i}{E_{Al}}\left(\frac{r_o^2+r_i^2}{r_o^2-r_i^2}+\nu_{Al}\right)+\frac{r_i}{E_{St}}(1-\nu_{St})} \quad \text{(eq. 16)}$$

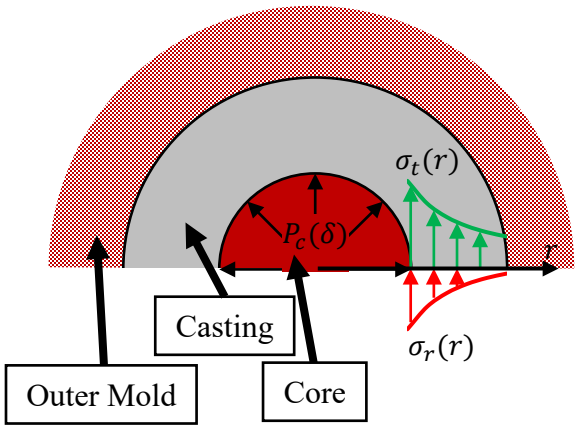

Figure 26: Bulk stress state prior to ejection due to the thermal interference between the casting and core.

The thermal interference is related to the coefficients of thermal expansion, α_{Al} and α_{St}, and the change in temperature, ΔT_{Al} and ΔT_{St} (eq. 17). During initial casting solidification and cooling, the steel is heating up and the aluminum is cooling. In this case, the steel change in temperature is negative adding to the interference. Assuming a coefficient of thermal expansion (CTE) of aluminum being roughly constant with temperature at 20 μm/m°C the theoretical interference strain can be plotted (Figure 27).

$$\delta = (\alpha_{Al}\Delta T_{Al} - \alpha_{St}\Delta T_{St})r_i \quad \text{(eq. 17)}$$

The yield stress was computed by using the elastic modulus (eq. 18) from Roy *et al.* and back calculation of the 0.002 offset yield stress in the L-H relationship [17]. The Poissons' ratio, ν, was assumed to be 0.3 (eq. 17). This was plotted versus temperature to evaluate whether the elastic stress assumption of eq. 16 is acceptable (Figure 27). Comparing the yield strain to the thermal strain reveals some plastic deformation occurs for all thermal strains in the axis-symmetric case (Figure 27). The thermal strains are small and the strain hardening coefficient is low at elevated temperatures. For these reasons, the yield stress is assumed to be a good estimate of the stress state prior to ejection.

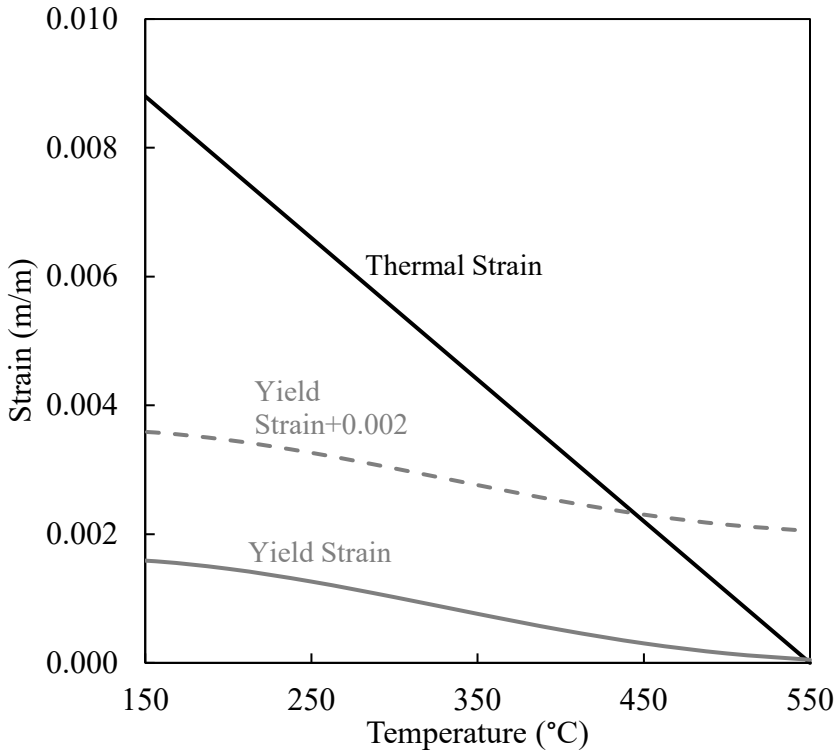

Figure 27: Thermal strain compared to the yield strain as calculated using an 0.002 offset of elastic modulus in eq. 18.

$$E = 5.08 \times 10^4 \left(1 + \frac{300-T}{2T_{melt}}\right)(1+v) \qquad \text{(eq. 18)}$$

Using this assumption, the contact pressure was calculated using the Von Mises stress. It is a widely used failure criterion for ductile materials such as aluminum [75], which is particularly true at the elevated ejection temperatures in HPDC where the aluminum has high plasticity. The Von Mises stress due to shrinkage, $\hat{\sigma}_{sh}$, can be simplified assuming the stress state only contains tangential and radial components (eq. 19). Setting this shrinkage stress equal to the YS and replacing the tangential and radial stresses with their equations for the axis-symmetric case (eqs. 14 and 15) yields an expression that relates the contact pressure to the yield stress (eq. 20).

Contact pressure for an arbitrarily sized cylindrical casting can now be substituted into eq. 8 and simplified (eq. 21). Grouping the terms in this way puts the material properties on the left-hand side of the inequality and the geometric and lubrication term on the right-hand side. The ratio on the left-hand side of eq. 21 is readily calculated and plotted (Figure 28). It decreases as the temperature decreases.

$$\hat{\sigma}_{sh} = \sqrt{\sigma_t^2 - \sigma_t\sigma_r + \sigma_r^2} \quad \text{(eq. 19)}$$

$$\sigma_{YS} = P_c\sqrt{\left(\frac{r_o^2-r_i^2}{r_o^2+r_i^2}\right)^2 + \left(\frac{r_o^2-r_i^2}{r_o^2+r_i^2}\right) + 1} \quad \text{(eq. 20)}$$

$$\frac{\sigma_{YS}}{\sigma_{UTS}} < \frac{\sqrt{\left(\frac{r_o^2-r_i^2}{r_o^2+r_i^2}\right)^2 + \left(\frac{r_o^2-r_i^2}{r_o^2+r_i^2}\right) + 1}}{\sqrt{3}}\frac{Tr}{\mu} \quad \text{(eq. 21)}$$

Determining the threshold ratio of YS and UTS below which soldering does not occur for a cylindrical casting requires examining the right-hand side of eq. 21. At a limiting case, the first ratio approaches 1 for large r_o relative to r_i. Making this simplification and assuming $Tr = 0.7$, critical values are plotted as horizontal lines. Three friction coefficients were plotted with the YS/UTS ratio (Figure 28), and the coefficients typical for reported friction coefficients at elevated temperatures [56], [95]. Where these lines intersect is the critical temperature above which soldering is likely. Lowering friction reduces soldering tendency as well as decreasing the ejection temperature.

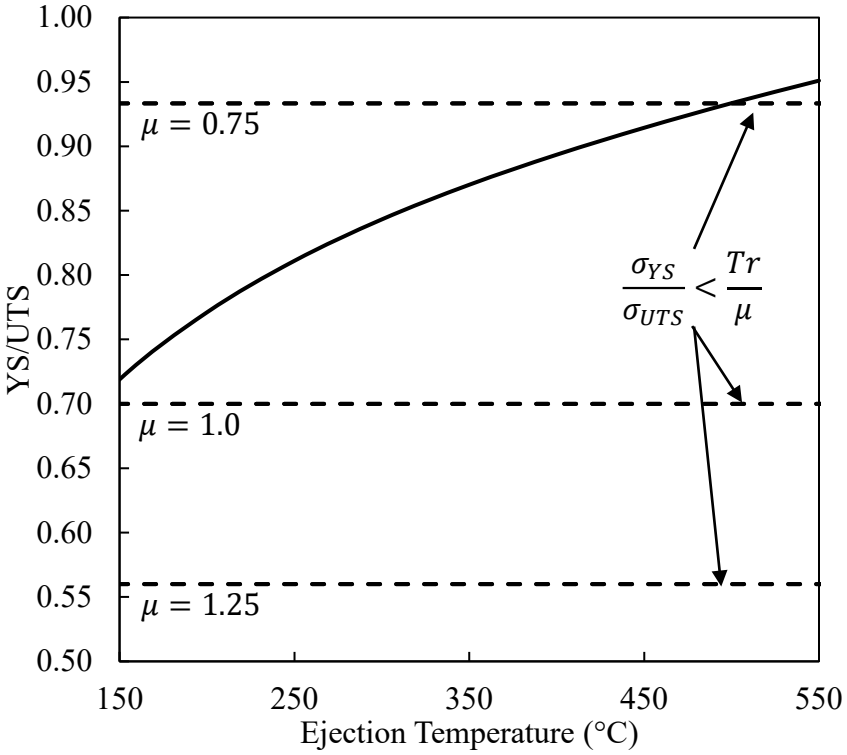

Figure 28: Predicted soldering likelihood of a cylindrical casting (eq. 21) based on the alloy described in eq. 9 versus the ejection temperature.

6.3 Hot Core Ejection Experiment:

A test was developed to examine the temperature effect (eq. 21) where cores were removed from a cylindrical casting at elevated temperature. The castings were poured into a sand mold with an embedded core (Figure 29 and Appendix A). Cores were made from 4140 steel with a 0.5° draft on the casting surface, and the core surface was left as machined. Sand molds were produced with a cold setting resin binder. Sand was used for the mold material to enable a uniform ejection temperature within the casting, which better matches the first principles model of the ejection stresses. Slower cooling rates also improved the uncertainty in the ejection temperature. The outer diameter was of the casting was constant at approximately 40 mm. A draft of 5° was applied on the outside of the casting to enable mold making.

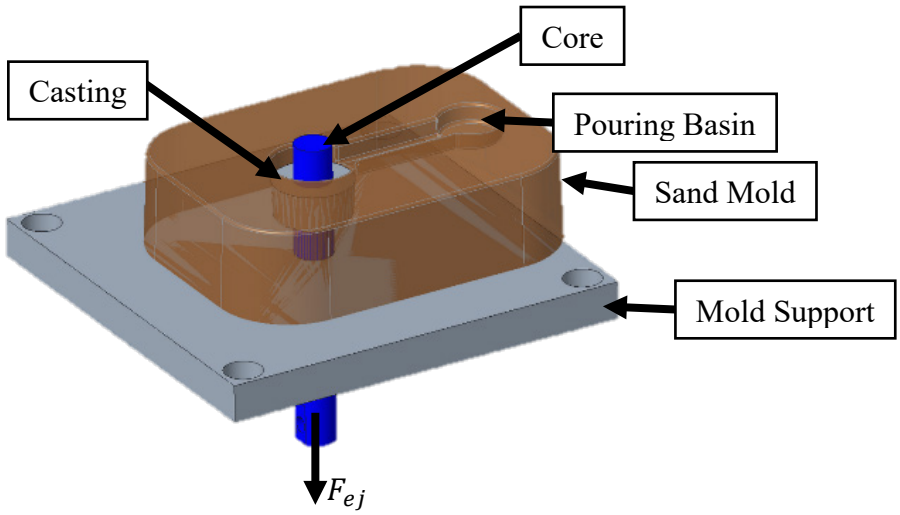

Figure 29: Assembly view of the hot ejection test apparatus the casting, core, sand mold, and support plate.

For all tests, the casting/core contact length was approximately 12.5 mm. Filling was stopped once the mold was full. Ejection temperatures were tested between 555°C and 450°C with the ejection force breaking the sand molds at 450°C. Alloy chemistry conformed to the aluminum association alloy A362 (Table 4). Temperatures were recorded with a k-type thermocouple embedded in the sand mold on the outer surface of the casting. Ejection force was measured with a load cell. Displacement of the core was measured with a LVDT.

6.4 Hot Ejection Test Results and Discussion:

The hypothesis was partially confirmed by the hot ejection test, in that within a single casting cycle aluminum would adhere to the core (Figure 30). However, this was not a massive buildup, and it was not as temperature dependent as predicted. These discrepancies are likely due to two observations. First, the contact was not uniform as shown by surface shrinkage (Figure 31). Without uniform contact, the contact pressure

would be concentrated, and the assumption of axis symmetry is no longer valid. Second, the range of temperatures tested have small differences in the strain hardening coefficient. From 450°C to 555°C the strain hardening coefficient was predicted to be between 0.03 and 0.02 (eq. 11). This is roughly one tenth of the strain hardening coefficient at room temperature, and the result is a low tolerance for shear stress due to friction (Figure 28).

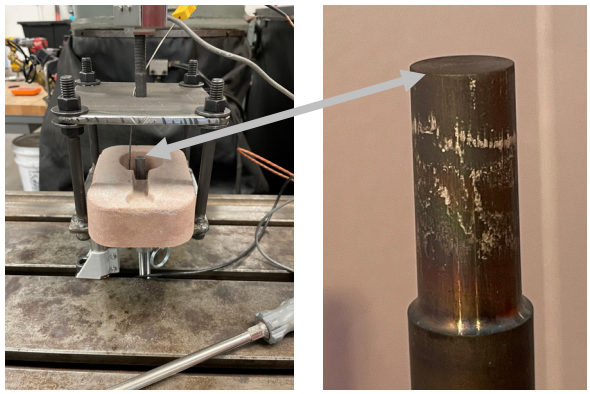

(a) (b)

Figure 30: (a) Example of experimental rig prepared for casting. (b) Incipient soldering clearly shown on the case where ejection occurred at 550°C.

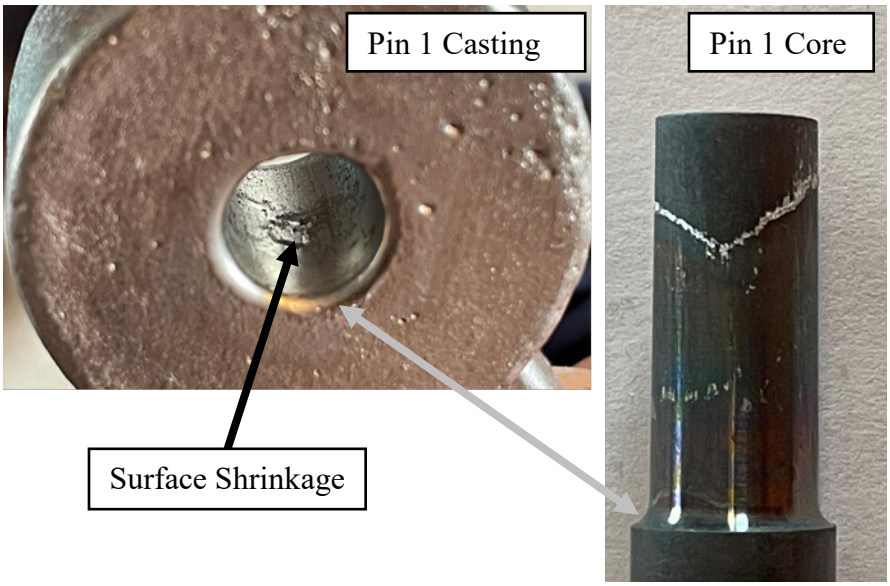

Figure 31: Casting surface for hot ejection test showing surface shrinkage (casting) and aluminum buildup (core).

Hot ejection of a core from a cylinder promised to be useful because of the simple relationship. However, matching the axis symmetric ideal case proved difficult in practice. The contact pressure can be a range of values as it is dependent on the solidified geometry. Outside of axis-symmetric cases it is easy to imagine a wide range of potential

contact pressures. For example, a rectangular geometry will have different contact pressures based on the length of each side (Figure 32). Fortunately, 3D computer simulations can predict the effect of shape on the local contact pressure.

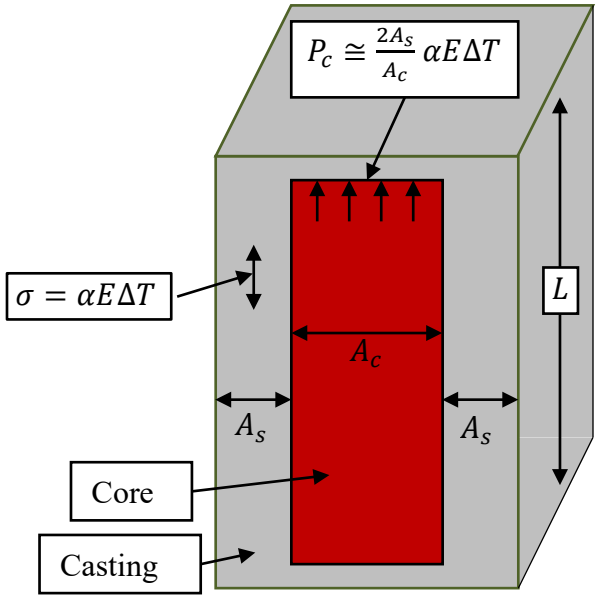

Figure 32: Rectangular example showing that the contact pressure is proportional to the thickness of the casting relative to the bearing area, A_c, on the core.

6.5 3D Modeling:

Industrial HPDC castings were simulated in MAGMASOFT to model the Tresca friction factor during the casting process [59]. One example is a mature die that was previously studied for soldering reduction (Figure 33) [8]. Seven warmup casting cycles were computed prior to filling and solidification. Lubricant spray, die filling, solidification, and ejection times were selected to mimic the industrial process as close as possible. All major die inserts were considered within the simulation. A second industrial example was simulated prior to trialing the die (Figure 34), and warmup cycles and filling were not computed because these simulations were created before the die was manufactured. In both cases, MAGMASTRESS calculated the contact pressure between the casting and die during solidification up until the specified ejection time. User results of the Tresca condition (eq. 13) were calculated by dividing the contact pressure by the temperature dependent ultimate tensile strength. The alloy simulated was A360, and all alloy properties were the default MAGMASOFT properties.

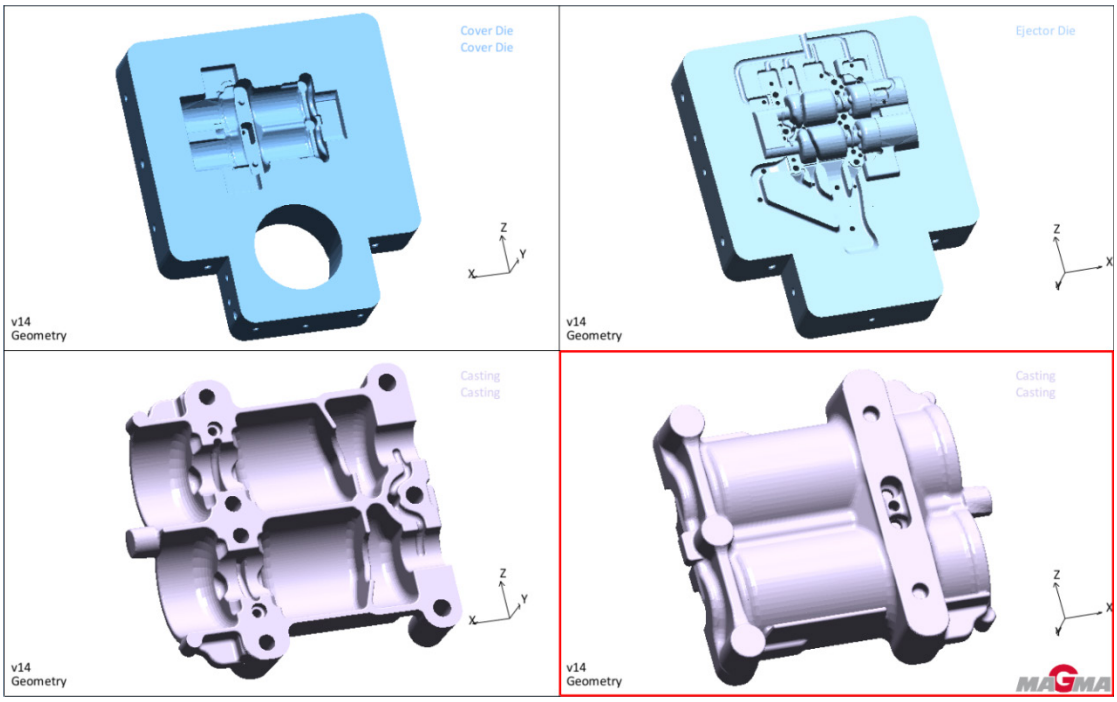

Figure 33: Example die simulated in MAGMASOFT to test the validity of the Tresca friction factor to predict HPDC soldering.

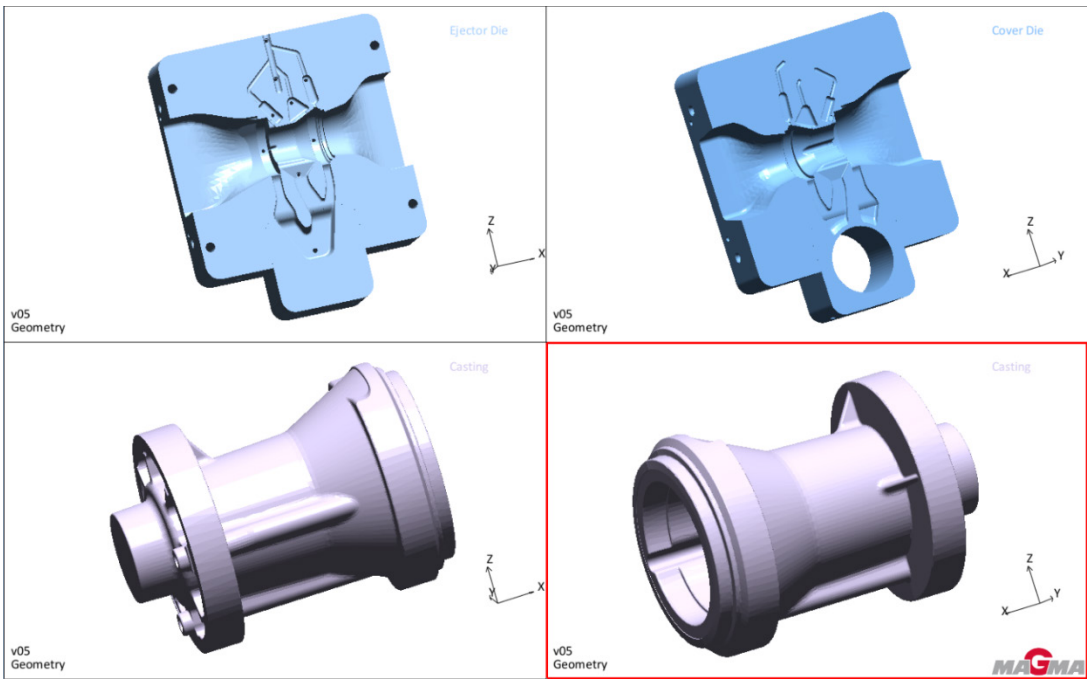

Figure 34: Second industrial HPDC example for comparison of the Tresca friction factor with HPDC soldering.

Calculation of the Tresca condition for both examples was possible using the result calculator available in MAGMASOFT (Figure 35 a and c). This prediction was compared to the condition of the dies after producing over 100 castings at Mercury Marine in Fond du Lac, WI (Figure 35 b and d). Locations of soldering and relative severity are well predicted using this friction-based prediction.

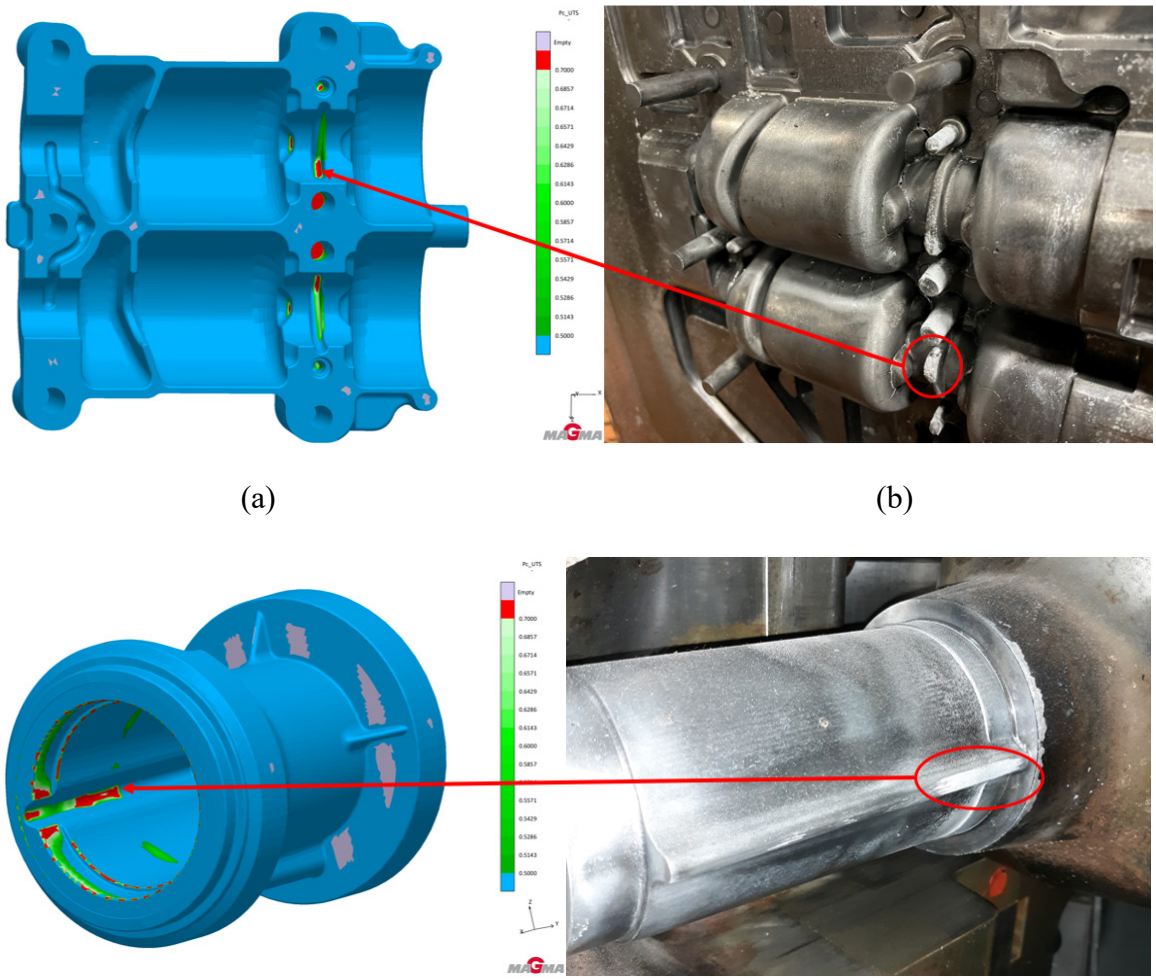

(a) (b)

(c) (d)

Figure 35: Comparison of the contact pressure scaled by UTS in MAGMA (a) and (c) with the production die casting die at the end of a production run (b) and (d).

The strong dependence of soldering on temperature is also clearly shown in the simulation. Two locations were selected in the first example for detailed review. One area develops a high friction factor then it rapidly declines (Figure 36 black lines). The other area also increases but does not decrease as significantly prior to ejection (Figure 36 grey lines). The increase in soldering friction factor is due to the thermal contraction of the

casting driving up the contact pressure locally. The decrease occurs when the casting start cooling sufficiently for the UTS to reduce the Tresca friction factor more rapidly than the contact pressure increases it (eq. 13).

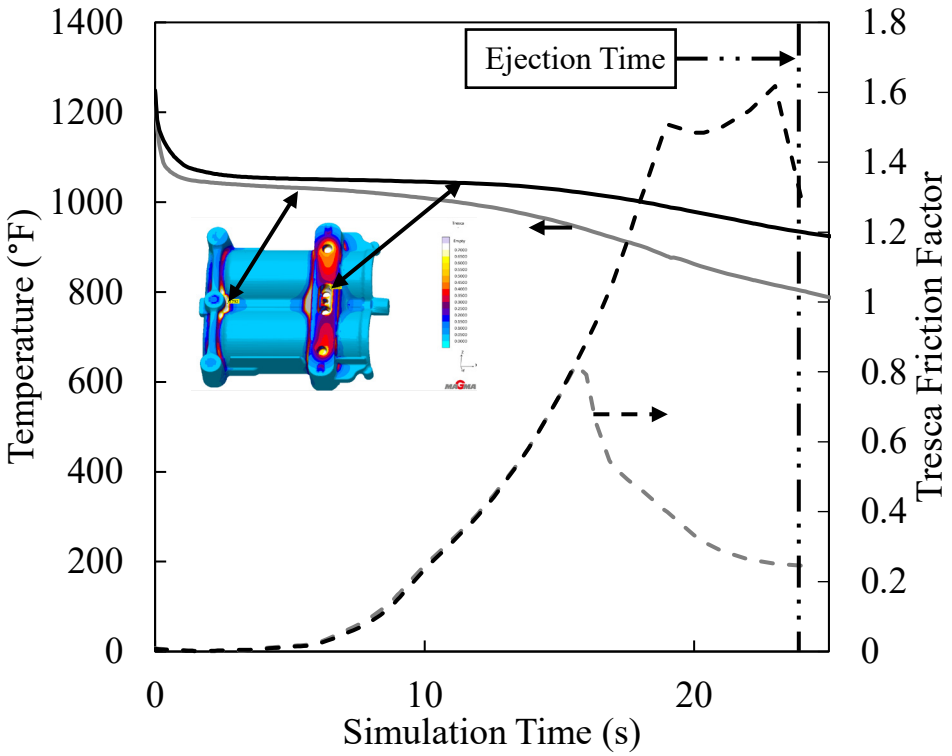

Figure 36: Predicted soldering friction factor (right hand axis) vs simulation time. The temperatures at the same locations are plotted on the left-hand axis. Both locations exhibit increasing then decreasing soldering tendency related to the local temperature of the casting.

This new modeling approach gives the die casting engineer a tool to anticipate and troubleshoot soldering behavior. As shown in Figure 36 adjustments as simple as ejection time can affect which locations solder. However, it is important to realize the strong dependence of the model to the material properties.

A brief examination of the literature suggests high temperature properties can vary significantly. Alankar and Wells investigated the high temperature strength of as cast wrought alloys [97]. They found that the high temperature strength can be quite different between alloys such as 6111, 3104 and 5183 (Figure 37). Similar experiments may show the effective alloy additions to die casting alloys to improve strength above 350°C.

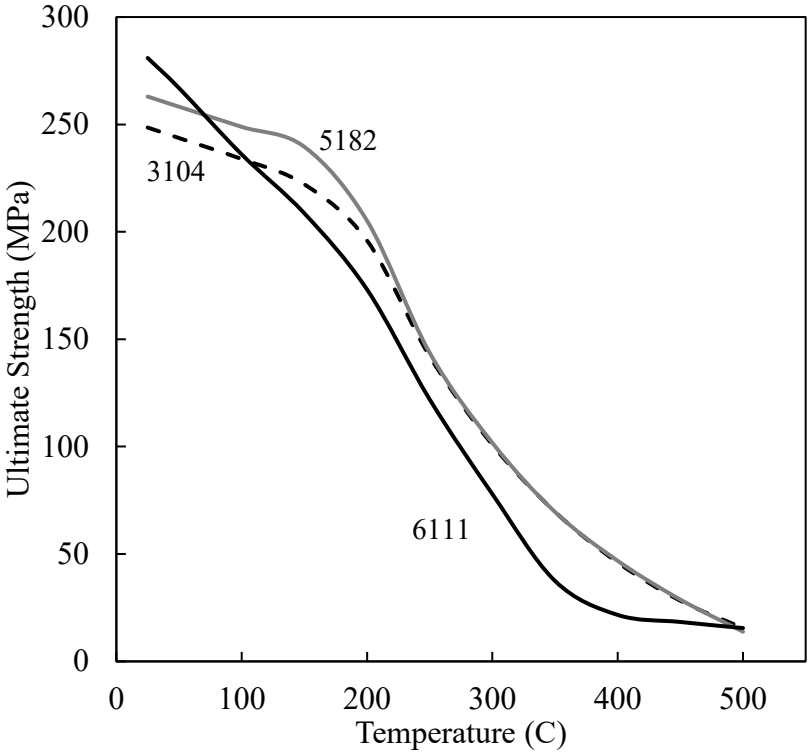

Figure 37: Hot Compression strength (assuming UTS at onset of necking) vs test temperature of typical wrought aluminum alloys in the as cast state [97]. UTS was assumed to occur at the onset of necking.

Identification of the soldering dependence on the high temperature strength of the aluminum alloy is useful, but ultimately not the best opportunity for HPDC foundries. The alloys used in HPDC are difficult to change due to the nature of the process and alloy specification. Rapidly applying this novel friction model will require leveraging the simulation tools to select common alloys and process conditions to reduce soldering. This will enable process designs with the lowest likelihood for soldering over a broad range of process settings. Such inputs that affect the soldering include alloy selection, casting design, die design, and process.

7 Optimizing HPDC for Reduced Sticking and Soldering

Optimizing friction in HPDC has the potential to reduce all forms of adhesion, namely sticking and soldering. These adhesion defects have opposite requirements for their reduction. As illustrated in Figure 3 and supported in previous chapters, sticking is reduced with higher ejection temperatures. Soldering is improved by reducing friction, contact pressure, and ejection temperature. The optimum casting conditions will occur when the ejection force and the local Tresca friction conditions are minimized. Both these constraints establish the limits of ejectability for a casting. Once ejection limits are established, process design and operational variables are considered to maximize this operational window. This concept is illustrated by returning to a core in the tube casting (Figure 7), and one-dimensional numerical simulations reveal the operational window (Figure 38).

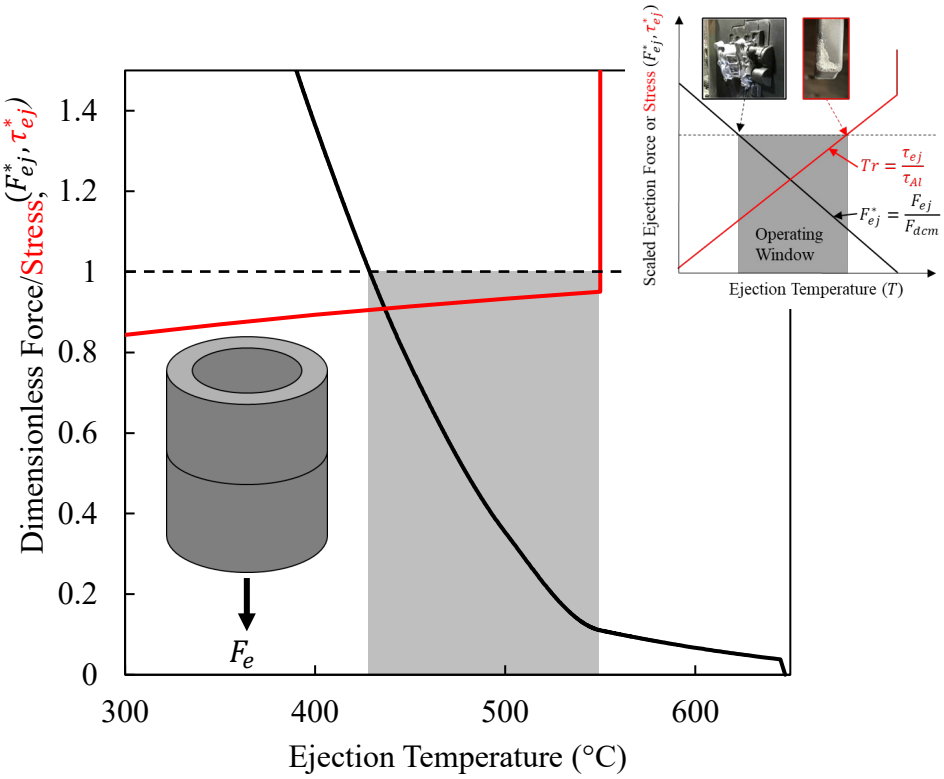

Figure 38: The limits of ejection to avoid sticking and soldering. This is the axis-symmetric case of the general conceptual model proposed in the introduction (Figure 3).

7.1 Axis-Symmetric Phenomenological Model:

There are two components required to predict the operating window for a hypothetical tube casting. First, the thermophysical properties of the casting alloys are required. Second, solidification and cooling were computed. The alloy dependent

temperature versus time prediction was used to calculate the contact pressure. With that pressure the ejection force is predicted over time.

7.1.1 Thermodynamic Modeling:

An investigation of the effect of thermophysical properties was conducted as a function of alloy composition. A broader cross section of alloys was also evaluated for their latent heat of fusion. This is because alloy selection has a significant effect on the solidification time of the casting. HPDC alloys A380, A362, A365, and A518 were all simulated. Both A380 and A362 were simulated with 1 and 0.25 weight percent iron to determine the effect of iron additions. The most common sand and permanent mold alloy, A356, was used as a benchmark. The chemical composition of each alloy is listed in Table 4.

An initial assessment compared the common HPDC alloy A380 to A356 (which is not used in HPDC due to increased sticking and soldering [2]). Typical compositions were assumed to be near the mid-range (Table 4 A380_Typ and A356_Typ), and they were thermodynamically modeled to predict density and enthalpy (Figure 39 a and b). A380 was considered to have iron and manganese near the maximum composition limit as recommended to avoid HPDC soldering. A356 was modeled with slightly elevated magnesium which is preferred to improve strength. Multiplying the density by the enthalpy creates the volumetric heat release for each alloy. This quantity was integrated to plot the cumulative heat release for solidification and cooling (Figure 39 c). Approximately 5% more heat is released when solidifying the A380 alloy versus A356. Thermal conductivity cannot easily be predicted because it depends on the amount of each element in and out of solution. In lieu of modeling, thermal conductivity was assumed to be an approximate linear fit to data from the literature (Figure 39 d) [100], [101].

Table 4: Alloys that were simulated in ThermoCalc [77] for analysis. There chemical compositions represent a typical composition for an initial assessment of the operational window. All other alloys were used to evaluate the effect of alloy on the total heat release as this has a large effect on the size of the operational window.

Alloy	**Cu (%)**	**Fe (%)**	**Mg (%)**	**Mn (%)**	**Si (%)**	**Zn (%)**
A380_Typ	3.5	1.0	0.05	0.35	9.0	1.0
A356_Typ	0.1	0.15	0.4	0.05	7.0	0.05
A380	3.5	0.25	0.05	0.2	8.5	1.0
A362	0.1	0.25	0.6	0.3	11	0.2
A365	0.1	0.25	0.45	0.7	10.5	0.2
A518	0.1	0.2	8.0	0.2	0.1	0.05
A356	0.1	0.2	0.3	0.1	7.0	0.1

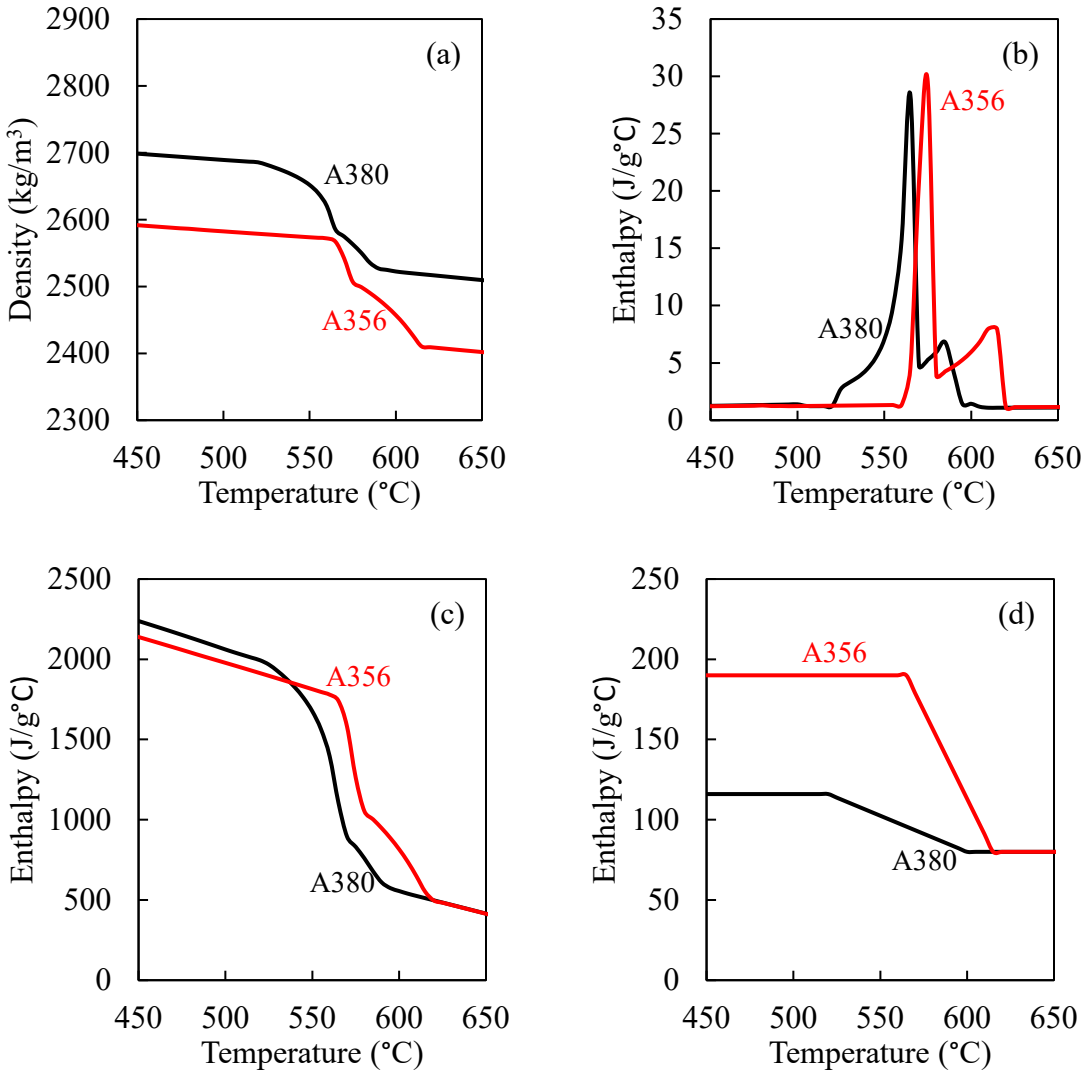

Figure 39: Density (a) and enthalpy (b) of the alloys in Table 4 as predicted by ThermoCalc equilibrium calculations [77]. Cumulative heat release (c) during solidification and cooling of the alloys. (d) Linearized thermal conductivity vs temperature for both alloys based on available literature measurements [100], [101].

Thermal properties of each alloy were calculated using the Scheil equation with back diffusion and a cooling rate of 10°C/s. Scheil is the appropriate model for solidification of aluminum based on the scaling discussion given by Dantzig and Rappaz [102]. Above the liquidus temperature and below the solidus equilibrium conditions were assumed. This results in small variations in the phase fractions that formed during solidification. However, these are all somewhat dilute alloys, and the resulting error was less than 0.4% at the solidus temperature. This is also clearly shown in the smooth transition between equilibrium and Scheil at the solidus temperature in the cumulative heat release plots (Figure 45). All simulations started at 800°C and cooled to 0°C. The

equilibrium calculations used a 10°C step size and the Scheil was 1°C. The system size and pressure were assumed as 1 mol and 1 atm respectively.

7.1.2 Solidification Modeling

Solidification and cooling of two alloys, A380_Typ and A356_Typ, in Table 4 were modeled using the MATLAB [76] version R2020B function PDEPE from the partial differential equation toolbox (eq. 22). Density (ρ) and heat capacity (c_p) are temperature (T) dependent and come directly from the equilibrium thermodynamic simulation. During solidification, the heat capacity includes the latent heat release, and they must be treated as temperature dependent within the differential. Thermal conductivity (k) is also temperature dependent and kept inside the differential on the right hand side of eq. 22. The heat transfer coefficient (HTC) between the casting and die was assumed to be 10,000 W/m^2 °K. This was accounted for by inserting a 10 micro-meter thick thermal resistance layer between the casting and die. Density and heat capacity of this layer was assumed to be unity, and the conductivity of this layer was the product of the desired HTC and the thickness of the barrier.

$$\frac{\partial \rho c_p T}{\partial t} = \nabla^2 kT \qquad \text{(eq. 22)}$$

For all conditions the core, casting, and outer die control volumes were linearly spaced and 0.5 mm thick. The tube thickness was 12 mm with an inner radius of 50 mm. All simulations assumed a 100 mm long tube, and the exterior portion of the die was 50 mm thick. The outer boundary of the mold was convectively cooled through a 10,000 W/m^2 °K heat transfer coefficient to 30°C. Initial metal temperature was uniform at 651°C. The initial die temperature was uniform and varied from 100°C to 250°C. Die thermophysical properties were constant throughout the simulation (Table 5). Casting properties were depended on the results of thermodynamic simulations and literature values. All simulations were run through 60 seconds of solidification and cooling, and all conditions solidified within that time.

Table 5: Die material properties used in 1D simulations.

Die Material	**Density (kg/m^3)**	**Conductivity (W/m°K)**	**Heat Capacity (J/kg)**
H13	7800	16.5	460
H13 High K	7800	25	460
Inconel	8442	12.5	410

Ejection force was assumed to be the contact pressure times the contact area and the coefficient of friction (eq. 6 and 22). The tangential stress was assumed to be the temperature dependent yield stress of the casting. Yield stress was computed according to eqs. 9 through 12. Eq. 20 was solved for the contact pressure assuming the average casting temperature across the thickness. This is a good approximation because the range

of temperatures in the casting was less than 5°C below the solidus temperature. The coefficient of friction was assumed to be 0.6.

An operating window was defined as the duration between two critical ejection times. The longest ejection time, $t_{e,max}$, occurred when the predicted ejection force exceeded the machine capability. For this study a 300 ton die casting machine with 100 kN of maximum ejection force was assumed [94]. Physically, a 100 mm diameter hydraulic cylinder with 140 bar of hydraulic pressure produces this ejection force. The shortest ejection time, $t_{e,min}$, was assumed to be at an ejection temperature of 540°C. It has been shown that some soldering is expected regardless of ejection temperature. However, it will be more severe at higher temperatures, and that casting is likely to deform during ejection. With these two times the ejection operating window can be computed by taking their difference. It is assumed that successful die casting is only possible within this window. Due to process variability, a larger window is preferred.

7.2 Results and Discussion of 1D modeling

Both the simulated temperature and predicted ejection force of the tube casting were plotted versus the simulated solidification and cooling time (Figure 40). As expected, the predicted temperature drop of the casting slows between the liquidus and solidus temperature due to the latent heat release. Ejection force increasing as the casting cools except for the brief time that the temperature is above the liquidus temperature (Figure 40 b). At 35 seconds the casting temperature is still over 350°C which corresponds to a yield strength of roughly 50 MPa in the aluminum.

The operating window was superimposed over the predicted ejection force versus time (Figure 41). Even at a relatively high ejection temperature of 350°C, the large casting contact area translates to a high ejection force exceeding 100 kN. This is despite having a low yield strength. Therefore, the hypothetical die casting machine cannot eject the casting after 21 seconds of cooling time. Soldering limitations make the minimum ejection time approximately 10 seconds. The result is an operating window of 10.8 seconds.

7.3 Alloy Effect on Ejection Limits

The casting alloy selection has an impact on the operating window because the thermophysical properties vary for each alloy as a function of the composition. For example, silicon, copper, and iron composition limits are different between A380_Typ and A356_Typ, Table 4. This causes the significant difference in total heat release of the alloys, Figure 39 (d).

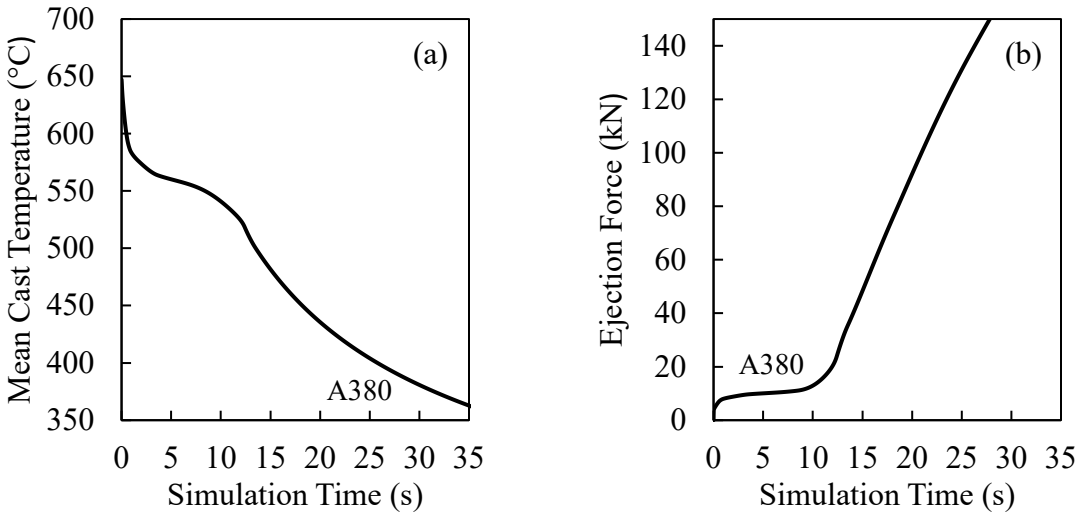

Figure 40: (a) Average casting temperature for a 12 mm tube casting with a 100 mm inner diameter. (b) Modeled contact pressure vs ejection time.

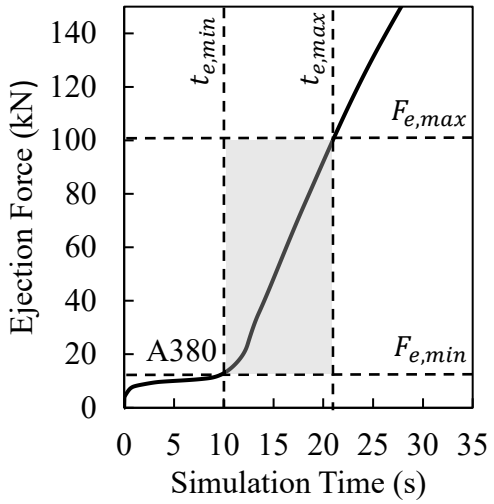

Figure 41: A schematic that illustrates the limits on acceptable ejection times. Excessively short ejection times lead to soldering from a galling mechanism. Long ejection times will stick from thermal contraction.

The higher solidus temperature of A356 holds the casting at a higher temperature than A380 during the initial cooling through solidification. However, the smaller solidification range and lower enthalpy of solidification translates to A356 cooling more rapidly than A380 to the 440°C ejection temperature that causes sticking (Figure 42 a).

Comparison of the predicted ejection force for both alloys was plotted relative to each other (Figure 42 b). The faster cooling A356 experiences increased contact pressure leading to higher ejection force. During the entire 10.8 second operating window of

A380, the ejection force for A356 is approximately 25% higher, and A356 requires a different operation window to avoid sticking and soldering (Figure 42 (b) and Table 6). That process window ($t_{e,max} - t_{e,min}$) is 20% smaller than A380. A356 would be more difficult to cast because it is less tolerant of process variation.

Table 6: Comparison of the modeled maximum and minimum ejection time for the A380 alloy vs the A356 alloy under identical casting conditions assuming a 100 mm diameter hydraulic cylinder with a 140 bar hydraulic pressure.

Alloy	$t_{e,min}$	$t_{e,max}$	$t_{e,max} - t_{e,min}$
A380	10.0	20.8	10.8
A356	9.5	18.0	8.5

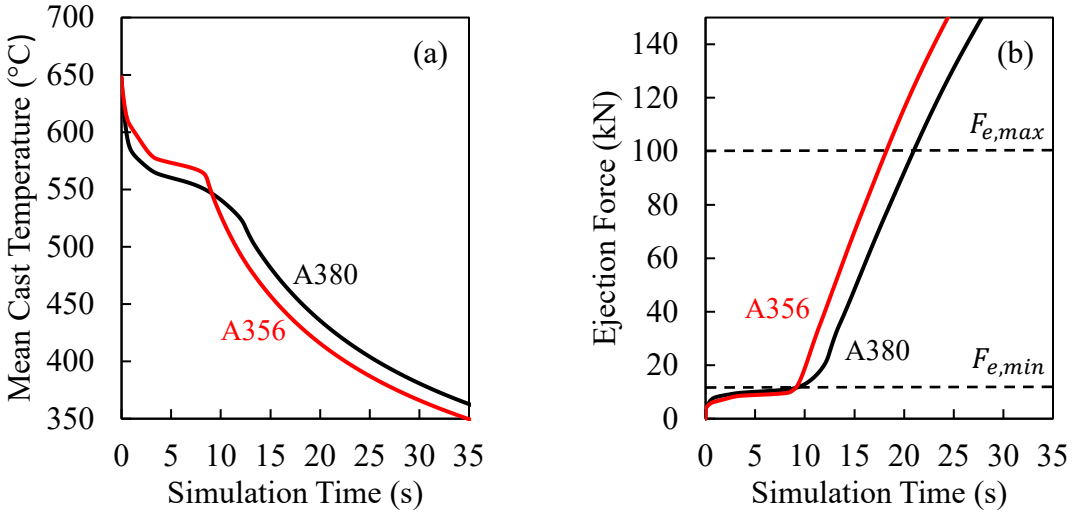

Figure 42: Predicted average casting temperature (a) and ejection force (b) of the alloys from Table 4

To avoid sticking A356 would need approximately 5-10% shorter ejection times than A380. This would enable the A356 to be ejected at the same temperature as A380. This will affect the thermal balance of the tool over multiple cycles. Whether the die will gain temperature or lose temperature cannot be known without fully defining the casting and die design. This is because the location and size of the internal cooling, the spray pattern, spray time, and die extraction time will all affect the thermal history. Regardless, either the process will run colder trending toward increased sticking or hotter trending towards increased soldering. Process redesign will be required to establish a successful process to cast A356.

Stuck castings are the worst failure in the HPDC process. Continuous cycling is interrupted, and the machine is down until the stuck part is removed. Often die damage occurs removing the stuck parts further reducing the productivity of the HPDC machine. Sticking occurs the colder the casting gets in the die. This is one reason why A356 is

more difficult to cast than A380. To avoid sticking the ejection temperatures should be maximized.

Soldering occurs when the hottest area of the die has a high contact pressure creating a locally high Tresca friction factor condition. Interestingly, contact pressure may be reduced when the median casting ejection temperature is raised, and anecdotally, this is an effective way to reduce soldering. When this occurs, the soldering is sometimes referred to as cold soldering [40]. However, the hottest areas of the die may get hotter if the ejection temperature is not raised carefully, and this is the reason avoiding sticking tends to create soldering issues.

7.4 Optimum Design Methodology to Reduce HPDC Adhesion

Other process variables affect the solidification and cooling rate of the casting. This will affect the size of the operating window to avoid sticking and soldering. These effects were investigated relative to casting design, cast alloy selection, die temperature, and die material selection. Casting design was evaluated by changing the casting thickness ($r_o - r_i$) and core diameter. Three alloys from Table 4 were compared: A356, A380, and 518. Four initial die temperatures were run: 100, 150, 200, and 250°C. Die materials were also tested from Table 5.

The main effects all affect the operating window by at least one second (Figure 43 and Figure 44), but none of the tested variables have significant interactions within the single simulated cycle (Appendix B). All the variables have a significant main effect on the operating window, but the strongest variable is the die temperature. This is not typically identified as a key variable. This is likely because it is difficult to modify. The bulk of the heating in HPDC come from consecutive casting cycles and managing the heat extraction from the die. Also, the die surface temperature changes dramatically throughout the cycle. This makes it difficult to even define a die temperature.

The strong dependence on die temperature should be interpreted as a general objective for hotter dies, while cooling the areas that are prone to soldering. A double benefit is gained by this approach. First, the larger ejection window is more tolerant of process variation. Second, the consistent and lower ejection forces translate to lower contact pressure in areas prone to soldering. These areas can now be treated with die coatings and enhanced thermal controls to locally reduce the friction and temperature.

Assuming the casting alloy cannot be changed, then the process design must be adjusted to accommodate difficult alloys. Outside of die temperature increases, insulative lubricants may be a good solution. Higher casting injection temperature or low thermal diffusivity die steels should also work, but these solutions have not been explored as they are far outside the last 100 years of HPDC process experience. Therefore, further study is recommended based on this novel friction-based approach to identify the adhesion process window for HPDC.

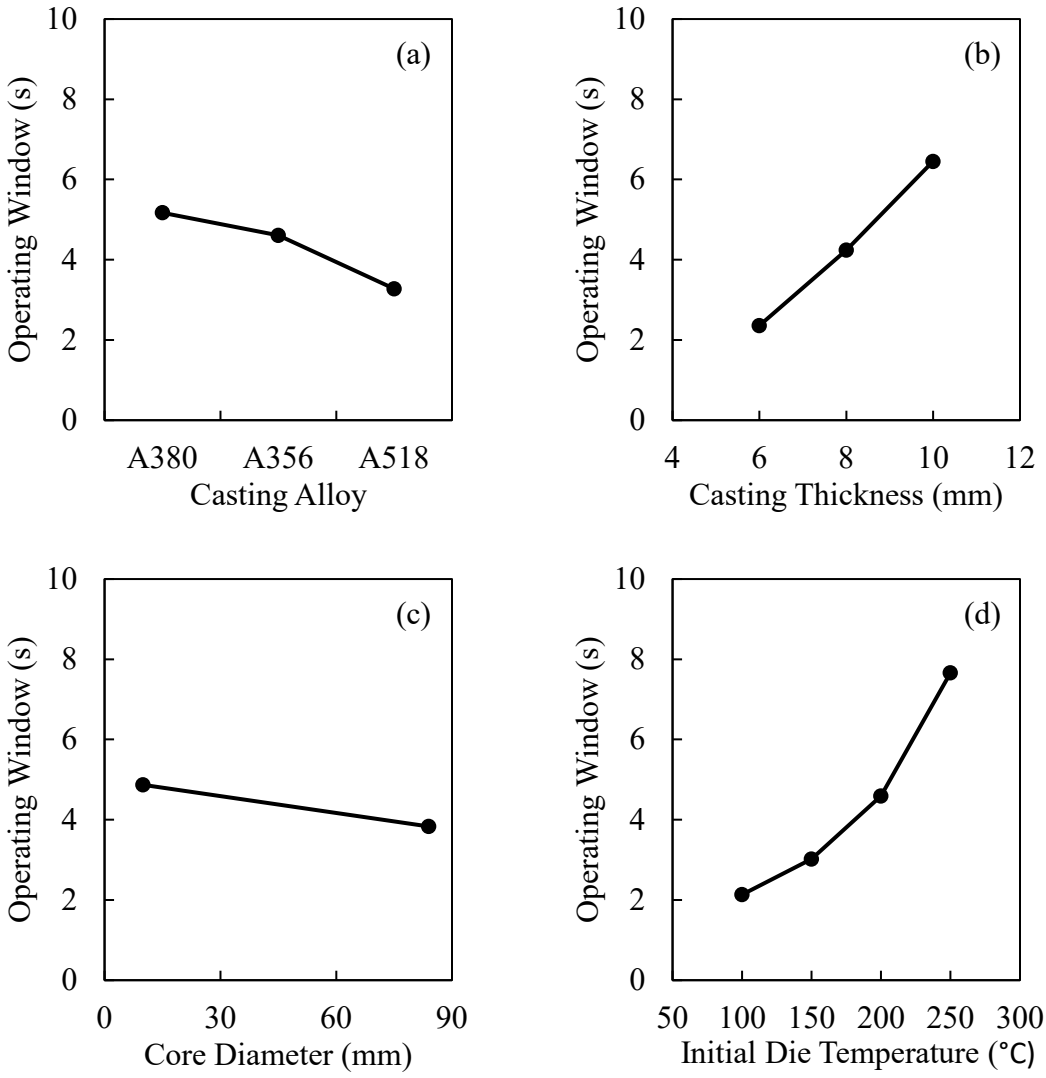

Figure 43: Main effects plots for prediction of the range of possible ejection times for a core in a tubular casting of various, thickness, casting alloy, core diameter, initial die temperature

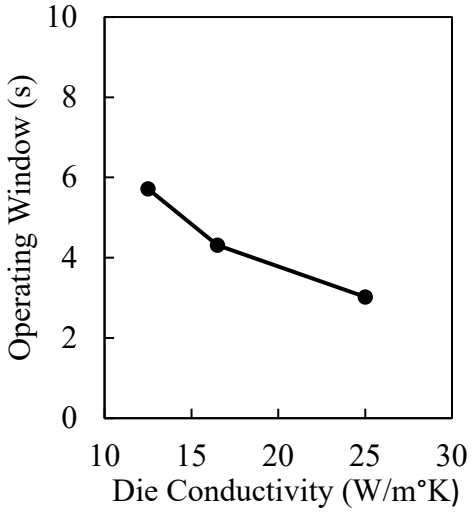

Figure 44: The main effect of die material changes from the full factorial simulation. Different die materials are discerned by their thermal conductivity in Table 5.

7.5 Alloy Optimization to Reduce Contact Pressure

Despite being a relatively low effect on the casting process, the alloy main effect is significant and known to affect the HPDC process (Figure 43 a) [10], [11]. This means some alloys are simply harder to cast than others. Using the ejection process window concept, maximizing the cast alloy latent heat of fusion will widen the window, and this is the main variable for the disparate behavior of A380 and A356 (Figure 39 b and d).

The cumulative volumetric heat release is plotted in Figure 45 for five chemistries in Table 4. A362 releases the most heat. HPDC alloy A518, which is like the commercial alloy family Magsimal, has the least heat release. A356 has the lowest heat release of the hypoeutectic aluminum-silicon alloys. However, it is more like the HPDC alloys, A380, A365, and A362 than A518. The North American Die Casting Association (NADCA) confirms in their 2018 product standards that A518 is a die casting alloy [2], but A356 has a higher cumulative heat release during solidification and cooling than A518 (Figure 45).

NADCA has created a relative rank of the castability of typical HPDC alloys. Alloy A518 is the most difficult on a host of potential casting defects (Figure 46). Most of these defects can be tied to the reduced heat release of A518 compared to other alloys. For example, the filling will be worse because the die will remove heat at a similar rate regardless of the alloy being cast. Less heat of solidification directly results in inferior filling capability. When the mold is partially filled hot cracking and leaking is more likely. 518 will also cool faster in the mold meaning the casting is more likely to stick when cast with similar thermal control and cycle time to the other HPDC alloys.

Comparing these alloys suggests that A356 and similar sand and permanent mold alloys can be high pressure die cast. Thermal control goals must be different like when

casting A518, but the fact A518 is castable means A356 is castable based on the thermo-mechanical model of solder and sticking. In fact, A356 should have lower sticking tendencies than A518. From the heat release data alone, A356 should rank around a 3 or 4 on the NADCA comparison in Figure 46. This also suggests that there is little value in designing an alloy for sticking and solder resistance based purely on their latent heat release. Instead, the process needs to be designed to accommodate the different heat release and strength characteristics of the alloy.

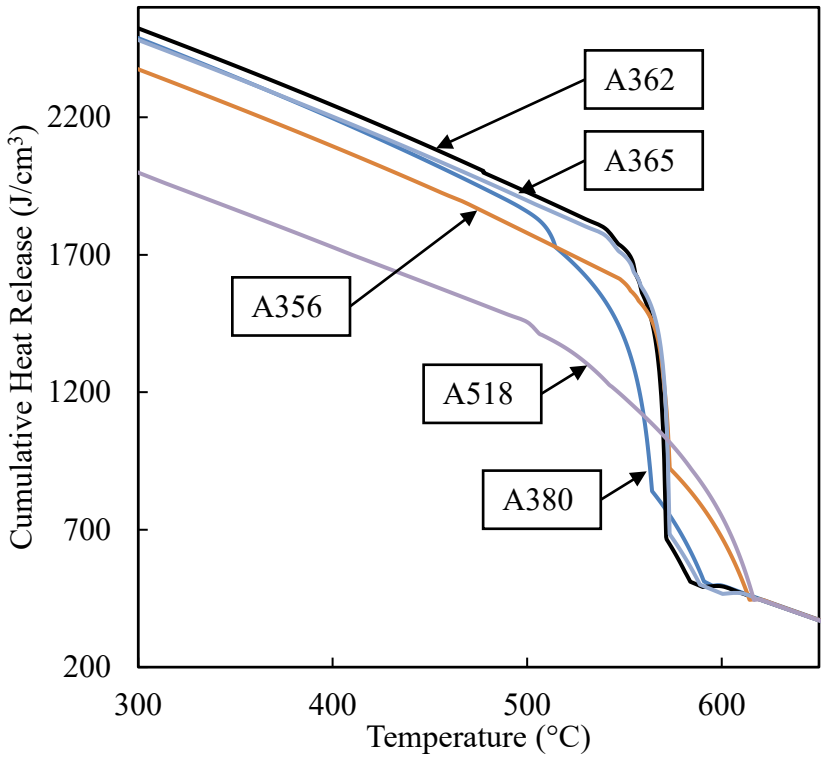

Figure 45: Enthalpy release of alloys in on a per volume basis during solidification and cooling.

The attention on the iron and manganese content for reducing adhesion in HPDC merits further discussion. Two friction related factors may explain the value of these alloy additions for reducing adhesion. First, precipitating energetic primary intermetallic phases add to the latent heat of the alloy, which is potentially significant. Second, these primary intermetallic phases (dispersoids) may increase the strength of the casting at high temperature.

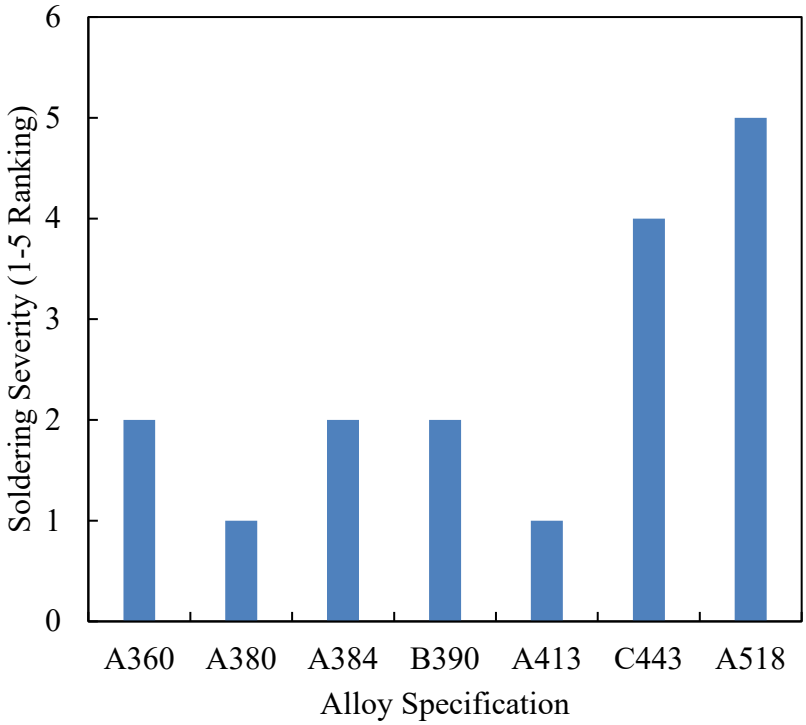

Figure 46: Soldering severity ranking from the NADCA Product Design Standards indicating A518 is castable but it has the worst die filling capacity and anti-solder capability [103].

The thermodynamic model of heat release was repeated for the A380 alloy with the iron increased to 1 wt% and the manganese increased to 0.3 wt%. Only the solidification heat release was run because the solid heat capacity and density is not significantly different with these small alloy changes. The result of adding these elements is a cumulative heat release increase by approximately 3% (Figure 47), which possibly contributes to a more consistent HPDC process.

This suggests a possible explanation of the interest in iron from the early years [35], [39]. It is likely that early die casting alloys ran near the original 2% iron that was allowed in A380 and A360. Like A319 (a sand cast alloy) there was near immediate pressure to remove iron to avoid nuisance cracking from brittle parts. Since die casters had already developed processes to cast assuming 2% iron they immediately ran into sticking issues. As a single factor adding iron to aluminum-silicon alloys will make them less sticky from the increased heat release. Over time, the language was imprecise, and sticking was associated with solder and it became common to use the terms interchangeably. This all happened prior to 1972 when research in die casting started in earnest, and influx of researchers adopted the concept that solder causes sticking. For the last 50 years the research was framed as a search for the cause of soldering to solve all adhesion issues in HPDC, when any alloy is hypothetically castable after adjusting the HPDC process.

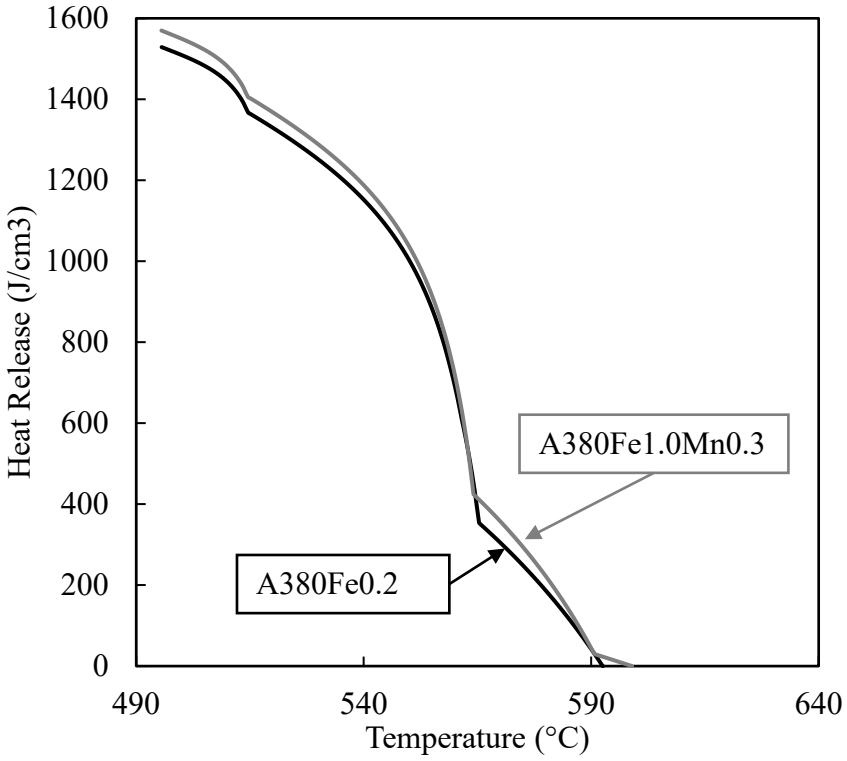

Figure 47: Cumulative heat release during solidification for A380 with 0.2 wt% iron and 0.2 wt% manganese compared to the same alloy with 1 wt% iron and 0.3 wt% manganese. There is a 3% reduction in heat released when iron and manganese are lowered.

The effect of iron and manganese on the high temperature properties of Al-Si alloys has not been well studied. There has been some study up to 200°C for combustion engine application, but to apply to HPDC adhesion the properties are needed up near the solidus temperature of the casting. These properties should be the subject of future work.

8 Conclusions

Friction from thermomechanical interference between the casting and the die was shown as the likely mechanism that causes aluminum to adhere to a HPDC die. Through room temperature ejection tests it was demonstrated that ejection force behaves like an interference fit without the need for a correction term to account for an inherent adhesive force. Similarly, at high temperatures hot ejection tests and 3D simulations show that local soldering correlates to high Tresca friction factors. For these reasons, it is recommended that adhesion defects in HPDC investigated as a frictional wear problem.

Minimizing contact pressure is the most effective way to reduce adhesion issues in HPDC. To achieve this, the optimum design methodology is one that first seeks to maximize casting ejection temperature. Once this has been accomplished, 3D simulation can be used to identify and minimize the temperature of areas that are prone to soldering. These areas can be approximated as the concave features which eject at temperatures near the solidus.

Cooling of the hottest areas of a casting is the simplest solution to soldering. When this is not possible using conventional methods, additive manufacturing offers improved design freedom for conformal cooling passages in the die. In addition, wear resistant coatings are available that have been demonstrated to prevent the rapid destruction of the tooling when soldering does occur. Soldering is, however, best managed when it is properly predicted, and the proposed thermomechanical model promises to enhance the ability to predict soldering.

Al-Mg and Al-Ni alloys are particularly interesting for their unique mechanical properties. They do not need heat treatment reducing cost. These alloys are notoriously difficult to cast, but they may be customized for easy HPDC by applying the thermomechanical model. Small alloy additions may improve the high temperature strength of these alloys systems and reduce their soldering tendency. Similarly, low thermal conductivity tools would aid in filling the die and reduce the sticking by reducing the cooling of these difficult alloys.

Even with the proper mechanism for adhesion identified some cast geometries may not be castable without some die wear due to soldering. In these cases, the well-established reaction between the cast material and die accelerates the failure of the die. Fortunately, many coating systems have been developed that eliminate the potential for these reactions. Further development of these coatings for reduced friction would enhance their effectiveness.

Finally, a commercial casting simulation code was used to develop and apply the criteria for sticking and soldering. As these tools continue to advance, it is now possible to quickly troubleshoot die castings virtually and identify solutions. With increasing availability of stochastic modeling, the power of these simulation codes will continue to increase in their predictive power, especially if they incorporate the proper physical and mechanical mechanisms for prediction of adhesion defects.

9 References

[1] S. P. Udvardy, “2019 State of the Die Casting Industry,” *Die Casting Engineer*, no. January, p. 6, 2019.

[2] *2018 Product Specification Standards for Die Castings*, 2018th ed. North American Die Casting Association.

[3] R. J. Donahue and G. K. Sigworth, “Die Casting Alloys that will Allow the Die Caster to Compete with Alloys A356, A357, 358 and 359 in PM Applications,” p. 17.

[4] Aoyama, Shunzo, Akase, Makota, Sakamoto, Katsumi, and Umemura, Teruyoshi, “Die Lubricant Deposit and Its Effect on Ejection in Die Casting,” vol. T91-112.

[5] R. A. Miller, “Fluidity from a Heat Transfer Perspective,” in *NADCA Transactions*, Ohio, Sep. 2016, vol. T16-081. Accessed: Apr. 10, 2018. [Online]. Available: https://www.diecasting.org/archive/transactions/T16-081.pdf

[6] R. N. Lumley, I. J. Polmear, H. Groot, and J. Ferrier, “Thermal characteristics of heat-treated aluminum high-pressure die-castings,” *Scr. Mater.*, vol. 58, no. 11, pp. 1006–1009, Jun. 2008, doi: 10.1016/j.scriptamat.2008.01.031.

[7] D. Blondheim, Jr. and A. Monroe, “Macro Porosity Formation - A Study in High Pressure Die Casting,” *Int. J. Met.*, 2021, doi: https://doi.org/10.1007/s40962-021-00602-x.

[8] B. Wang, G. R. Bourne, A. L. Korenyi-Both, S. P. Midson, and M. J. Kaufman, “An investigation of the use of PVD die coatings to minimize or eliminate lubrication during high pressure die casting,” in *North American Die Casting Congress*, 2016, vol. T16-061.

[9] Chu, Yeou-Li, Cheng, Patrick, and Shivpuri, Rajiv, “Soldering Phenomenon in Aluminum Die Casting: Possible Causes and Cures,” in *North American Die Casting Congress*, Cleveland, OH, Oct. 1993, pp. 361–372.

[10] Tosa, Hiroki and Urakami, Akio, “Factors Influencing Die Casting Ejection,” in *North American Die Casting Congress*, Chicago, IL, 1972, vol. T72-041.

[11] B. Wang, G. R. Bourne, A. L. Korenyi-Both, A. K. Monroe, S. P. Midson, and M. J. Kaufman, “Method to evaluate the adhesion behavior of aluminum-based alloys on various materials and coatings for lube-free die casting,” *J. Mater. Process. Technol.*, vol. 237, pp. 386–393, 2016, doi: 10.1016/j.jmatprotec.2016.06.031.

[12] S.-B. Kim, Y.-H. Yim, and D.-H. Roh, “Prediction of Die Soldering in Die Casting by a Numerical Algorithm based on the Combination of Thermal and Fluid Factors Verified with Experimental Results,” in *Die Casting Congress and Tabletop*, Cleveland, OH, 2019, p. 9.

[13] K. Domkin, J. H. Hattel, and J. Thorborg, “Modeling of high temperature- and diffusion-controlled die soldering in aluminum high pressure die casting,” *J. Mater. Process. Technol.*, vol. 209, no. 8, pp. 4051–4061, 2009, doi: 10.1016/j.jmatprotec.2008.09.031.

[14] D. Tabor, “Friction - the present state of our understanding,” *J. Lubr. Technol.*, vol. 103, no. 2, pp. 169–179, Apr. 1981.

[15] F. Widerøe and T. Welo, “Conditions for Sticking Friction between Aluminium Alloy AA6060 and Tool Steel in Hot Forming,” *Key Eng. Mater.*, vol. 491, pp. 121–128, Sep. 2011, doi: 10.4028/www.scientific.net/KEM.491.121.

[16] H. Wang and C. A. Loong, “Experimental Studies on Ejection FORCES of a die cast Aluminum Part,” in *North American Die Casting Congress*, Cleveland, OH, 1999, vol. T99-052.
[17] M. J. Roy, D. M. Maijer, and L. Dancoine, “Constitutive behavior of as-cast A356,” *Mater. Sci. Eng. A*, vol. 548, pp. 195–205, Jun. 2012, doi: 10.1016/j.msea.2012.03.106.
[18] Shankar, Samantha and Apelian, Diran, “Die Soldering: Mechanism of the interface reaction between molten aluminum alloy and tool steel,” vol. 33B, no. June 2002, pp. 465–476, doi: 10.1007/s11663-002-0057-7.
[19] *ASM Handbook: Welding, Brazing, and Soldering*, vol. 6. ASM International (R), Materials Park, Ohio, USA, 1993.
[20] A. Long, D. Thornhill, C. Armstrong, and D. Watson, “Predicting die life from die temperature for high pressure dies casting aluminium alloy,” *Appl. Therm. Eng.*, vol. 44, pp. 100–107, Nov. 2012, doi: 10.1016/j.applthermaleng.2012.03.045.
[21] A. Long, D. Thornhill, C. Armstrong, and D. Watson, “Determination of the heat transfer coefficient at the metal–die interface for high pressure die cast AlSi9Cu3Fe,” *Appl. Therm. Eng.*, vol. 31, no. 17–18, pp. 3996–4006, Dec. 2011, doi: 10.1016/j.applthermaleng.2011.07.052.
[22] Z. W. Chen, “Formation and progression of die soldering during high pressure die casting,” *Mater. Sci. Eng. A*, vol. 397, no. 1–2, pp. 356–369, 2005, doi: 10.1016/j.msea.2005.02.057.
[23] Y. Zhu, D. Schwam, J. F. Wallace, and S. Birceanu, “Evaluation of soldering, washout and thermal fatigue resistance of advanced metal materials for aluminum die-casting dies,” *Mater. Sci. Eng. A*, vol. 379, no. 1–2, pp. 420–431, 2004, doi: 10.1016/j.msea.2004.03.020.
[24] Chu, Yeou-Li, Balasubramaniam, Srikanth, Rajan, Rajendra, and Shivpuri, Rajiv, “A Study of the Cast Alloy-Die Surface Interactions in Aluminum Die Casting,” in *North American Die Casting Congress*, Minneapolis, MN, 1997, vol. T97-075. [Online]. Available: https://diecasting.org/wcm/Technology/Technical_Archive/wcm/Technology/Technical_Archive.aspx?hkey=62f825ba-424c-41c3-b10f-3b860771ffa4
[25] S. Gulizia, M. Z. Jahedi, and E. D. Doyle, “Performance evaluation of PVD coatings for high pressure die casting,” *Surf. Coat. Technol.*, vol. 140, no. 3, pp. 200–205, Jun. 2001, doi: 10.1016/S0257-8972(01)01037-4.
[26] Hairy, P. and Richard, M., “Reduction of Sticking in Pressure Die Casting by Surface Treatment,” in *North American Die Casting Congress*, 1997, vol. T97-102.
[27] K. Bobzin, T. Brögelmann, U. Hartmann, and N. C. Kruppe, “Analysis of CrN/AlN/Al2O3 and two industrially used coatings deposited on die casting cores after application in an aluminum die casting machine,” *Surf. Coat. Technol.*, vol. 308, pp. 374–382, Dec. 2016, doi: 10.1016/j.surfcoat.2016.09.040.
[28] Q. Han and S. Viswanathan, “Analysis of the Mechanism of Die Soldering in Aluminum Die Casting,” *Metall. Mater. Trans. A*, vol. 34A, no. January, pp. 139–146, 2003.

[29] Shankar, Sumanth and Apelian, Diran, “Mechanism and Preventive Measures for Die Soldering during Al Casting in a Ferrous Mold,” *JOM*, vol. 54, no. August 2002, pp. 47–54, doi: 10.1007/BF02711867.
[30] C. Mitterer, F. Holler, F. Üstel, and D. Heim, “Application of hard coatings in aluminium die casting — soldering, erosion and thermal fatigue behaviour,” *Surf. Coat. Technol.*, vol. 125, no. 1–3, pp. 233–239, Mar. 2000, doi: 10.1016/S0257-8972(99)00557-5.
[31] Norstrom, Lars-Ake, Klarenfjord, Bengt, and Svensson, Maths, “General Aspects on ‘Washout’ Mechanisms in Aluminum Die Casting Dies,” 1993, vol. T93-075–1.
[32] M. Yu, R. Shivpuri, and R. A. Rapp, “Effects of Molten Aluminum on H13 Dies and Coatings,” *J. Mater. Eng. Perform.*, vol. 4, no. 2, pp. 175–181, Apr. 1995.
[33] R. J. Barnhurst, D. Argo, and W. Walkington, “NADCA Sponsored Research: The Causes of Soldering in Zinc Die Casting,” in *Die Casting Congress*, 1997, vol. T97-033.
[34] M. Stern, “PROGRESS_OF_DIE-CASTING_INDUSTRY,” in *Transactions of the American Foundrymen’s Association*, 1930, vol. 37, pp. 723–733.
[35] W. Bonsack, “Trends in Aluminum Casting Alloys,” in *Transactions of the American Foundrymen’s Association*, 1950, vol. 76, pp. 69–75.
[36] D. L. Colwell and E. Trela, “New Aluminum Die Casting Alloys,” in *Transactions of the American Foundrymen’s Association*, 1954, vol. 93, pp. 359–364.
[37] D. L. Colwell and O. Tichy, “Machinability of Aluminum Die Castings,” in *Transactions of the American Foundrymen’s Association*, 1956, vol. 92, pp. 236–241.
[38] S. U. Siena, “Die Casting Aluminum Alloys by the Cold Chamber Process,” 1944.
[39] W. Bonsack, “Iron-The Problematic Factor in Quality Of Aluminum Alloy Die Castings,” in *Transactions of the American Foundrymen’s Association*, 1961, vol. 114, pp. 712–720.
[40] Holz, Earl K., “Trouble Shooting Aluminum Die Casting Quality Problems,” in *7th SDCE International Die Casting Congress*, Chicago, IL, 1972, vol. T72-043.
[41] Kajoch, Wladyslaw and Fajkiel, Alexander, “Testing the Soldering Tendencies of Aluminum Die Casting Alloy,” in *North American Die Casting Congress*, Detroit, MI, Oct. 1991, vol. T91-034, pp. 67–74.
[42] W. Jonsson, “THE EFFECT OF IRON AND MAGNESIUM ON TEH PROPERTIES OF ALUMINUM DIE CASTING ALLOYS,” Nov. 1964, p. 8.
[43] Chu, Yeou-Li, Cheng, Patrick, and Shivpuri, Rajiv, “Investigation of the soldering problem in aluminum die casting - Phenomena, mechanism and protection,” National Science Foundation Engineering Research Center for Net Shape Manufacturing, NADCA Technical Archive, ERC/NSM-C-93-36, Sep. 1993.
[44] Y. Tsuchiya, H. Kawaura, K. Hashimoto, H. Inagaki, and T. Arai, “Core Pin Failure in Aluminum Die Casting and the Effect of Surface Treatment,” in *The Many Faces of Die Casting*, Minneapolis, MN, 1997, vol. T97-103.
[45] Z. W. Chen, D. T. Fraser, and M. Z. Jahedi, “Structures of intermetallic phases formed during immersion of H13 tool steel in an Al–11Si–3Cu die casting alloy melt,” *Mater. Sci. Eng. A*, vol. 260, no. 1–2, pp. 188–196, Feb. 1999, doi: 10.1016/S0921-5093(98)00963-0.

[46] R. J. Barnhurst, D. Argo, and W. Walkington, “NADCA Sponsored Research: The Causes of Soldering in Zinc Die Casting,” in *Die Casting Congress*, 1997, vol. T97-033.
[47] J. Song, X. Wang, T. DenOuden, and Q. Han, “Evolution of Intermetallic Phases in Soldering of the Die Casting of Aluminum Alloys,” *Metall. Mater. Trans. A*, vol. 47, no. 6, pp. 2609–2615, 2016, doi: 10.1007/s11661-016-3454-2.
[48] A. Duarte, F. J. Oliveira, and F. M. Costa, “Characterisation of interface formed at 650°C between AISI H13 steel and Al–12Si–1Cu aluminium melt,” *Int. J. Cast Met. Res.*, vol. 23, no. 4, pp. 231–239, Aug. 2010, doi: 10.1179/136404610X12665088537455.
[49] S. Sumanth and A. Diran, “The Role of Aluminum Alloy Chemistry and Die Material on Die Soldering,” in *North American Die Casting Congress*, Cleveland, OH, 1999, vol. T99-083. [Online]. Available: https://diecasting.org/wcm/Technology/Technical_Archive/wcm/Technology/Technical_Archive.aspx?hkey=62f825ba-424c-41c3-b10f-3b860771ffa4
[50] M. Vilaseca, S. Molas, and D. Casellas, “High temperature tribological behaviour of tool steels during sliding against aluminium,” *Wear*, 2011, doi: 10.1016/j.wear.2011.07.007.
[51] P. Terek *et al.*, “Effects of die core treatments and surface finishes on the sticking and galling tendency of Al-Si alloy casting during ejection,” *Wear*, vol. 356–357, pp. 122–134, Jun. 2016, doi: https://doi.org/10.1016/j.wear.2016.03.016.
[52] H. Cagin, “Techniques for Removing Stuck Castings,” in *NADCA Transactions*, Jun. 1981, vol. T81-025, p. 4.
[53] P. Terek *et al.*, “The Influence of CrAlN Coating Chemical Composition on Soldering Resistance in Contact with Al-Si-Cu Alloy,” *Mater. Proc.*, vol. 2, no. 1, p. 28, May 2020, doi: 10.3390/CIWC2020-06837.
[54] P. Terek, L. Kovačević, A. Miletić, D. Kukuruzović, S. Baloš, and B. Škorić, “Improved ejection test for evaluation of soldering tendency of cast alloy to die core materials,” *J. Mater. Process. Technol.*, vol. 266, pp. 114–124, Apr. 2019, doi: 10.1016/j.jmatprotec.2018.10.038.
[55] Chen, Z. W. and Jahedi, M. Z., “Die erosion and its effect on soldering formation in high pressure die casting of aluminum alloys,” *Mater. Des.*, vol. 20, pp. 303–309, 1999.
[56] J. Jerina and M. Kalin, “Initiation and evolution of the aluminium-alloy transfer on hot-work tool steel at temperatures from 20 °C to 500 °C,” *Wear*, vol. 319, no. 1–2, pp. 234–244, Nov. 2014, doi: 10.1016/j.wear.2014.07.021.
[57] R. Kimura, M. Yoshida, G. Sasaki, J. Pan, and H. Fukunaga, “Characterization of heat insulating and lubricating ability of powder lubricants for clean and high quality die casting,” *J. Mater. Process. Technol.*, vol. 130–131, pp. 289–293, Dec. 2002, doi: 10.1016/S0924-0136(02)00808-7.
[58] N. Nishi, “Challenge to Ultra Thin-Wall Zinc Die Casting under 0.5 mm Thickness,” *Cast. Eng.*, no. September 2007, p. 5, 2007.
[59] *MAGMAsoft*. Kackerstrasse 11, 52072 Aachen, Germany: MAGMA Gmbh, 2019.

[60] T. Cedorge and J. Colton, “Draft angle and surface roughness effects on sterolighography molds,” *Polym. Eng. Sci. Newtown*, vol. 40, no. 7, p. 1581, Jul. 2000.
[61] A. E. Palmer and J. S. Colton, “Failure mechanisms in stereolithography injection molding tooling,” *Polym. Eng. Sci.*, vol. 40, no. 6, pp. 1395–1404, Jun. 2000, doi: 10.1002/pen.11269.
[62] G. T. Pham and J. S. Colton, “Ejection force modeling for stereolithography injection molding tools,” *Polym. Eng. Sci.*, vol. 42, no. 4, pp. 681–693, Apr. 2002, doi: 10.1002/pen.10981.
[63] B. Omar and K. Barney, “Prediction of Local Part-Mold and Ejection Force in Injection Molding,” *Trans. ASME*, vol. 127, no. August 2005, pp. 598–604, Aug. 2005, doi: 10.1115/1.1951785.
[64] S. Tetsuo, K. Nobuhiro, S. Kenji, K. Yoshikazu, and T. Ayumu, “An experimental study on ejection forces of injection molding,” *J. Int. Soc. Precis. Eng. Nanotechnol.*, vol. 24, pp. 270–273, 2000, doi: 0141-6359/00/.
[65] M. Sorgato, D. Masato, and G. Lucchetta, “Effects of machined cavity texture on ejection force in micro injection molding,” *Precis. Eng.*, vol. 50, pp. 440–448, 2017, doi: 10.1016/j.precisioneng.2017.06.019.
[66] Monroe, Alexander, Gaddam, Deepika, and Glim, Beau, “Preliminary Study on Ejection Force Prediction,” *NADCA Congr. Tabletop*, vol. T16-083, 2016.
[67] A. L. ALTIERI and P. H. STEEN, “Adhesion Upon Solidification and Detachment in the Melt Spinning of Metals,” *Metall. Mater. Trans. B*, vol. VOLUME 45B, pp. 2262–2268, Dec. 2014, doi: 10.1007/s11663-014-0128-6.
[68] M. D. Hanna, “Tribological evaluation of aluminum and magnesium sheet forming at high temperatures,” *Wear*, vol. 267, no. 5–8, pp. 1046–1050, Jun. 2009, doi: 10.1016/j.wear.2009.01.007.
[69] H. Kitano, K. Dohda, M. Kalin, and K. F. Ehmann, “Galling growth analysis in metal forming,” *Manuf. Lett.*, vol. 16, pp. 32–35, Apr. 2018, doi: 10.1016/j.mfglet.2018.03.003.
[70] E. Huttunen-Saarivirta, L. Kilpi, T. J. Hakala, J. Metsäjoki, and H. Ronkainen, “Insights into the behaviour of tool steel-aluminium alloy tribopair at different temperatures,” *Tribol. Int.*, vol. 119, pp. 567–584, Mar. 2018, doi: 10.1016/j.triboint.2017.11.041.
[71] L. Wang and H. Yang, “Friction in aluminium extrusion—part 2: A review of friction models for aluminium extrusion,” *Tribol. Int.*, vol. 56, pp. 99–106, Dec. 2012, doi: 10.1016/j.triboint.2012.06.006.
[72] X. Ma, M. de Rooij, and D. Schipper, “A load dependent friction model for fully plastic contact conditions,” *Wear*, vol. 269, no. 11–12, pp. 790–796, Oct. 2010, doi: 10.1016/j.wear.2010.08.005.
[73] X. Ma, M. B. de Rooij, and D. J. Schipper, “Friction conditions in the bearing area of an aluminium extrusion process,” *Wear*, vol. 278–279, pp. 1–8, Mar. 2012, doi: 10.1016/j.wear.2011.11.001.
[74] L. Wang, J. Zhou, J. Duszczyk, and L. Katgerman, “Friction in aluminium extrusion—Part 1: A review of friction testing techniques for aluminium

extrusion," *Tribol. Int.*, vol. 56, pp. 89–98, Dec. 2012, doi: 10.1016/j.triboint.2012.01.012.
[75] J. Shigley, C. Mischke, and R. Budynas, *Mechanical Engineering Design*, 7th Edition. McGraw-Hill, 2004.
[76] *MATLAB*. Natick, Massachusetts: Mathworks, 2020.
[77] J. O. Andersson, T. Helander, P. F. Shi, and B. Sundman, *Thermo-Calc and DICTRA, Computational tools for material science*. 2002.
[78] H. Springer, A. Kostka, J. F. dos Santos, and D. Raabe, "Influence of intermetallic phases and Kirkendall-porosity on the mechanical properties of joints between steel and aluminium alloys," *Mater. Sci. Eng. A*, vol. 528, no. 13–14, pp. 4630–4642, May 2011, doi: 10.1016/j.msea.2011.02.057.
[79] H. Springer, A. Kostka, E. J. Payton, D. Raabe, A. Kaysser-Pyzalla, and G. Eggeler, "On the formation and growth of intermetallic phases during interdiffusion between low-carbon steel and aluminum alloys," *Acta Mater.*, vol. 59, no. 4, pp. 1586–1600, Feb. 2011, doi: 10.1016/j.actamat.2010.11.023.
[80] V. Jindal, V. C. Srivastava, A. Das, and R. N. Ghosh, "Reactive diffusion in the roll bonded iron–aluminum system," *Mater. Lett.*, vol. 60, no. 13–14, pp. 1758–1761, Jun. 2006, doi: 10.1016/j.matlet.2005.12.013.
[81] Z. W. Chen, "Formation and progression of die soldering during high pressure die casting," *Mater. Sci. Eng. A*, vol. 397, no. 1–2, pp. 356–369, 2005, doi: 10.1016/j.msea.2005.02.057.
[82] C. Z. W., J. M.Z., and L. J.A., "Metallurgical Phenomena in Die/Casting Interfacial Regions During High Pressure Die Casting of Aluminum Alloys," in *North American Die Casting Congress*, Cleveland, OH, 1999, vol. T99-084.
[83] A. Bouayad, C. Gerometta, A. Belkebir, and A. Ambari, "Kinetic interactions between solid iron and molten aluminium," *Mater. Sci. Eng. A*, vol. 363, no. 1–2, pp. 53–61, Dec. 2003, doi: 10.1016/S0921-5093(03)00469-6.
[84] F. Yin, M. Zhao, Y. Liu, W. Han, and Z. Li, "Effect of Si on growth kinetics of intermetallic compounds during reaction between solid iron and molten aluminum," *Trans. Nonferrous Met. Soc. China*, vol. 23, no. 2, pp. 556–561, Feb. 2013, doi: 10.1016/S1003-6326(13)62499-1.
[85] G. Eggeler, W. Auer, and H. Kaesche, "REACTIONS BETWEEN LOW ALLOYED STEEL AND INITIALLY PURE AS WELL AS IRON-SATURATED ALUMINUM MELTS BETWEEN 670 AND 800-DEGREES-C," *Z. Met.*, vol. 77, no. 4, pp. 239–244, 1986.
[86] Makhlouf M. Makhlouf and Diran Apelian, "Casting Characteristics of Aluminum Die Casting Alloys," DOE/ID/13716, 792701, Feb. 2002. doi: 10.2172/792701.
[87] A. Zovi and F. Casarotto, "SILAFONT-36, THE LOW IRON DUCTILE DIE CASTING ALLOY DEVELOPMENT AND APPLICATIONS," *Metall. Ital.*, 2007, [Online]. Available: https://www.fracturae.com/index.php/aim/article/view/517/488
[88] Chu, Yeou-Li, Balasubramaniam, Srikanth, Rajan, Rajendra, and Shivpuri, Rajiv, "A Study of the Cast Alloy-Die Surface Interactions in Aluminum Die Casting," vol. T97-075, 1997.

[89] Yu, Mulong, Chu, Yeou-Li, and Shivpuri, Rajiv, "A Study of Corrosion of Die Materials and Die Coatings in Aluminum Die Casting," in *North American Die Casting Congress*, Cleveland, OH, Oct. 1993, vol. T93-072, pp. 191–198.
[90] M. Movahedi, A. H. Kokabi, and S. M. Seyed Reihani, "Investigation on the bond strength of Al-1100/St-12 roll bonded sheets, optimization and characterization," *Mater. Des.*, vol. 32, no. 6, pp. 3143–3149, Jun. 2011, doi: 10.1016/j.matdes.2011.02.057.
[91] M. Roulin and J. W. Luster, "Strength and Structure of Furnace-Brazed Joints between Aluminum and Stainless Steel," *Weld. Res. Suppl.*, vol. 78, no. 5, pp. 151–155, May 1999.
[92] J. Vrenken, C. Goos, T. Veldt, and W. Braunschweig, "Fluxless Laser Brazing of Aluminium to Steel," *Join. Automot. Eng.*, 2009, [Online]. Available: Fluxless Laser Brazing of Aluminium to Steel
[93] Tosa, Hiroki and Urakami, Akio, "Factors Influencing Die Casting Ejection," in *North American Die Casting Congress*, Chicago, IL, Oct. 1972, vol. T72-041.
[94] "Buhler Evolution Die Casting Machine Brochure." Buhler. Accessed: May 01, 2021. [Online]. Available: https://www.buhlergroup.com/content/buhlergroup/global/en/products/evolution_die-castingmachineevolution.html
[95] J. Lu, Y. Song, L. Hua, P. Zhou, and G. Xie, "Effect of temperature on friction and galling behavior of 7075 aluminum alloy sheet based on ball-on-plate sliding test," *Tribol. Int.*, vol. 140, p. 105872, Dec. 2019, doi: 10.1016/j.triboint.2019.105872.
[96] C. M. Estey, S. L. Cockcroft, D. M. Maijer, and C. Hermesmann, "Constitutive behaviour of A356 during the quenching operation," *Mater. Sci. Eng. A*, vol. 383, no. 2, pp. 245–251, Oct. 2004, doi: 10.1016/j.msea.2004.06.004.
[97] A. Alankar and M. A. Wells, "Constitutive behavior of as-cast aluminum alloys AA3104, AA5182 and AA6111 at below solidus temperatures," *Mater. Sci. Eng. A*, vol. 527, no. 29–30, pp. 7812–7820, Nov. 2010, doi: 10.1016/j.msea.2010.08.056.
[98] C. H. Cáceres, "A Rationale for the Quality Index of Al-Si-Mg Casting Alloys," p. 17, 1998.
[99] F. A. Nichols, "Plastic instabilities and uniaxial tensile ductilities," *Acta Metall.*, vol. 28, no. 6, pp. 663–673, Jun. 1980, doi: 10.1016/0001-6160(80)90144-3.
[100] R. Overfelt, S. Bakhtiyarov, and R. Taylor, "Thermophysical properties of A201, A319, and A356 aluminium casting alloys," *High Temp.-High Press.*, vol. 34, no. 4, pp. 401–409, 2002, doi: 10.1068/htjr052.
[101] R. Brandt and G. Neuer, "Electrical Resistivity and Thermal Conductivity of Pure Aluminum and Aluminum Alloys up to and above the Melting Temperature," *Int. J. Thermophys.*, vol. 28, no. 5, pp. 1429–1446, Nov. 2007, doi: 10.1007/s10765-006-0144-0.
[102] J. A. Dantzig and M. Rappaz, *Solidification*, 1 st. EPFL Press, 2009.
[103] P. Brancaleon, "Specifications and Standards Development for Enhanced Casting Performance through Examination of Mechanical Properties versus Casting Section Thickness," in *NADCA Transactions*, Virtual Event, 2020, p. 7.

A Drawings of test molds

A.1 Print of room temperature ejection mold

All dimensions are in millimeters, and many core pin draft anlges were employed for tests.

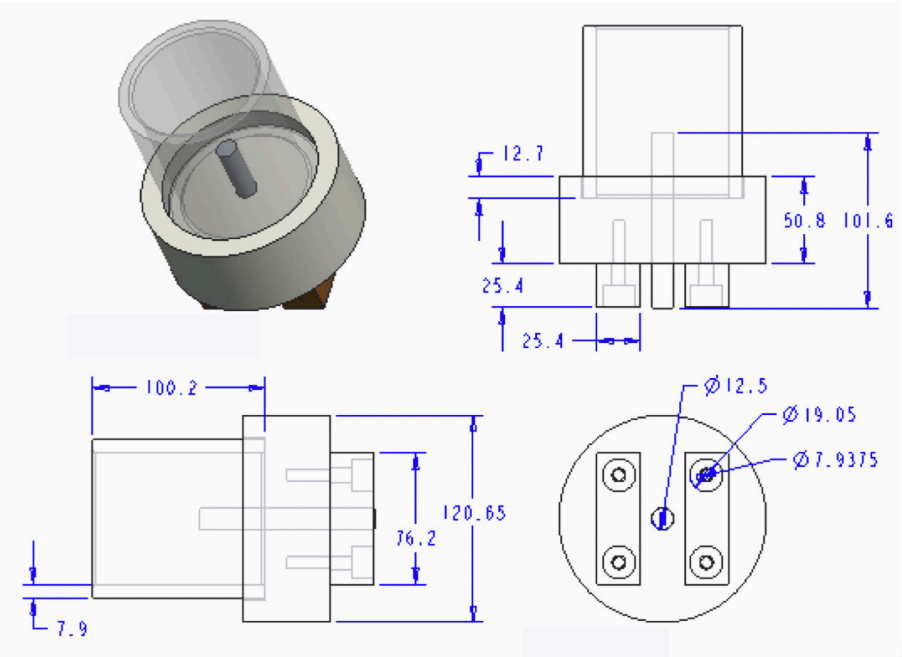

A.2 Print of hot ejection test core

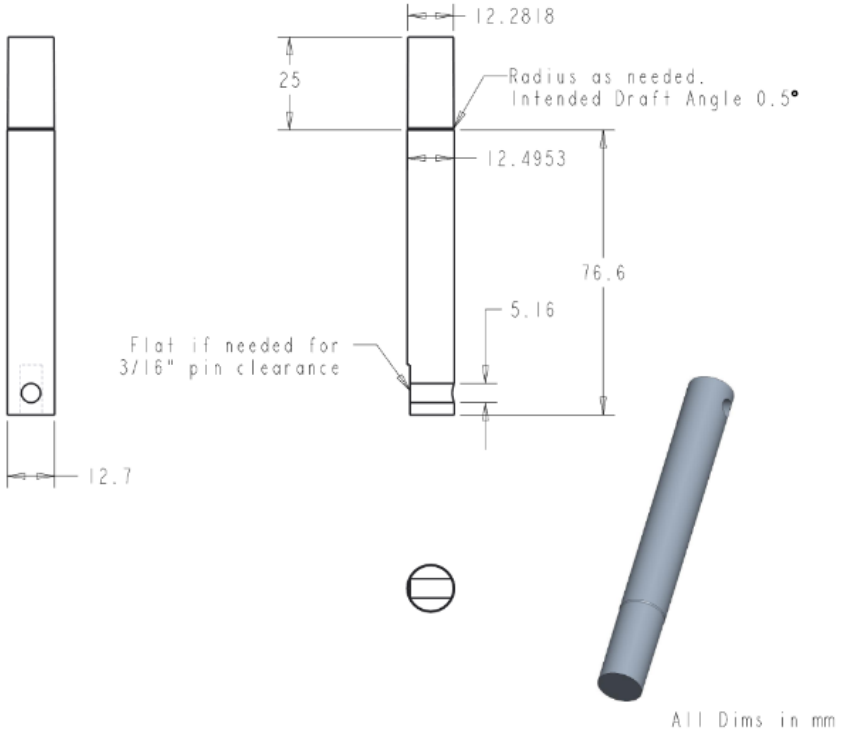

A.3 Print of hot ejection test mold

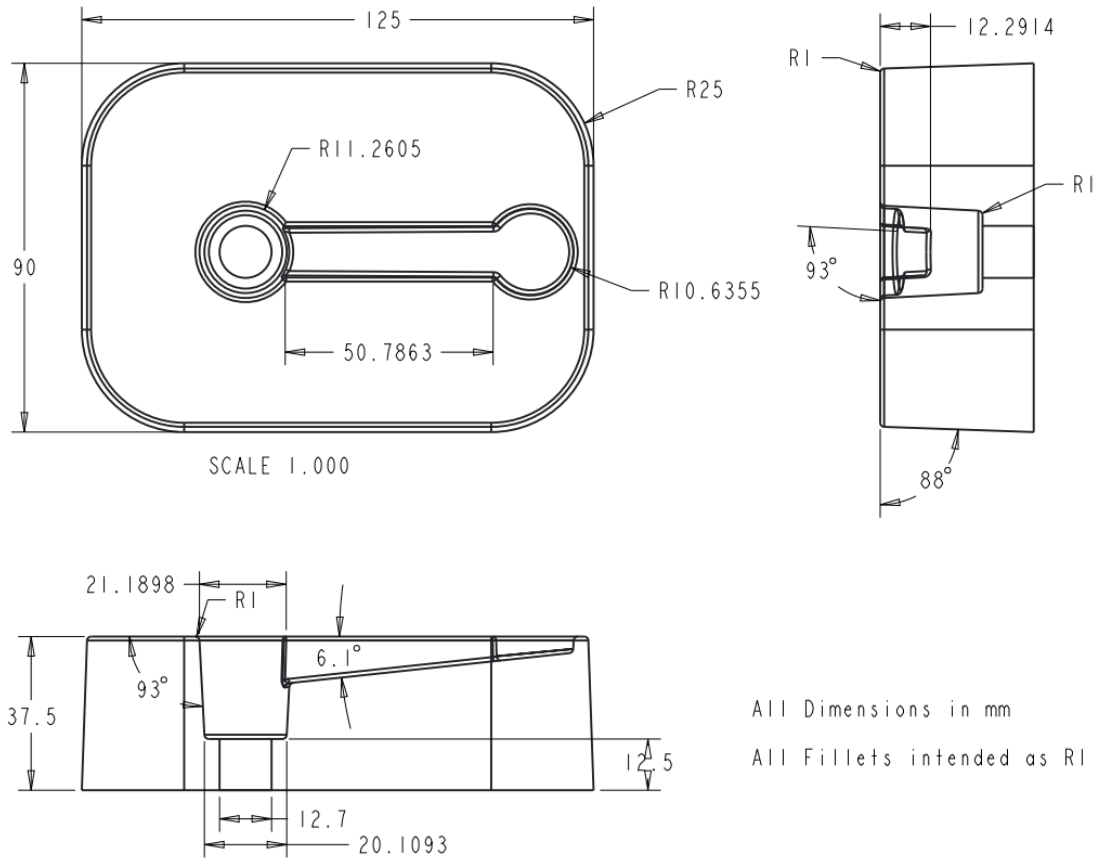

B Interaction plots of processing conditions vs operating window

B.1 Interaction plots of alloy composition vs other variables

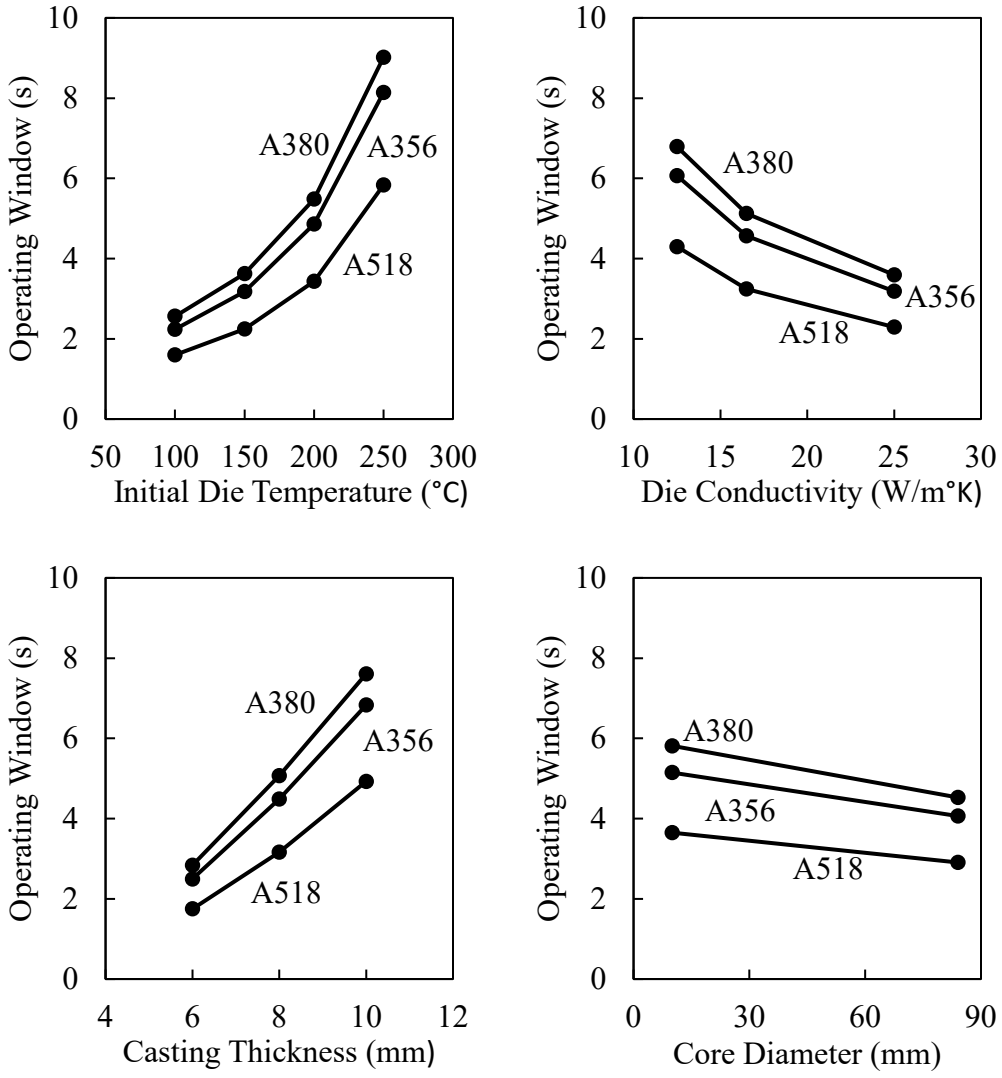

B.2 Interaction plots of die temperature vs other variables

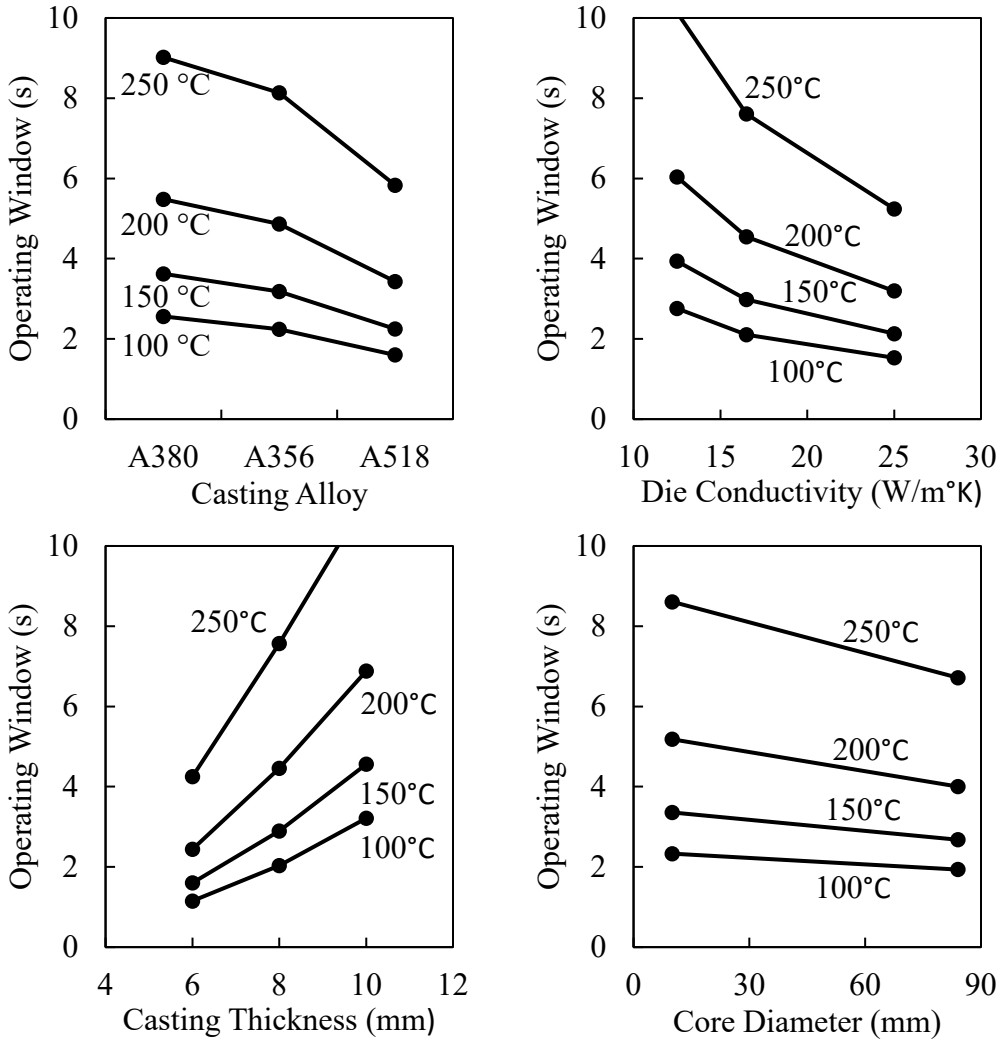

B.3 Interaction plots of die material from Table 5 vs other variables

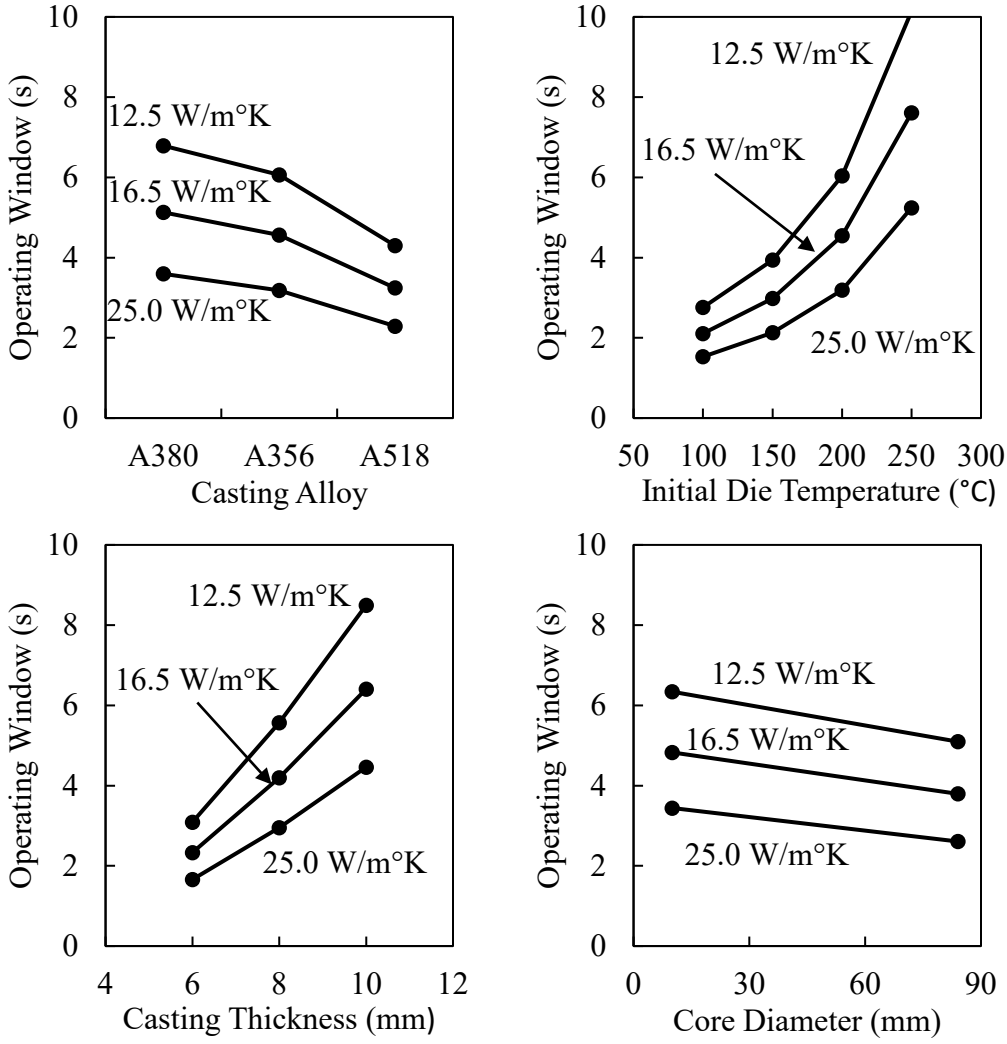

B.4 Interaction plots of casting thickness vs other variables

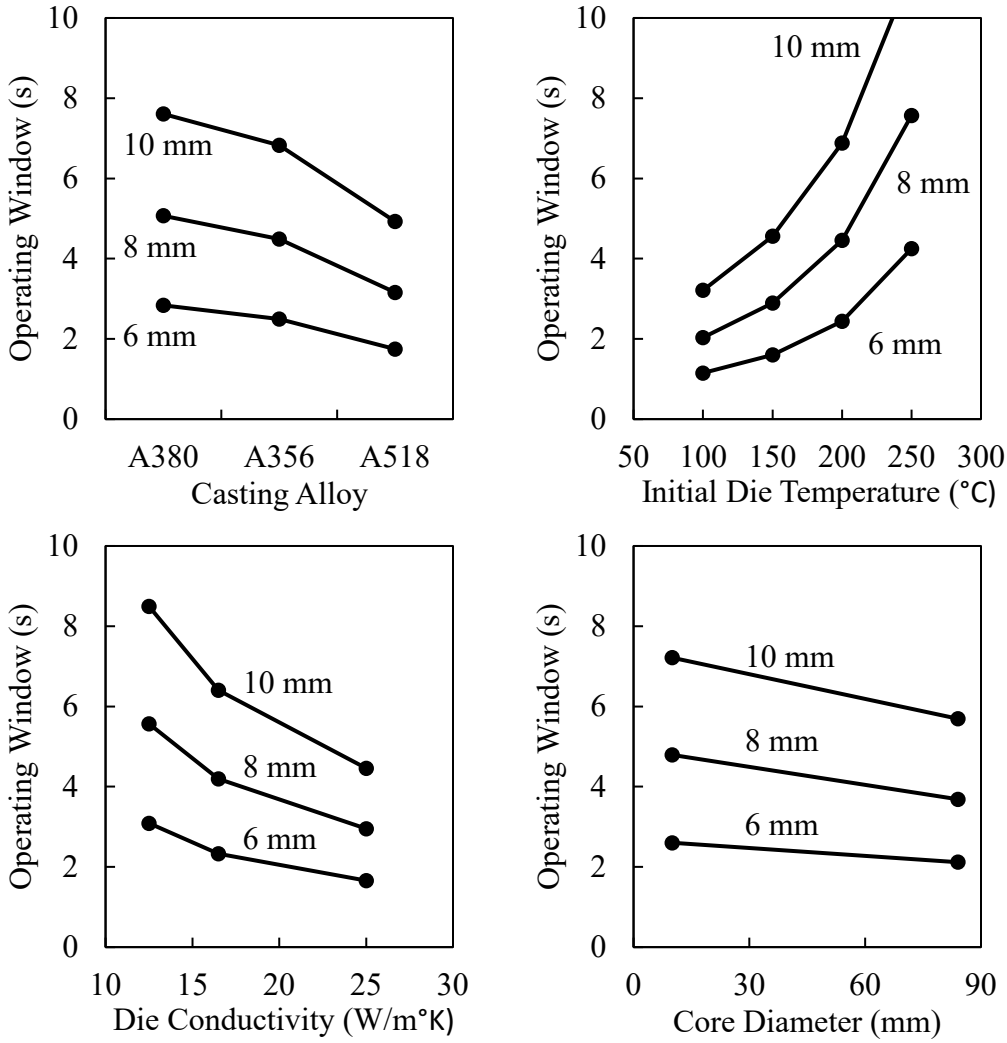

B.5 Interaction plots of casting diameter vs other variables